Autophagy-Mediated Antigen Presentation in Central Nervous System Autoimmunity

---

Dissertation

zur

Erlangung der naturwissenschaftlichen Doktorwürde

(Dr. sc. nat.)

vorgelegt der

Mathematisch-naturwissenschaftlichen Fakultät

der

Universität Zürich

von

Christina Sina

aus

Deutschland

Promotionskomitee

Prof. Dr. rer. nat. Christian Münz (Vorsitz)

Prof. Dr. med. Jan Lünemann (Leitung der Dissertation)

Prof. Dr. rer. nat. Burkhard Becher

Zürich, 2014

Table of Contents

Abbreviations

ACK	Ammonium-chloride-potassium
AMBRA1	Activating molecule in Beclin-1-regulated autophagy protein 1
APC	Antigen presenting cell
Atg	Autophagy-related gene
β2-m	β2-microglobulin
bp	Base pair
BBB	Blood brain barrier
BCA	Bicinchoninic acid
BCL-2	B cell lymphoma 2
BCR	B cell receptor
Beclin1 (Atg6)	B cell lymphoma-2 (Bcl-2) interacting coiled-coil protein
BM-DC	Bone marrow-derived dendritic cell
BSA	Bovine serum albumin
CD + number	Cluster of differentiation
CD	Crohn's disease
cDC	Conventional/Classical DC
CFA	Complete Freund's Adjuvant
CFSE	Carboxyfluorescein succinimidyl ester
CLIP	Class II-associated invariant chain peptide
CMA	Chaperone-mediated autophagy
CNS	Central nervous system
Cre	Cyclization (or causes) recombination enzyme
CTL	Cytotoxic T cell lymphocytes
CTRL	Control
2D2	Mouse strain that carries MOG–specific TCRs
DAMP	Danger-associated molecular pattern
DAPI	4',6-diamidino-2-phenylindole
DC	Dendritic cell
DFCP1	Double FYVE-containing protein 1
DMSO	Dimethyl sulfoxide
DNA	Desoxyribonucleic acid
DNase	Desoxyribonuclease
DNA-IC	DNA-immuno complexes
dNTP	Desoxyribonucleotide
DRiPs	Defective ribosomal products

EAE	Experimental autoimmune encephalomyelitis
EBV	Epstein-Barr virus
EDTA	(Ethylenedinitrilo)tetraacetic acid
EGFP	Enhanced green fluorescent protein
ER	Endoplasmatic reticulum
FACS	Fluorescent activated cell sorting
FCS	Fetal calve serum
FcγR	Fcγ receptors
FcR	Receptor, fragment crystallizing
FIP200	Focal adhesion kinase (FAK) family interacting protein of 200 kDa
Fl or flox	DNA sequence that is flanked by two loxP sites
Flt3L	FMS Like Tyrosine Kinase 3 Ligand
Foxp3	Forkhead box P3
FSC	Forward scatter
FYVE	Zinc finger FYVE (Fab1p, YOTB, Vac1p, EEA1) domain
GILT	Gamma-interferon inducible lysosomal thiol reductase
GM-CSF	Granulocyte macrophage colony-stimulating factor
HERV	Human endogenous retrovirus
HHV-6	Human herpesvirus-6
HLA	Human leukocyte antigen
HRP	Horseradish peroxidase
ICAM1	Intercellular adhesion molecule 1
ICS	Intracellular cytokine staining
iDTR	Inducible diphtheria toxin receptor
IFN	Interferon
IgG	Immunoglobulin G
Ii	Invariant chain
IL	Interleukin
IM	Infectious mononucleosis
iNOS	Inducible nitric-oxide synthase
int	Intermediate (expression)
i.p.	Intra peritoneal (injection)
IRGM1	Immunity-related GTPase
ITGaM	Integrin aM
kb	kilobase pairs
kDa	Kilo Dalton
KFERQ	One-letter code for amino acid sequence Lys-Phe-Glu-Arg-Gln

KO	Knock out
LAMP-2a	Lysosomal membrane-associated protein 2a
LAP	LC3-associated phagocytosis
LC3	Microtubule-associated protein 1A/1B-light chain 3
loxP	Locus of crossover (x) in P1
LPS	Lipopolysaccharide
MACS	Magnetic activated cell sorting
MBP	Myelin basic protein
MIIC	MHC class II loading compartments
MKLSV	One-letter code for amino acid sequence Met-Lys-Leu-Ser-Val
MHC	Major histocompatibility complex
MS	Multiple sclerosis
moDC	Monocyte-derived DCs
MOG	Myelin oligodendrocyte glycoprotein
mRNA	Messenger RNA
mTOR	Mammalian target of rapamycin
NBR1	Neighbor of BRCA1 gene 1
NK cells	Natural killer cells
NKT cells	Natural killer T cells
p62 (SQSTM1)	Ubiquitin-binding protein involved in cell signaling
PAGE	Polyacrylamide gel electrophoresis
Pam3CSK4	Pam3Cys-Ser-(Lys)4, Synthetic triacylated lipoprotein
PAMPs	Pathogen associated molecular patterns
PAS	Pre-autophagosomal structure
PBS	Phosphate buffered saline
PCR	Polymerase chain reaction
pDC	Plasmacytoid DC
PFA	Paraformaldehyde
PI3K	Phosphatidylinositide 3-kinase
PI3P	Phosphatidylinositol3-phosphate
PLP	Proteolipid protein
PMA	Phorbol-12-myristate-13-acetate
PNS	Peripheral nervous system
PRR	Pattern recognition receptor
PtdSer	Phosphatidylserine
PTx	*Pertussis* toxin
RA	Rheumatoid arthritis

RNA	Ribonucleic acid
rpm	Rounds per minute
S1P	Sphingosine-1-phosphate
s.c.	Subcutaneous (injection)
SDS	Sodium dodecyl sulfate
SLE	Systemic lupus erythematosus
SNP	Single nucleotide polymorphism
SSC	Side scatter
ssRNA	Single stranded RNA
TAP-1 and 2	Transporter associated with antigen processing-1 and -2
TBE	Tris-borate-EDTA buffer
T cell	T lymphocyte, matured in the thymus
TCR	T cell receptor
TEM	Transmission electron microscopy
TGF	Transforming growth factor
Th	T helper cell
TIM-4	T cell immunoglobulin mucin-4
Tip DC	TNF inducible nitric oxide synthase (iNOS)-producing DCs
TLR	Toll-like receptor
TNF	Tumor necrosis factor
Treg	Regulatory T cell
ULK-1	Uncoordinated (UNC)-51-like kinase 1
VLA-4	Very late activating antigen-4
VMP1	Vacuole membrane protein 1
VPS34	Vacuolar protein sorting protein 34; is a class III PI 3-kinase
VZV	Varicalle-zoster virus
WIPI	WD (Trp-Asp)-repeat proteins interacting with phosphoinositides
WT	Wildtype
ZNS	Zentrales Nervensystem

Zusammenfassung

Multiple Sklerose (MS) ist eine Autoimmunerkrankung des zentralen Nervensystems (ZNS). Untersuchungen des Mausmodells für MS, namentlich Experimentelle autoimmune Enzephalomyelitis (EAE), konnten zeigen, dass autoreaktive $CD4^+$ T-Zellen eine herausragende Rolle in der Entwicklung von EAE spielen. Jedoch ist bisher unklar, ob Selbstantigene des Myelins über den klassischen MHC Klasse II Prozessierungsweg, Autophagie oder LC3-assoziierte Phagozytose (LAP) degradiert und gegenüber $CD4^+$ T-Zellen präsentiert werden. Mit Bezug auf LAP konnte gezeigt werden, dass extrazelluläres Material über diesen Weg abgebaut werden kann und zudem nimmt die Anzahl von $LC3^+$ Vesikeln in Microglia-Zellen am Höhepunkt der EAE zu. Basierend auf diesen Daten haben wir angenommen, dass die Präsentation von Autoantigenen durch LAP die Aktivierung von autoreaktiven T-Zellen unterstützt.

Um diese Hypothese zu bestätigen, haben wir den Einfluss von Atg5-Defizienz in $CD11c^+$ Zellen auf die Entwicklung der EAE untersucht. Wir haben gezeigt, dass die Defizienz von Atg5 in $CD11c^+$ Zellen keine Rolle bei der Entwicklung von aktiver EAE spielt und dass dieses Ergebnis davon unabhängig ist, ob MOG-Peptid oder MOG-Protein zur Induktion der Krankheit verwendet worden ist. Überraschenderweise resultierte die Induktion der adoptiven Transfer-EAE darin, dass EAE- Symptome in Atg5-defizienten Mäusen nahezu abwesend waren, während Atg5-Kontroll Mäuse normale EAE-Symptome entwickelt haben. Um diese gegensätzlichen Ergebnisse besser verstehen zu können, wurden MOG-spezifische T-Zellen mit primären $Atg5^+$ oder $Atg5^-$ $CD11c^+$ Zellen, in der Gegenwart von MOG-Peptid, MOG-Protein oder Kugeln, welche mit MOG-Protein beschichtet waren, co-kultiviert. Hierbei ergab die Messung der Proliferation von T-Zellen, dass T Zellen in der Gegenwart von $Atg5^-$ $CD11c^+$ Zellen mehr proliferieren als in der Gegenwart von $Atg5^+$ $CD11c^+$ Zellen. Um die Antigenpräsentation weitergehend zu untersuchen, wurden sowohl $Atg5^+$ als auch $Atg5^-$ BM-DCs generiert, die mit Kugeln inkubiert wurden, welche MOG-Protein, Pam3CSK4 oder MOG-Protein plus Pam3CSK4 beschichtet waren. Bei diesen Untersuchungen konnten keine LC3-assoziierten Phagosomen erkannt werden und somit keine Rückschlüsse über die Rolle von LAP während der Prozessierung von extrazellulären Autoantigenen gezogen werden.

Weitere *in vitro* und *in vivo* Experimente werden notwendig sein, um die unterschiedlichen Ergebnisse in der aktiven und adoptiven Transfer-EAE erklären zu können. Zum einen müssten die T-Zell- und Antigenpräsentierende Zellinfiltrate in das ZNS am Höhepunkt der Krankheit untersucht werden. Diese Untersuchungen könnten darüber Aufschluss geben, welche Zellen das ZNS infiltrieren und welche Effektorfunktionen diese besitzen. Darüber hinaus könnte der Antigenprozessierungsweg untersucht werden, indem LAP durch bekannte Faktoren, wie beispielsweise TLR-Stimulierung, FcR-Bindung oder mit der Verwendung von “eat me” Signalen, ausgelöst wird. Alle Experimente zusammengenommen, könnten somit neue Einblicke dahin gehend ermöglichen, über welchen Prozessierungsweg extrazelluläre Autoantigene verarbeitet werden und wie $CD4^+$ autoreaktive T-Zellen dazu aktiviert werden, EAE oder MS zu induzieren.

Summary

Multiple sclerosis (MS) is an autoimmune disease of the central nervous system (CNS). The commonly used mouse model for MS, namely experimental autoimmune encephalomyelitis (EAE), revealed that the main driving forces in the development of EAE are autoreactive $CD4^+$ T cells.

The exact antigen processing route of how myelin self-antigens are processed and presented has not been described yet and the classical MHC class II pathway, the autophagy pathway and LC3-associated phagocytosis (LAP) are potential degradation pathways that might lead to MHC class II presentation of myelin antigen. It has recently been shown that extracellular material can be degraded by LAP and previous studies of our laboratory indicate that the presence of $LC3^+$ vesicles in microglia increases at the peak of EAE. Based on these data, we hypothesized that LAP-dependent presentation of autoantigens facilitates the activation of autoreactive T cells.

To address this question, we investigated whether autophagy deficiency in $CD11c^+$ cells influences the development of EAE. We demonstrated that Atg5-deficiency in $CD11c^+$ cells does not play a role in active EAE, neither triggered by MOG peptide nor MOG protein. Surprisingly, induction of adoptive transfer EAE via the adoptive transfer of autoreactive $CD4^+$ T cells resulted in the almost complete absence of EAE symptoms in Atg5-deficient mice whereas Atg5 control mice developed EAE symptoms. In order to better understand these findings, *in vitro* experiments to study the role of Atg5 in antigen presentation were performed. A co-culture experiment in which MOG peptide-specific T cell receptor transgenic T cells from 2D2 mice were co-cultured with splenic $Atg5^+$ or $Atg5^-$ $CD11c^+$ cells in the presence of MOG peptide, MOG protein or beads coated with MOG protein was performed. Checking for T cell proliferation, it was shown that T cells in the presence of $Atg5^-$ $CD11c^+$ proliferated more than in the presence of $Atg5^+$ $CD11c^+$ cells. In an alternative approach to investigate antigen processing pathways in antigen presenting cells (APCs), bone marrow-derived dendritic cells (BM-DCs) were generated from Atg5-deficient and Atg5 control mice and incubated with beads coated with MOG protein, the TLR agonist Pam3CSK4 or MOG protein with Pam3CSK4. Screening for $LC3^+$ vesicles that might be an indication for LAP, did not yield any unambigous LC3-associated phagosomes.

Conclusively, further *in vitro* and *in vivo* investigations are necessary to identify the mechanism that leads to the absence of EAE symptoms in Atg5-deficient mice in adoptive transfer EAE, but not in active EAE. Firstly, T cell and APC infiltrates into the CNS at peak of disease need to be examined. These experiments would offer valuable clues which cells infiltrate and which effector functions they fulfill. With regard to *in vitro* studies, antigen processing and presentation characteristics could be studied by inducing LAP by known factors such as TLR stimulation, Fc receptor (FcR) engagement or “eat me” signals.

In conclusions, our findings would give newly insights of how extracellular self-antigen is processed and how $CD4^+$ autoreactive T cells are triggered to induce EAE, or even MS.

1 Introduction

1.1 The Immune System

The body harbours a plethora of diverse effector cells and molecules that function in the body's defence against pathogens and other exogenous factors that might cause damage to their host. The entire system consisting of effector cells and molecules is called the immune system. Immunity describes the capability of the body to protect itself against these exogenous and damaging factors.

The immune system can be divided into two arms: the innate and adaptive immune system. The innate immune system is defined as the „first line of defense" and is mainly based on physical barriers, such as the skin, toxic molecules and phagocytic cells that phagogcytose and eliminate the pathogenic invader. The innate immune response is initiated immediately after an infection and acts in response to molecular patterns, which are found in pathogens or indicate cell damage. Nevertheless, it is irreplaceable to instruct the adaptive immune response. The adaptive immune system, on the other hand, is highly specific against exogenous pathogenic factors and does own „memory" functions. This memory function allows the immune system to respond faster and more efficiently when encountering a thread for a second time. Generally, a substance that is able to generate an adaptive immune response is named antigen (*anti*body *gen*erating) (term coined by Paul Ehrlich around 1900).

The adaptive immune response is executed by a class of leukocytes called lymphocytes and one distinguishes humoral (antibody-mediated) and cellular immune responses, which are mediated by two classes of lymphocytes, namely B cells and T cells, respectively. During the humoral immune response, B cells recognize an antigen by means of their B cell receptor (BCR) that leads to the activation of the B cell and, eventually, to the release of antibodies into extracellular fluids such as blood, tear fluid or breast milk. While circulating, antibodies bind their specific antigen, which originally caused the release of this antibody. The binding of the antibody to the antigen might result in the neutralization or inactivation of the antigen by binding to structures that otherwise might interact with cell surface structures of the host. Additionally, the antibody binding might initiate the destruction of the invader since it facilitates the uptake of it by cells of the innate immune system.

The main players of the cellular immune system are lymphocytes called T cells that develop in the thymus, which is a lymphoepithelial organ. T cells recognize their specific antigen with a T cell receptor (TCR) and can be further subdivided into cytotoxic T cell lymphocytes (CTL) and T helper (Th) cells. Based on their unique expression of the co-receptor molecules CD8 and CD4, CTLs are also known as $CD8^+$ T cells and Th cells as $CD4^+$ T cells, respectively. $CD8^+$ T cells have the capability to kill cancer cells, infected cells or otherwise defect cells in order to maintain integrity of the host. On the other hand, once $CD4^+$ T cells recognize an antigen, they secrete high amounts of inflammatory cytokines in order to activate B cells and macrophages and, hence, destroy the

invading pathogen. As mentioned above, T cells recognize their antigen by a TCR. In order to do so, the antigen needs to be presented by an antigen presenting molecule named major histocompatibility (MHC) molecule that is present on antigen presenting cells (APCs).

An APC is a cell type that is able to process protein antigens and dissect them into small peptide fragments. These antigenic fragments are bound to MHC molecules and displayed as a peptide:MHC complex on the cell surface. The peptide:MHC complex is recognized by T cells by means of their TCR and this interaction leads to the activation of the T cell.

Principally, there are two different types of MHC molecules, namely, MHC class I and class II molecules. MHC class I molecules are present on most nucleated cells and present peptides from cytosolic proteins to $CD8^+$ T cells. On the other hand, MHC class II molecules bind peptides that are derived from extracellular material and are recognized by $CD4^+$ T cells. MHC class II molecules are mainly restricted to dendritic cells (DCs), macrophages and B cells which form the group of professional APCs. Professional APCs are most efficient in uptake, processing and presenting of exogenous antigen and constitutively express MHC class II molecules. The expression of co-stimulatory molecules is another feature that defines professional APCs. Contrary, non-professional APCs are less efficient in antigen uptake and processing and do not constitutively present MHC class II molecules, but their expression can be triggered by cytokine stimulation. The group of non-professional APCs includes the following cells: fibroblasts, thymic epithelial cells, glial cells, pancreatic β-cells and vascular endothelial cells.

The close interaction between the innate and adaptive immune system and the resulting immune response with cytokine secretion, antigen capture and presentation as well as pathogen elimination ensures the durability and survival of the host.

1.2 Autoimmunity

Autoimmunity is described as an immune reaction that is directed against antigens that originated from or produced by the host – so-called self-antigens. Thus, in the case of autoimmunity, the body's own immune system is not able to distinguish between self and non-self-antigens. This disequilibrium might lead to a strong immune response against various host tissues mediated via self-molecules. This, in turn, might cause severe damage of the affected organ possibly instigating the manifestation of an autoimmune disease.

1.2.1 Autoimmune Diseases

Autoimmune diseases are caused by an immune reaction against self-antigens and might lead to severe tissue damage of the affected organ. Amongst the most prevalent autoimmune diseases are systemic lupus erythematosus (SLE), type 1 diabetes mellitus and rheumatoid arthritis (RA) as well as multiple sclerosis (MS). Briefly, in SLE autoantibodies and autoreactive T cells target self-DNA,

chromatin-associated proteins and ubiquitous ribonucleoproteins resulting in phenotypes such as glomerulonephritis, vasculitis or skin rash (Teresa Bailey et al., 2011). In type 1 diabetes mellitus the body produces autoreactive T cells against antigens of the pancreatic islets which results in the destruction of insulin-producing pancreatic β-cells and, thus, in depletion of this hormon (Atkinson, 2012). A third example for an autoimmune disease is RA during which autoreactive T cells against the capsule around the joints (synovium) are formed. This results in an inflammation and destruction of joints and, finally, in arthritis (Imboden, 2009). In MS, autoreactive T and B cells are directed against self-antigens of the central nervous system (CNS). Sclerotic plaques are formed and the myelin layer around the axons is disrupted which leads to loss of myelin and scarring. Clinically, patients may present variable symptoms dependent on the locations of the lesions within the CNS. Typical manifestations include loss of sensitivity or alteration in sensation, muscle weakness, very pronounced reflexes, muscle spasms, or difficulties with coordination and balance (ataxia) (Sospedra and Martin, 2005).

1.2.2 Origin and Causes of Autoimmunity

The immune system comprises a diversity of different effector mechanisms to eliminate a wide range of pathogens and it is, under physiological conditions, able to distinguish between self and non-self antigens. In order to develop such a self-tolerance, the immune system needs to discriminate autoreactive from non-autoreactive lymphocytes. Principally, there are two mechanisms that lead to self-tolerance: central and peripheral tolerance.

1.2.2.1 Principle Mechanisms of Central Tolerance

Central tolerance develops in the thymus via negative selection and subsequent deletion of thymocytes that recognize self-antigen. The process of negative selection takes place during the entire development of lymphocytes and is located to the cortex and medulla of the thymus. Thymic epithelial cells express and present self-antigens on their cell surface. Alternatively, self-antigen is transported to the thymus where local APCs process and present these self-antigens for the aforementioned selection process. A developing lymphocyte that recognizes a self-peptide:MHC complex with its TCR too strongly will be eliminated by programmed cell death (apoptosis). The deletion of a T cell that is reactive to a self-peptide:MHC complex thereby decreases the likelihood of releasing an autoreactive T cell into the periphery, where it might cause damage by being activated (Hogquist et al., 2005).

1.2.2.2 Principle Mechanisms of Peripheral Tolerance

Autoreactive lymphocytes can be eliminated during the process of central tolerance as elucidated above. If self-antigens are neither produced nor transported to the primary lymphoid organs or the process of central tolerance was incomplete, self-reactive lymphocytes need to be kept in check by peripheral tolerance. Freshly matured self-reactive lymphocytes that leave the primary lymphoid organs and might encounter their self-antigen will be eliminated. The main three mechanisms of inducing peripheral tolerance are: cell death by apoptosis, inducing an anergic state of the lymphocytes that renders them unresponsive to self-peptide:MHC complexes or suppression by regulatory T cells (Treg). Tregs comprise a subset of $CD4^+$ T cells their main function being to suppress the activation of an immune response, regulation of lymphocyte homeostasis and induction of immune tolerance by, among other mechanisms, the secretion of interleukin (IL)-10, transforming growth factor (TGF)-β and IL-35 (Walker and Abbas, 2002).

Next to these regulatory cell functions, morphological characteristics, namely immunological privileged areas in the body that cannot be accessed by immune cells, contribute to the reduction of autoimmunity. Sites of immune privilege are not drained by the lymphatic system and include for example the brain and the eye (Wekerle and Sun, 2010).

1.2.2.3 Triggers of Autoimmune Diseases

Autoimmune diseases are rather complex and various mechanisms have been described for the development of the disorders. Accordingly, a wide range of triggers that are potential causes of autoimmune diseases are currently under discussion. Genetic as well as environmental factors may contribute to the pathogenesis of autoimmune diseases and are explained by using the example of MS in the following section.

1.2.3 Multiple Sclerosis

MS is a demyelinating autoimmune disorder that mainly affects young adults. The name of this disease is attributed to the fact that hard (sclerotic) lesions are formed in the white matter of the brain. As a neurological disease that is characterized by local demyelination in the CNS, MS is believed to be an autoimmune reaction against various antigens of the myelin sheath that surrounds the axon. Typical brain antigens affected are myelin basic protein (MBP), proteolipid protein (PLP) and myelin oligodendrocyte glycoprotein (MOG). The immune response results in severe damage of the myelin sheath and, based on this damage, electrical signals cannot be conducted properly anymore and the affected conductivity might result in a variety of neurological symptoms (Sospedra and Martin, 2005).

Depending on the course of disease, MS can be classified into two main categories: relapsing remitting and primary progressive MS. Relapsing remitting MS is defined as the occurrence of

exacerbating symptoms and complete remission of symptoms and can result in a relatively mild degree of disability. This type of MS eventually develops into secondary progressive MS that is defined by changing from a relapsing and remitting disease course into a steady and gradual worsening of disease symptoms. This shift in symptoms typically appears 15 to 20 years after first being diagnosed with MS. On the other hand, primary progressive MS is characterized by lack of remission and a continuous progression of disability (Lublin and Reingold, 1996).

1.2.3.1 Etiology of MS

The exact etiology of MS is still unknown, but there is evidence that the underlying cause of the condition is based on immunopathogenic processes and that both genetic and environmental factors contribute to the pathogenesis of MS. An interrelationship of both factors is likely.

Genetic Predisposition and Hereditary Factors

With regard to the cause of MS, some individuals show a clear genetic predisposition. Amongst all genes that are associated with a higher susceptibility to autoimmune diseases, the human leukocyte antigen (HLA) haplotype is known to confer the highest genetic risk in developing MS. The strongest genetic risk factor is the HLA-DRB1*1501 allele (Schmidt et al., 2007). Additionally, other HLA-DRB1 alleles, namely DR3 (DRB1*0301) and DR4 (DRB1*0405, DQA1*0301 and DQB1*0302) are associated with a relative higher risk rate of roughly threefold in heterozygous individuals and an elevated risk rate by sixfold in homozygous individuals (Ascherio et al., 2012).

The correlation between the HLA haplotype and MS can be explained by use of the two following models. Firstly, the susceptibility to an autoimmune disease is dependent on the efficiency of the MHC molecule to present an autoantigen to an autoreactive T cell. This means in turn that a defective MHC molecule might have the ability to present self-antigens in a superior way and, thus, might lead to the unintended activation of autoreactive T cells. Secondly, the correlation between the MHC haplotype and the susceptibility to autoimmune diseases might go back to the role of MHC molecules in the establishment of the TCR repertoire. According to this hypothesis, during the process of negative selection, MHC molecules loaded with self-antigen might promote the positive selection of self-reactive thymocytes instead of inducing their elimination. Association to MHC class I alleles (Cree et al., 2010) and other non-MHC regions have been also described (International Multiple Sclerosis Genetics Consortium (IMSGC) et al., 2013), but are less well defined.

The search for other, unrelated HLA haplotype genes that may confer the risk of MS is ongoing. The gene CYP27B1 that encodes for 25-hydroxyvitamin D-1α hydroxlyase has been associated with an increase in risk to develop MS (Ramagopalan et al., 2011). And based on further genetic approaches, such as genome-wide association studies and genome projects, more MS susceptibility

loci have been identified. These loci include, amongst others, IL-2 receptor α, IL-7 receptor α, CLEC16A, IRF8, IL12A and others (Qiu et al., 2013).

In parallel, demographic studies have shown that women show a higher risk of developing autoimmunity than men (Voskuhl and Gold, 2012). Furthermore, a high degree of heritability of autoimmune disease was established in studies of twins and siblings and it was shown that the risk of suffering from MS is lower in Hispanic, black and Asian populations than in Caucasian populations (Wallin et al., 2004).

Geographical and Environmental Factors

The geographical distribution of autoimmune diseases shows a regular pattern with regard to continents, countries and ethnic groups in that the incidence of MS decreases form north to south in the northern hemisphere and the opposite way around in the southern hemisphere (so-called latitude gradient) (Acheson et al., 1960). This is in line with studies that showed that autoimmunity is less common in developing countries than in industrial countries. Deeper insights into genetics and environmental factors were gained by immigration studies. In these studies the movement of people from areas where MS is very common to areas where it is less common and vice versa were conducted (Gale and Martyn, 1995). The tracking of migration of people from high MS risk to low MS risk regions revealed that the risk of suffering from MS decreases the younger the age of the migrant. This relation suggests a connection between MS risk and environmental factors (Gale and Martyn, 1995; McLeod et al., 2011). Additional epidemiological and clinical studies have revealed that there is a negative correlation between the occurrence of certain infections in early childhood, the socio-economic status and the development MS. This correlation is described by the hygiene hypothesis (Bach, 2002).

Another environmental factor that contributes to MS is the level of vitamin D and the amount of sun light exposure. In this context, a negative correlation between vitamin D level and MS incidence was shown (van der Mei et al., 2001). Furthermore, smoking of cigarettes increases the risk of suffering from MS enormously when comparing ever smokers to never smokers (Hernán et al., 2005; Riise et al., 2003; Sundström et al., 2008). All these environmental factors were also reviewed by (Ascherio and Munger, 2007; Milo and Kahana, 2010; Shapira et al., 2010).

Pathogenic Factors that Contribute to MS

The role of infectious and viral triggers in MS etiology and pathology is still under debate. But there are studies that describe the connection between pathogens and MS and which try to explain how infections might trigger autoimmune responses in MS. Viruses that have been described to be associated with MS are: Herpesviruses such as Varicalle-zoster virus (VZV), human herpesvirus-6 (HHV-6) and Epstein-Barr virus (EBV) as well as the human endogenous retroviruses (HERVs) (Kakalacheva et al., 2011).

Amongst all viruses being described to be associated with triggering MS, EBV is the most promising candidate. EBV is an orally transmitted virus ("kissing disease") and immediately infects the recipient. While EBV infection of children is generally asymptomatic, EBV infection during adolescence or adulthood often results in the clinical illness infectious mononucleosis (IM) that is characterized by fever, lymphadenopathy, pharyngitis and fatigue. Epidemiological studies have linked symptomatic infectious mononucleosis and MS and associated EBV infection with the development of MS. This assumption is based on results showing a strong interconnection between infectious mononucleosis and MS with regard to age, geographical location and socioeconomic status. Furthermore, an elevated serum level of antibodies against a mixture of EBV nuclear antigens was associated with an increased risk for developing MS (Ascherio and Munger, 2010; Kakalacheva et al., 2011).

Potential molecular mechanisms of how pathogens might induce autoimmunity include: bystander activation, adjuvant effect, superantigen activation, molecular mimicry, epitope spreading and viral support of autoreactive cell survival and are illustrated in Figure 1.1.

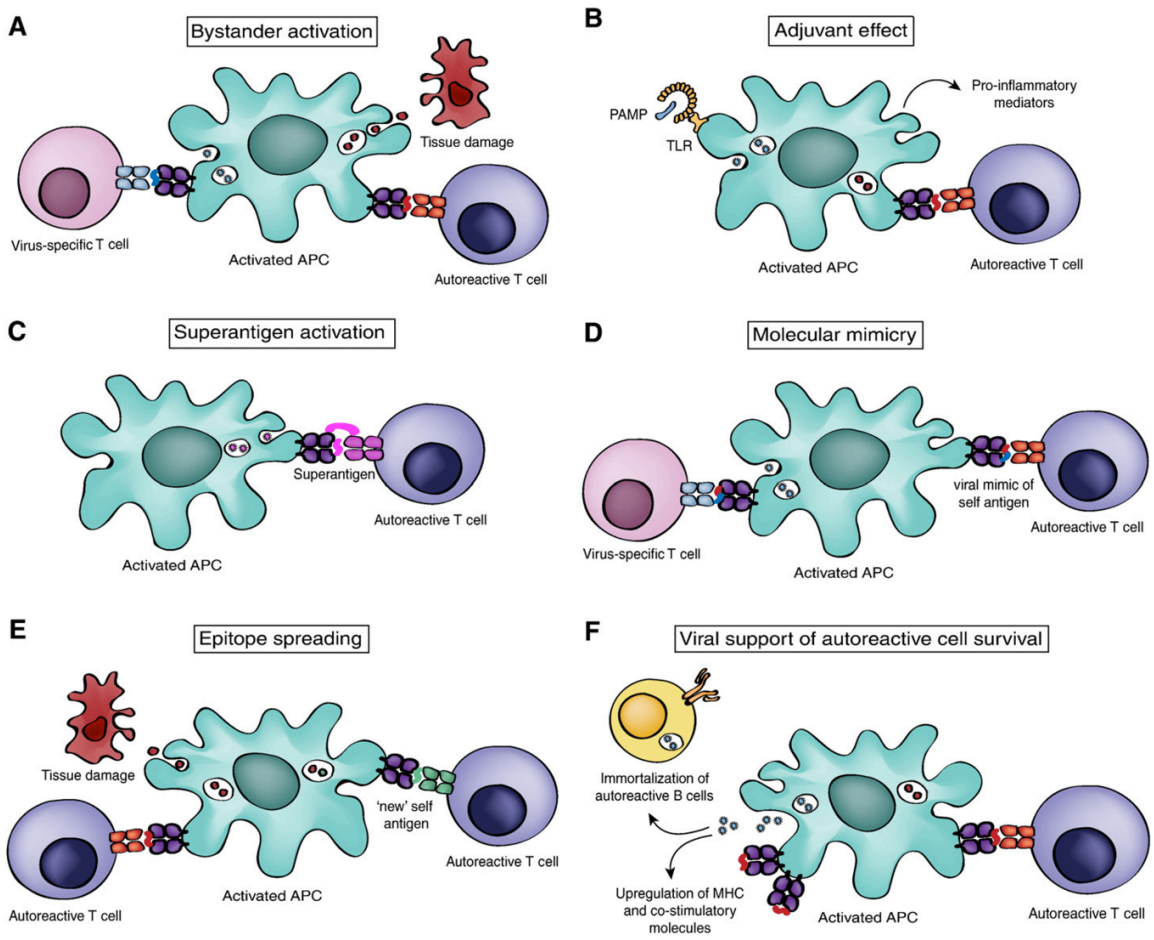

Figure 1.1: Molecular mechanisms of pathogen-induced autoimmunity. (A) bystander activation, **(B)** adjuvant effect, **(C)** superantigen activation, **(D)** molecular mimicry, **(E)** epitope spreading and **(F)** viral support of autoreactive cell survival. Figure from (Kakalacheva et al., 2011).

Bystander activation of autoreactive lymphocytes is facilitated via infectious factors (Figure 1.1A). During the process of an infection, an immune response is caused that leads to the release of immune mediators and co-stimulatory molecules. These inflammatory conditions might influence noninvolved lymphocytes (so-called bystanders) that are not antigen specific. Especially under conditions when tissue is affected and destroyed, a high number of self-antigen is released and presented by APCs to self-reactive lymphocytes that are then activated in a so-called bystander activation process (Fujinami et al., 2006; McCoy et al., 2006).

Another aspect of how autoreactive lymphocytes could be activated is the adjuvant effect (Figure 1.1B). Generally, the activation of APCs by binding of pathogen associated molecular patterns (PAMPs) by pattern recognition receptors (PRRs) leads to the activation of APCs and the release of pro-inflammatory mediators. If an autoreactive T cell interacts with a self-peptide:MHC molecule simultaneously, the inflammatory mediators might function as an adjuvant and might lead to the activation of these autoreactive T cells.

Furthermore, superantigens might play a role in the development of autoimmunity (Figure 1.1C). A superantigen is an antigen that can direct the binding of an MHC class II molecule to a TCR by binding to non-polymorphic regions of the MHC class II molecule and the conserved regions of the TCR Vβ domain without a specifically bound peptide. This event results in the crosslinking of those two molecules and, potentially, to the unspecific activation of T cells. In this context, one of the best-known superantigens is *staphylococcal* enterotoxin (Brocke et al., 1993).

Another mechanism of pathogen-induced immunity is termed molecular mimicry (Figure 1.1D). Pathogens express proteins or carbohydrates that resemble the host's own structures. Under inflammatory conditions these self-mimicking structures might be presented to autoreactive T cells and induce their activation. As mentioned earlier, there are some immunological privileged areas in the body that cannot be accessed by immune cells. During an infection or a severe trauma, these cell or tissue barriers can be disrupted and self-material that is sequestered under normal conditions now becomes accessible to autoreactive lymphocytes and might lead to their activation. This entire process is called epitope spreading and is illustrated in Figure 1.1E (Fujinami et al., 2006; McCoy et al., 2006).

Furthermore, a viral infection activates APCs and induces the upregulation of MHC and co-stimulatory molecules. This might cause the conversion into an effector state and might support the survival of autoreactive lymphocytes (Figure 1.1F).

1.2.3.2 Pathogenesis of MS

Disregarding the potential and ultimate trigger of MS, proinflammatory conditions lead to an immune response in the CNS and a certain sequence of pathogenic steps (Hemmer et al., 2002; Sospedra and Martin, 2005; Steinman, 2009). A short overview of these steps is illustrated in Figure 1.2.

The presumed initial step in the pathogenesis of MS is the activation of autoreactive T cells and B cells in the periphery. The activation is caused by antigen that is either released from the CNS into the circulation or an alternative activation process by cross-reactive foreign antigens. After activation of autoreactive lymphocytes in the periphery, the cells start to proliferate. The second step includes the transmigration of these clonally expanded cells through the blood brain barrier (BBB) into the brain parenchyma. The pro-inflammatory cytokines and chemokines that are produced by infiltrating immune cells, promote the activation of CNS-resident cells such as microglia and astrocytes and the recruitment of further immune cells. Once present in the CNS, T cells and B cells encounter their specific antigen that is either presented by APCs or naturally occurring in the tissue, respectively. Activated $CD8^+$ T cells induce damage to cells that present self-peptide:MHC complexes on their surfaces and $CD4^+$ T cells release inflammatory cytokines after encountering their specific antigen on MHC class II molecules. Additionally, plasma cells release myelin-specific antibodies that bind their antigen and lead to opsonization of cells and, in a next step, to damage of the myelin sheath. Attracted by inflammatory cytokines, macrophages are also recruited to the CNS, where they release further immune mediators and phagocytose target cells leading to a high level of CNS tissue damage.

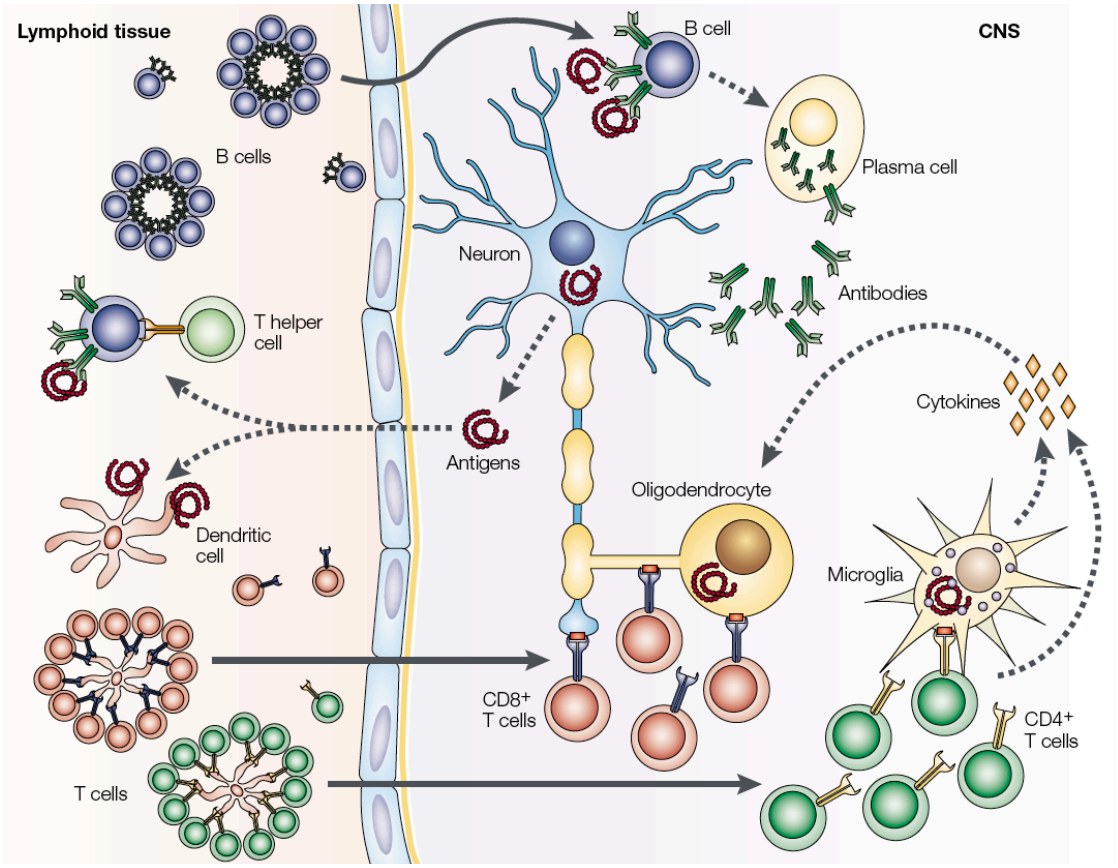

Figure 1.2: Pathogenesis of MS. The pathogenesis of MS can be subdivided into the following steps: Activation of autoreactive lymphocytes in the periphery, transmigration of autoreactive lymphocytes into the CNS, release of pro-inflammatory cytokines and chemokines, recruitment of resident cells and further immune cells, reactivation of autoreactive lymphocytes and destruction of CNS tissue in the inflammatory stage. Figure from (Hemmer et al., 2002).

1.2.3.3 Animal Model for MS

A murine animal model that is used to study the mechanistic basis of autoimmune demyelinating diseases and to test therapeutic approaches is called experimental autoimmune encephalomyelitis (EAE) (Gold et al., 2006) and was first described by Olitsky and Yager 65 years ago (Olitsky and Yager, 1949). EAE is an antigen-induced animal model and can be actively induced by the injection of CNS antigens in combination with Complete Freund's Adjuvant (CFA) which is an oil-based adjuvant containing mycobacteria. CNS antigens can be applied in form of homogenate of the CNS (Brown and McFarlin, 1981), in form of brain antigens such as MBP (Fritz et al., 1983), PLP (Trotter et al., 1987) or MOG (Mendel et al., 1995) or, alternatively, with peptides representing the major encephalitogenic regions of MBP ($MBP_{84–104}$), PLP ($PLP_{139–151}$ or $PLP_{178–191}$), or MOG (MOG_{35-55} or $MOG_{92–106}$). It is noted that MOG_{35-55} is highly encephalitogenic in C57BL/6 mice – the genetic background that was used in this study. In addition to self-antigen and CFA, *Pertussis* toxin (PTx) which, originally, is an exotoxin produced by the bacterium *Bordetella pertussis* and causes whooping cough, is necessary to induce EAE. The true role of PTx is still under discussion, but PTx was described to facilitate immune cell entry into the CNS (Kerfoot et al., 2004). Furthermore, PTx is also known to break T cell tolerance and to promote clonal expansion and cytokine production by T cells (Kamradt et al., 1991; Shive et al., 2000; Waldner et al., 2004).

In the EAE mouse model clinical disease symptoms arise 10 to 15 days after immunization. Initial disease symptoms are a flaccid, limp tail and paralysis of hind legs with progression of symptoms to the front legs and a potential culmination in a completely moribund state. This disease course describes the classic EAE model and reflects the preferential targeting of inflammation to the spinal cord and to some extent to the cerebellum.

In contrast to active induction of EAE, EAE can also be induced by adoptive transfer of autoreactive T cells. In the adoptive transfer EAE model, donor mice are primed and autoreactive T cells are isolated from these donors. In a next step, the autoreactive T cells are expanded *in vitro* in the presence of neuroantigen and are then adoptively transferred to syngeneic naïve recipient mice. The first adoptive transfer experiment was done with rats. In these experiments, lymph node cells from rats that had been immunized with spinal cord homogenate were transferred into naïve mice that then developed EAE symptoms (Paterson, 1960). Over time it could be shown that antigen-specific T cells are actually responsible for transfering the disease (Ben-Nun et al., 1981) and, in a next step, it was shown that MHC class II-restricted $CD4^+$ T cells that are either MBP (Zamvil et al., 1985) or MOG-specific (Bettelli et al., 2003) can induce disease in recipient mice. All these experiments clearly showed that $CD4^+$ T cells mainly mediate EAE.

Spontaneous development of EAE in wildtype mice is not known. But there are TCR transgenic mice that spontaneously develop EAE without the administration of neuroantigen or adjuvant (Goverman et al., 1993; Krishnamoorthy et al., 2006; Pöllinger et al., 2009).

1.2.3.4 Pathogenesis of EAE

The main pathogenic steps of EAE are similar to the ones believed to be essential for MS (chapter 1.2.3.2). As mentioned above, normal wildtype mice do not develop spontaneous EAE. Thus, in order to induce EAE, peripheral myelin-specific $CD4^+$ T cells that escaped tolerogenic mechanisms, need to be primed in the periphery by injection of CNS antigen with adjuvant. In a next step, the activated $CD4^+$ T cells expand in the peripheral lymphoid organs and migrate to the CNS. In the CNS, the BBB is most likely broken down by the application of PTx (Kerfoot et al., 2004) and allows T cell entry into the CNS where they need to be reactivated by local APCs that present myelin peptide. The subsequent secretion of pro-inflammatory cytokines and the expression of co-stimulatory molecules initiate a cascade of events that triggers the recruitment of macrophages to the site of inflammation. Macrophages are known to secrete pro-inflammatory mediators such as tumor necrosis factor (TNF)-α and IL-1, which support the infiltration of T cells, B cells and macrophages. Consequently, an inflammatory milieu is provided and due to the neuroinflammatory response, CNS damage is caused and focal plaques of demyelination are formed.

1.3 Basic Principles of Antigen Processing and Presentation

Antigen processing is an intracellular procedure that converts proteins from the extracellular space or cytosol into peptides. These peptides are loaded onto MHC molecules to be presented to T cells. There are two classical pathways of antigen processing and presentation: the MHC class I pathway for the processing and presentation of cytosolic proteins and the MHC class II pathway for processing and presentation of extracellular proteins (Figure 1.3).

1.3.1 MHC Class I Antigen Presentation Pathway

In every cell endogenous messenger RNA (mRNA) or even mRNA that originates from pathogens that reside in the cytosol are translated constantly. During this process not only correctly folded proteins are synthesized, but also a high amount of misfolded proteins that are called defective ribosomal products (DRiPs) (Li et al., 2011a). Additionally, short-lived, old or excessive proteins need to be removed from the cell to ensure a functional environment. All these targets are immediately recognized and labeled with multiple ubiquitin units (poly-ubiquitination) and are then directly targeted to the proteasome where they are proteolysed into small peptide fragments (Pickart, 2001). The peptide fragments are transported into the endoplasmatic reticulum (ER) by transporters called transporters associated with antigen processing-1 and -2 (TAP1 and TAP2) for loading onto MHC class I molecules (Abele and Tampé, 2004).

In parallel, within the ER, the polymorphic heavy chain and a light chain called β2-microglobulin (β2m) subunit are assembled to form the MHC class I:β2m complex. Until a peptide has been loaded to the complex, the MHC class I:β2m complex is stabilized by the ER chaperone proteins

calreticulin, ERp57, protein disulfide isomerase (PDI) and tapasin. Tapasin also functions as an adaptor protein between the assembled MHC class I molecule and the TAP transporter (Wearsch and Cresswell, 2008). Generally, the binding groove of the MHC class I molecule accommodates peptides of 8–9 amino acids.

Once the peptide fragments have arrived in the ER and the MHC class I molecule has been assembled, peptides are loaded onto MHC class I molecules and are guided to leave the ER to present the peptide:MHC class I complex on the cell surface. In case peptides and MHC class I molecules are not assembled successfully, they are returned to the cytosol for subsequent degradation (Blum et al., 2013; Neefjes et al., 2011).

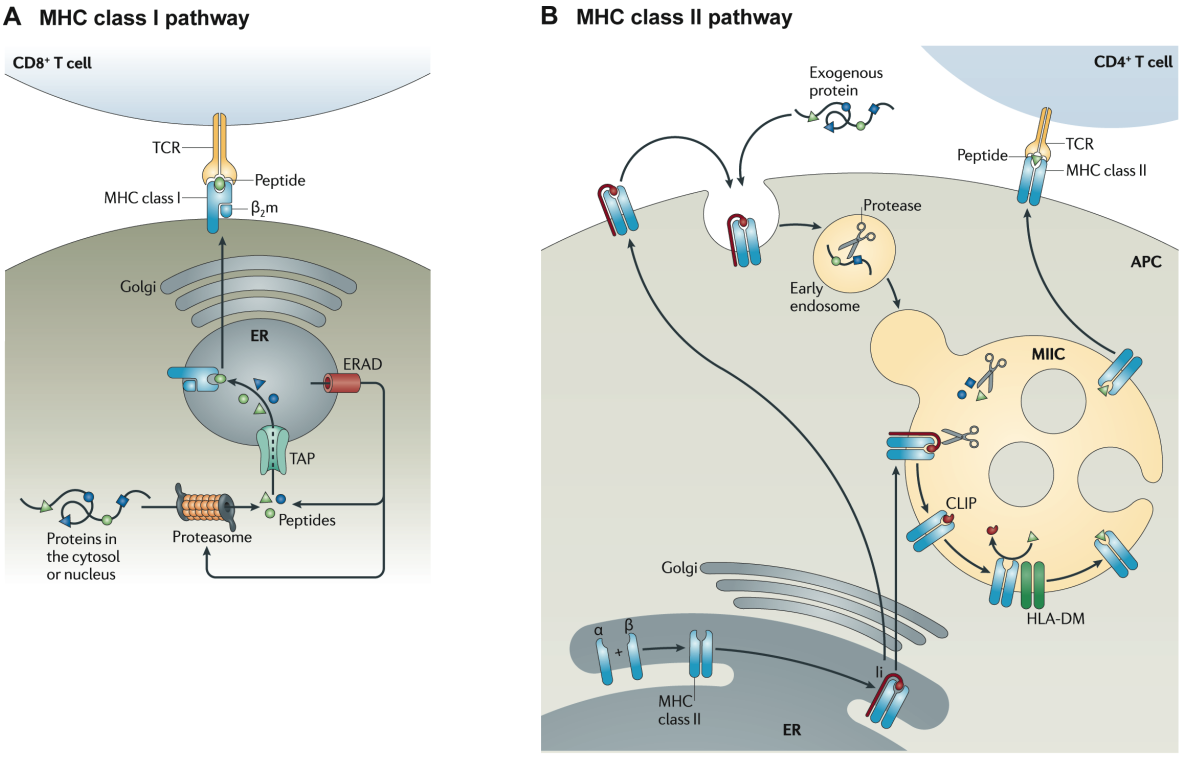

Figure 1.3: The basic principles of MHC class I and MHC class II antigen presentation. (A) MHC class I pathway: proteins in the cytosol are targeted by poly-ubiquitinylation and are proteolytically degraded within the proteasome. Degraded peptides are transported from the cytosol to the ER where the peptide:MHC class I complex is assembled. The peptide:MHC class I complex is transported to the cell surface and presented to $CD8^+$ T cells. **(B)** MHC class II pathway: extracellular proteins are taken up by APCs and are processed in endosomal and lysosomal vesicles. In the MHC class II loading compartment, processed peptides are associated with MHC class II molecules. The peptide:MHC class II complex is displayed on the cell surface and presented to $CD4^+$ T cells. Figure from (Neefjes et al., 2011).

1.3.2 MHC Class II Antigen Presentation Pathway

Extracellular antigens are taken up by APCs by phagocytosis. The emerging phagosomes, or early endosomes, fuse with lysosomal vesicles which results in the stepwise acidification of the endosome and, thereby, in the activation of proteases (Huotari and Helenius, 2011). The cysteine

proteases cathepsin S and L are the most important proteases in the degradation process of vesicular antigens (Watts, 2001). Before cargo is degraded to peptide fragments within the lysosome, the enzyme gamma-interferon inducible lysosomal thiol reductase (GILT) facilitates the unfolding of the proteins by reducing intramolecular disulfide bonds and, thus, making the endocytosed protein accessible for further enzymatic processing (Phan et al., 2000).

The transmembrane α- and β-chains of the MHC class II molecules are assembled in the ER like normal glycoproteins. The unspecific binding of peptides to the MHC class II molecule is prevented by the occupation of the binding groove by the invariant chain (Ii). An additional role of the invariant chain is to guide the transfer of the MHC class II molecule from the ER to the MHC class II loading compartment (MIIC). MIICs are late endosomal compartments where loading of the MHC class II molecule with peptide fragments is performed. On the way from the ER to the MIICs the pH within the vesicle constantly decreases. Under these conditions the invariant chain is cleaved off and only the class II-associated invariant chain peptide (CLIP) stays with the MHC class II molecule (Busch et al., 2000). Within the MIIC, the MHC class II molecule is associated with a molecule called HLA-DM (H2-M in mice), which prevents aggregation of MHC class II molecules and ensures stability of the molecule. Furthermore, HLA-DM catalyzes the removal of the CLIP fragment as well as the loading of a peptide antigen derived from a protein degraded in the endosomal pathway (Schulze and Wucherpfennig, 2012). The appropriate length of such a peptide antigen is 10 to 16 amino acids. In B cells, thymic epithelial cells and certain DC subsets, the HLA-DM molecule can be bound by a HLA-DO molecule (H2-O in mice), which modulates the activity of HLA-DM (Guce et al., 2013). Once the peptide:MHC class II complex is assembled, it is transported to the cell surface where the peptide cargo is presented to $CD4^+$ T cells. (Blum et al., 2013; Neefjes et al., 2011)

1.3.3 Cross Presentation Pathways

Cross presentation is an antigen presentation pathway in which extracellular antigens are presented on MHC class I molecules and that is most prominent in DCs. Generally, cells have the ability to capture extracellular antigen by phagocytosis. But in the context of cross-presentation, the phagosome does not enter the MHC class II antigen presentation pathway (chapter 1.3.2), but the so-called cytosolic or vacuolar pathway. If the phagosome enters the cytosolic pathway, the antigen is first exported to the cytosol. In the cytosol the antigen is degraded by proteasomal degradation and then transported into the ER or into the phagosome where the antigenic peptide fragments are loaded onto MHC class I molecules by either ER loading or phagosomal loading, respectively. Alternatively, in the vacuolar pathway, the phagosomal cargo is directly degraded in the phagosome and loaded onto MHC class I molecules for antigen presentation (Joffre et al., 2012).

On the other hand, it could also be shown that intracellular protein can be presented by MHC class II molecules. In this context, it was shown that self-antigens originated from the cell surface and the

endosomal network are presented on MHC class II molecules (Chicz et al., 1993; Hunt et al., 1992), but also molecules of cytoplasmic or nuclear origin could be detected in other studies (Dengjel et al., 2005; Dongre et al., 2001). Even though the underlying mechanism of presentation of self-antigen via MHC class II molecules is not perfectly clear, there is evidence that macroautophagy might play a role in delivering these molecules to the MHC class II loading compartment (Dörfel et al., 2005; Nimmerjahn et al., 2003; Paludan et al., 2005). The role of macroautophagy in antigen presentation will be discussed in more detail in chapter 1.3.5.

1.3.4 Presentation of Non-Protein Antigens to Subsets of T Cells

Non-protein antigens that are presented by APCs include lipids and glycolipids, small phosphorylated proteins and alkyl amines. Lipids and glycolipids are displayed by the non-classical MHC molecule CD1 (Moody and Porcelli, 2003). CD1 is an MHC class I-like molecule and is mainly expressed on cells specialized for antigen presentation. The antigen bound to CD1 molecules is recognized by natural killer T cells (NKT cells). NKT cells are a T cell subset defined by expressing markers characteristic for both natural killer (NK) cells and T lymphocytes and express αβ TCRs that have a very limited diversity.

On the other hand, some proteins, small phosphorylated proteins and alkyl amines are recognized by γδ T cells (Born et al., 2013). γδ T cells are a small population of T cells and the exact mechanism of how γδ T cells recognize ligands is still not known. There is evidence that ligand recognition does not depend on MHC presentation, but a diversity of cell surface structures were shown to be recognized by γδ T cells (Born et al., 2013).

1.3.5 Autophagic Pathways

Autophagy is a cell intrinsic process by which intracellular constituents are transported to the lysosome for degradation. The term autophagy was coined by Christian de Duve, renaming autolysis which was used by Ashford and Porter to describe vesicles that contained cellular organelles and lysosomal enzymes and connecting it to cellular catabolism (autophagy from the Greek “auto” for “self” and “phagein” meaning “to eat”) (Ashford and Porter, 1962; De Duve, 1963). Until today three types of autophagy have been described – namely, chaperone-mediated autophagy, microautophagy and macroautophagy (Figure 1.4).

Chaperone-mediated autophagy (CMA) is a highly selective form of autophagy. During CMA, proteins that show a KFERQ-like motif (KFERQ is the one-letter code for the amino acid sequence Lys-Phe-Glu-Arg-Gln) are recognized by Hsp70 chaperones (heat shock 70 kDa protein) and targeted to the lysosome. The selected protein surpasses the lysosomal membrane by help of the

lysosomal membrane-associated protein 2A (LAMP-2A) and is finally degraded in the lysosome. (Kaushik and Cuervo, 2012)

Another form of autophagy is microautophagy, which sequesters portions of the cytoplasm by the direct engulfment of the cytoplasm by the membrane of the lysosome or late endosome (mammals) or the vacuole (plants and fungi). During this process the cytosol is directly sequestered at the surface of the lysosome and no transport vesicles or adaptor proteins are involved. More specifically, small soluble substrates are engulfed by tubular invagination, whereas, during the process of selective microautophagy (e.g., micropexophagy, microautophagy of the nucleus, micromitophagy), the cargo is sequestered by arm-like protrusions. Noteworthy, non-selective microautophagy is regularly observed in mammalian cells, while the other three forms of selective microautophagy are frequently induced in yeast. Once the invagination is completed, the invaginating membrane is choked off and single membrane vesicles are released into the lysosomal lumen where the cargo is degraded. (Li et al., 2011b)

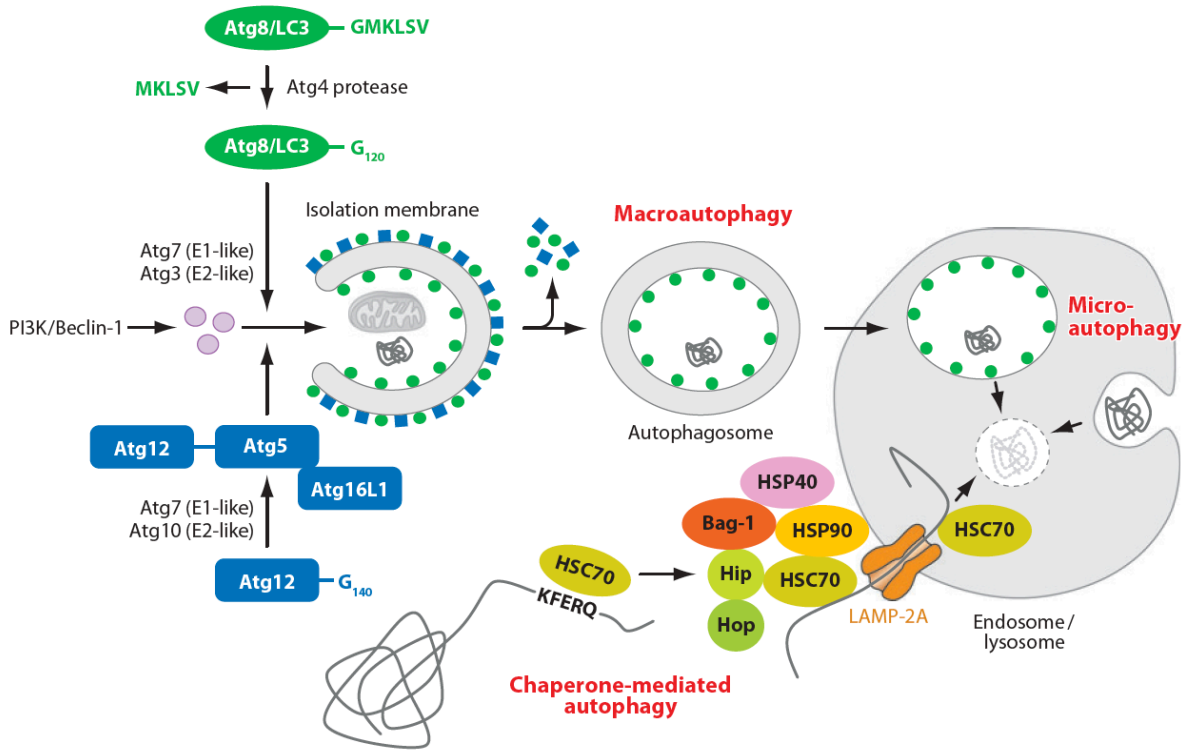

Figure 1.4: Types of autophagy and the main players in the formation of the macroautophagic isolation membrane. During macroautophagy an isolation membrane is formed around cytoplasmatic constituents. After completion of the isolation membrane, the autophagosome is formed and fuses with lysosomal vesicles for degradation of cargo. Additionally, key autophagy (Atg)-related proteins that are important in the formation of the isolation membrane are depicted. Microautophagy is a non-selective process in which the membrane of the lysosome directly engulfes cytoplasmic cargo for delivery to the lysosome. CMA is a highly selective pathway in which proteins carrying a KFERQ-like motif are recognized by Hsp70 chaperones. The targeted protein translocates into the lysosome through the LAMP-2A transporter. Figure from (Münz, 2009).

Macroautophagy is a conserved catabolic process, which is important for the maintenance of cellular homeostasis. During the process of macroautophagy, an isolation membrane sequesters a portion of the cytoplasm that contains cellular components such as organelles and pathogens as well as misfolded or long-lived proteins. The resulting vesicle is called the autophagosome. Once the autophagosome is assembled, lysosomal vesicles are recruited to the autophagosome, an autophagolysosome is formed and the cargo is degraded in the lysosome. Hereafter, macroautophagy will be referred to as autophagy and will be discussed in more detail below.

1.3.6 Autophagy

Nowadays, it is known that autophagy is involved in many different physiological processes, such as: generation of amino acids during starvation, clearing of redundant or nonfunctional proteins, regulation of availability of certain substrates, mammalian development as well as degradation of pathogens and antigen presentation. (Cecconi and Levine, 2008; Deretic and Levine, 2009; Levine and Kroemer, 2008; Menzies et al., 2011; Milo and Kahana, 2010; Mizushima and Levine, 2010; Mizushima et al., 2008; Virgin and Levine, 2009; White et al., 2010; Wong and Cuervo, 2010).

1.3.6.1 Regulation of Autophagy

Under steady state conditions, autophagy works at low levels, but it can be induced by various triggers, such as deprivation of nutrients, hormones, and energy (He and Klionsky, 2009). The key player in the regulation of autophagy is the mammalian target of rapamycin (mTOR), which is a central serine/threonine protein kinase of the nutrient-sensing pathway (Jung et al., 2010). Rapamycin can induce autophagy by inhibiting mTOR. Generally, the activity of mTOR is regulated by a diversity of signals such as growth factors, amino acids, glucose and energy status of the cell (Kim et al., 2002).

In addition to mTOR, other processes can also influence the level of autophagy. For example, anti-apoptotic proteins from the B cell lymphoma 2 (BCL-2) family inhibit autophagy (Pattingre et al., 2005), whereas, withdrawal of growth factors leads to the upregulation of autophagy to ensure maintenance of cellular functions (Lum et al., 2005). Autophagy is also upregulated in response to cellular stress such as hypoxia (Mazure and Pouysségur, 2010), oxidative stress (Lee et al., 2012), or ER stress (Deegan et al., 2013). Latter describes conditions that interfere with the proper function of the ER, such as accumulation of unfolded protein aggregates or excessive protein traffic. Autophagy also plays an important role in the removal of invading pathogens and the recognition of potential pathogens depends on the detection of PAMPs by PRRs such as Toll-like receptors (TLRs). For example, viral ssRNA (single-stranded RNA) induces autophagy via TLR7 (Delgado et al., 2008), whereas zymosan, a yeast-derived glucan, activates TLR2 and bacterial lipopolysaccharide (LPS) induces autophagy by binding to TLR4 (Xu et al., 2007a).

1.3.6.2 Assembly of the Autophagosome

Once autophagy is induced, an isolation membrane (also called phagophore) is formed (Figure 1.5). In total more than 30 autophagy-related proteins (Atg, from AuTophaGy) have been described to be involved in the formation of the autophagsosome (Mizushima and Komatsu, 2011).

The first step in the generation of the isolation membrane is the assembly of the ULK1 (uncoordinated (UNC)-51-like kinase 1) complex at the autophagosome formation site on the membrane of, for example, the ER, which is also known as phagophore assembly site or pre-autophagosomal structure (PAS) (Xie and Klionsky, 2007). The mammalian ULK1 complex comprises of the proteins ULK1, Atg13, FIP200 (focal adhesion kinase (FAK) family interacting protein of 200 kDa) and Atg101 (Itakura and Mizushima, 2010). Once this first initiation complex is assembled, the ULK1 complex induces the assembly of a second initiation complex, namely the class III PI3K (Phosphatidylinositide 3-kinase) complex. The latter constitutes of the Vps34 (vacuolar protein sorting protein 34), Vps15, Beclin1 (B cell lymphoma-2 (Bcl-2) interacting coiled-coil protein; also know as Atg6), Atg14(L) and AMBRA1 (activating molecule in Beclin-1-regulated autophagy protein 1) and is responsible for the production of phosphatidylinositol-3-phosphate (PI3P) on the membrane. PI3P binds to double FYVE-containing protein 1 (DFCP1) and both initiate the formation of the omegasome (Axe et al., 2008). The omegasome is a cup-shaped protrusion of the ER that serves as starting point for the generation of the autophagosome. In addition to PI3P and DFCP1 also Atg9, WIPIs (WD-repeat protein interacting with phosphoinositides) and VMP1 (vacuole membrane protein 1) can be found at this initiation point (Mizushima and Komatsu, 2011).

For the elongation, maturation and closure of the isolation membrane further steps are necessary and utilize two ubiquitin-like conjugation systems. The first conjugation system in action is the Atg12 conjugation system. To form this protein complex the E1-like enzyme Atg7 and the E2-like enzyme Atg10, which are an ubiqutin-activating enzyme and ubiqutin-conjugating enzyme, respectively, are necessary (Mizushima et al., 1998). Atg7 and Atg10 are responsible for the coupling of Atg12 to Atg5 (Mizushima et al., 1998) and, in a next step, Atg16L1 is also recruited to build the Atg5-Atg12/Atg16L1 complex. The Atg5-Atg12/Atg16L1 complex is one of the two complexes required for the conjugation of Atg8/LC3 (microtubule-associated protein 1A/1B-light chain 3) to phosphatidylethanloamine (PE) to the isolation membrane (Fujita et al., 2008; Hanada et al., 2007). The second conjugation system is called Atg8/LC3 conjugation system and consists of LC3, Atg4, Atg7 and Atg3. Atg4 is a cysteine protease that cleaves off the five C-terminal amino acids (MKLSV) of LC3 and makes its glycine residue accessible. In a next step, LC3 is activated by the E1-like enzyme Atg7 and conjugated by the E2-like enzyme Atg3 to PE on the outer and inner membrane of the isolation membrane (Ichimura et al., 2000). LC3 is responsible for the fusion of membrane vesicles that are of importance during the formation, elongation and closure of the isolation membrane (Nakatogawa et al., 2007; Xie et al., 2008). Furthermore, LC3 was described as

a receptor or an adaptor protein that is responsible for selective cargo incorporation into the autophagosome (Noda et al., 2010). The isolation membrane elongates and, finally, results in a double-membrane organelle that is called autophagosome. After the autophagosome is completed, LC3 bound to the outer membrane of the autophagosome is released by cleavage by the deconjugation enzyme Atg4 (Kirisako et al., 2000). On the other hand, LC3 bound to the inner membrane stays attached to it and is degraded together with the autophagosome once it reaches the lysosome.

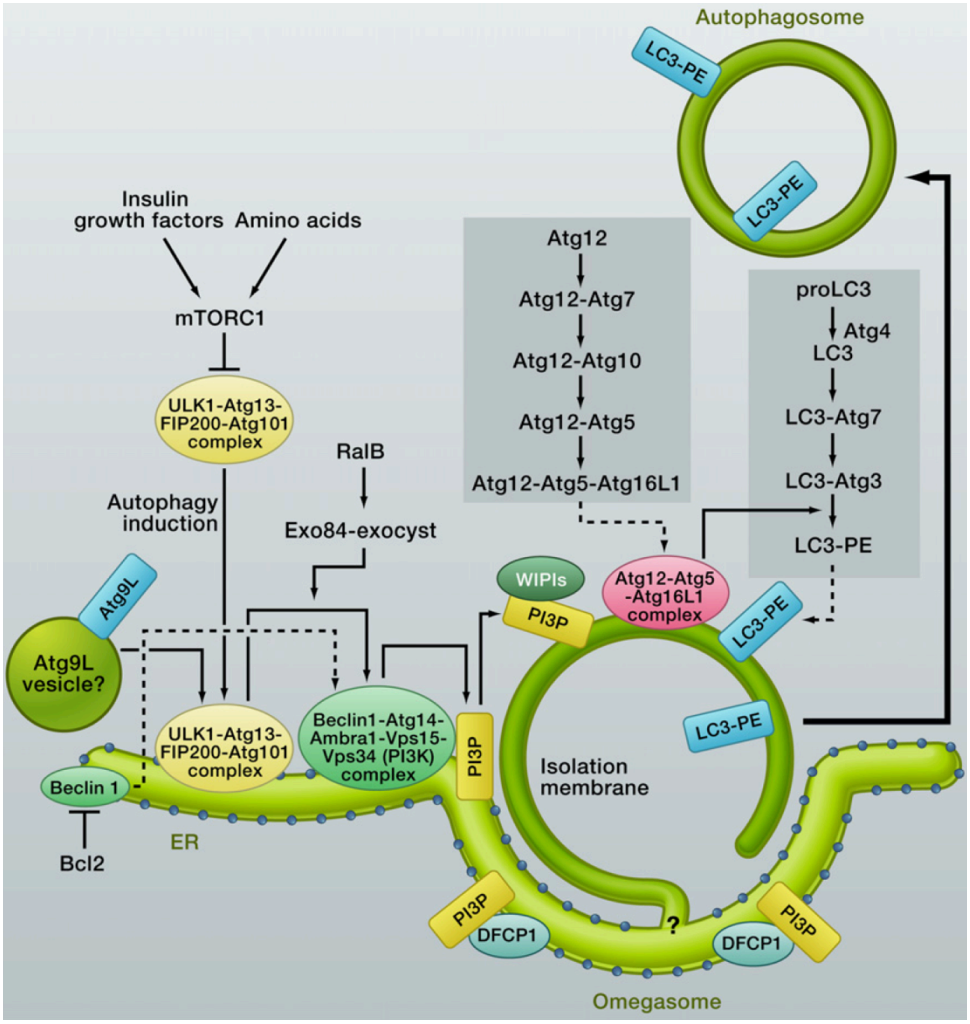

Figure 1.5: Formation of the autophagosome. Upon inhibition of mTORC1, autophagy is induced and the ULK1 complex is assembled and translocated to the ER membrane. The ULK1 complex initiates the assembly of the class III PI3K complex that produces PI3P and attaches it to the membrane. PI3P recruits DFCP1 and the formation of the omegasome is induced. The Atg5-Atg12/Atg16L1 complex plays an important role in the conjugation of Atg8/LC3 to PE and assists in the elongation and closure of the isolation membrane. Figure from (Mizushima and Komatsu, 2011).

The membrane source for the formation of the isolation membrane is still not clearly determined. Some of the potential membrane sources are believed to be organelles such as the ER, Golgi complex, mitochondria or endosomes, but also *de novo* synthesis of the membrane seems reasonable. And even the plasma membrane or nuclear membrane are considered potential starting

points of membrane supply (Tooze and Yoshimori, 2010).

Classically, autophagy was thought to be important for the degradation of unnecessary proteins and random uptake of cytosolic constituents. Meanwhile it was shown that autophagosomes also specifically bind to cargo by the assistance of adaptor proteins such as p62/SQSTM1 (sequestosome 1), NBR1 (neighbor of BRCA1 gene 1), NDP52, optineurin and TAX1BP1. These cargo receptors are responsible for the degradation of ubiquitinated substrates (Johansen and Lamark, 2011; Kraft et al., 2010). Additionally, it could be demonstrated that autophagy is involved in the selective degradation of organelles such as mitochondria (mitophagy) (Kim et al., 2007), peroxisomes (pexophagy) (Dunn et al., 2005), ribosomes (ribophagy) (Kraft et al., 2008), ER (reticulophagy) (Bernales et al., 2006) and intracellular microbes (xenophagy) (Klionsky et al., 2007).

1.3.6.3 LC3-Associated Phagocytosis

LC3-associated phagocytosis (LAP) is a newly characterized process that combines features from both phagocytosis and autophagy and was first described by Sanjuan *et al.* in 2007. In this study it was shown that a pathogen or particle that engages TLRs on murine macrophages induces phagocytosis and the recruitment of elements of the autophagic pathway. Beads that were coated with LPS (TLR4 agonist) and pathogen-derived surface molecules such as zymosan (TLR2 agonist) co-localized with LC3 on the phagosomal membrane which indicates that LAP is induced when a receptor-mediated signaling pathway is engaged (Sanjuan et al., 2007). LAP can be distinguished from canonical autophagy with regard to the following characteristics (Figure 1.6): LAP goes back to a single-membrane phagosome that can be detected by transmission electron microscopy (TEM), LAP causes a more rapid maturation of the phagosome and is independent of the ULK1 pre-initiation complex. On the other hand, LAP and autophagy show similar characteristics in terms of class III PI3K activity, LC3 recruitment and the requirement of Beclin1, Atg5 and Atg7 (Sanjuan et al., 2009).

Additionally, LAP was shown to be triggered by apoptotic cell bodies that display phosphatidylserine (PtdSer) on their surface by which they engage the T cell immunoglobulin mucin-4 (TIM4) receptor on the phagocytic cell (Martinez et al., 2011). DNA-antibody immune complexes that bind to Fc receptors (FcR) are also able to induce LAP (Henault et al., 2012) and entotic bodies are able to trigger the recruitment of LC3 in an endothelial cell line. But, in the latter case, it still needs to be determined how the engulfment of non-pathogens in the absence of “eat me” signals can promote LC3 targeting (Florey et al., 2011).

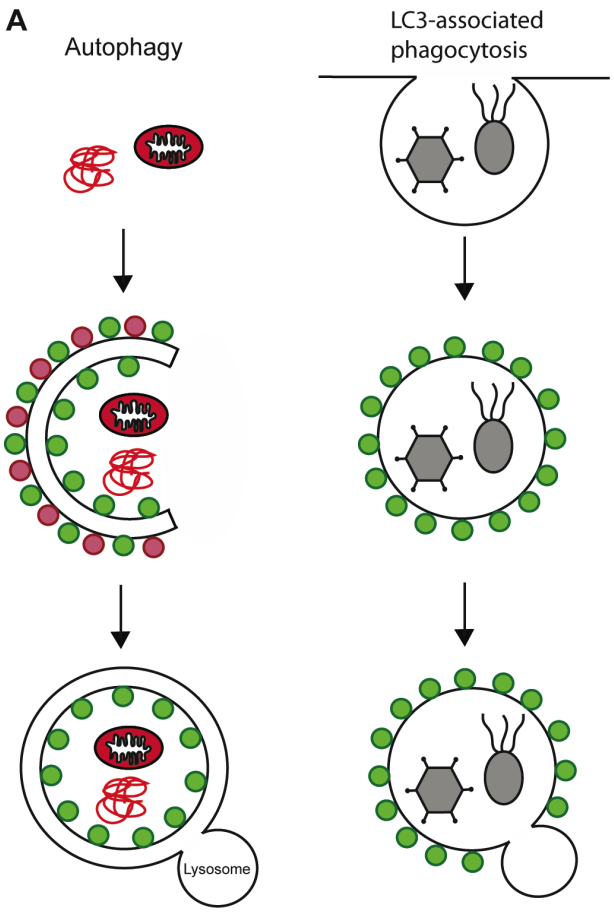

B

	Autophagy	LAP
double membrane	+	-
Beclin-1	+	+
LC3 recruitment	+	+
Atg5 and Atg7	+	+
class III PI3K activity	+	+
ULK1 and FIP200	+	-
more rapid maturation of phagosome	-	+

Figure 1.6: Comparison of autophagy and LAP. (A) Graphical comparison of autophagy and LAP. Autophagic isolation membrane engulfes mitochondrium and protein aggregate, whereas virus and bacterium are engulfed by phagocytosis. Red circles: Atg5-Atg12/Atg16L1 complex, green circles: LC3. Figure adopted from (Randow and Münz, 2012) **(B)** Comparison of hallmark proteins involved in either autophagy or LAP. Data are based on results from (Florey et al., 2011; Martinez et al., 2011; Sanjuan and Green, 2008).

Amongst these well-defined LAP processes, there are additional studies that describe processes that could be related to LAP, but are not clearly defined as LAP. One of these potential cellular signals are peptidoglycans that bind to NOD-like receptors such as NOD1 and NOD2. In this study it could be shown that LC3 and Atg16L are located at the site of the plasma membrane where the bacterium *Shigella flexneri* was engulfed (Travassos et al., 2010). Furthermore, beads coated with human immunoglobulin G (IgG) were taken up by RAW 264.7 cells, a murine macrophage-derived cell line by FcR-mediated endocytosis and induced the recruitment of LC3 to phasosomes (Huang et al., 2009). In another study, the autophagy-related proteins Vps34, Vps15 and Beclin1 were recruited to phagosomes containing beads that were coated with *Escherichia coli* (*E. coli*) outer membrane extract. Based on the fact that the class III PI3K complex (Vps34 Vps15 Beclin1 complex) is essential for the formation of the autophagosome, a potential association between the uptake of *E. coli* extract and LAP was suggested (Berger et al., 2010).

1.3.6.4 Role of Autophagy in Antigen Presentation, Immunity and Autoimmunity

Autophagy is known as an „auto-digestive“ process that engulfes intracellular components by an autophagosome which transports the cargo to the lysosome for degradation and recycling. Additionally, MHC class II molecules were thought to function solely for the presentation of exogenous and foreign peptide antigens. But it could actually be shown that MHC class II molecules are able to present intracellular antigen (Chicz et al., 1993) and that endogenous viral antigens are presented to $CD4^+$ T cells through an intracellular route using the example of measles and influenza antigens (Guéguen and Long, 1996). In subsequent years, the involvement of autophagy in the presentation of cytosolic model peptides by MHC class II molecules could be shown (Dörfel et al., 2005; Nimmerjahn et al., 2003; Paludan et al., 2005). It was demonstrated that autophagosomes constitutively form in MHC class II-positive cells - including DCs, B cells and epithelial cells. In these cells, autophagosomes continuously fused with multivesicular MIICs and targeting of antigen to autophagosomes via fusion to the autophagosome-associated protein Atg8/LC3 led to strongly enhanced MHC class II presentation to $CD4^+$ T cells (Schmid et al., 2007). These data showed that macroautophagy constitutively and efficiently delivers cytosolic proteins for MHC class II presentation. Not just intracellular self-antigens are targeted to MHC class II presentation, but also bacterial and viral antigens that are present in the cytoplasma can be presented on MHC class II molecules (Nimmerjahn et al., 2003; Paludan et al., 2005). In this context, it was hypothesized that the presentation of intracellular pathogenic antigen might be beneficial for the induction of Th cell functions.

The presentation of self-peptide on MHC class II molecules by the assistance of autophagy plays also an important role in the selection process of thymic $CD4^+$ T cells. In this regard, thymic epithelial cells deliver self-peptides via autophagy to MHC class II molecules for positive and negative selection in the thymus (Nedjic et al., 2008). Supporting these data, it was shown that autophagosomes fuse with MIICs in theses thymic epithelial cells (Kasai et al., 2009). Notably, inflammatory stimuli such as pro-inflammatory cytokines and TLR agonists upregulate macroautophagy in APCs suggesting that macroautophagy-mediated antigen processing could particularly enhance immune responses within inflamed tissues (Münz, 2009).

Autophagy has also been linked to the development of autoimmunity (Bhattacharya and Eissa, 2013). One of the autoimmune diseases associated with a deficiency in autophagy is SLE. Genome-wide associations studies have shown that single-nucleotide polymorphisms (SNPs) in the gene encoding the Atg5 protein can be related to SLE susceptibility (Pierdominici et al., 2012). Additionally, activation of mTOR was shown in SLE patients which further suggests an association between SLE and the autophagy machinery (Pierdominici et al., 2012). In the context of autophagy-deficiency, it was discussed that one of the potential causes of SLE might be the defective clearance of apoptotic cell corpses which might lead to the breakdown of self-tolerance, the activation of autoreactive lymphocytes and, finally, to the development of SLE (Gaipl et al., 2006).

Furthermore, autophagy was linked to the development of Crohn's disease (CD) by means of genome-wide association studies in which non-synonymous single nucleotide polymorphisms (SNP) in the autophagy gene ATG16L1 were associated with the susceptibility to this disease. And it was discussed that autophagy might lead to an altered immune response to commensal gut bacteria or an insufficient induction of tolerance (Prescott et al., 2007; Rioux et al., 2007).
A role of autophagy was also considered for the etiology of MS since an elevated expression of Atg5 was detected in blood samples of EAE mice (Alirezaei et al., 2009). It is assumed that Atg5 and IRGM (immunity-related GTPase) might positively effect the survival of mature effector $CD4^+$ T cells which might contribute to EAE and/or MS development (Xu et al., 2010).

1.3.6.5 DCs – The Model APC

DCs are professional APCs and are, thus, most efficient in the activation of naïve T cells and the initiation of T cell responses. DCs were first described by Ralph M. Steinman and Zanvil A. Cohn who termed this cell subset „dendritic cell" because of their tree-like morphology at certain development stages (dendrite = δένδρον or déndron being Greek for "tree") (Steinman and Cohn, 1973). Meanwhile, it is well known that theses cells are the major players in regulating the adaptive immune response.
DCs derive from the bone-marrow and can arise from lymphoid as well as myeloid precursor cells. Their precursors migrate from the bone-marrow through the blood to lymphoid organs or to peripheral non-lymphoid organs. They are mainly present in all tissues that are in contact with the external environment - such as epithelium of the skin, inner lining of the respiratory tract, and interstitium of most parenchymal organs. Based on their diverse origin cell-specific surface markers, location and immunological functions, three main DC subsets can be distinguished: plasmacytoid DCs, conventional DCs and inflammatory DCs. (Satpathy et al., 2012)
Plasmacytoid DCs (pDCs) show a round and spheric phenotype and need further development in order to acquire the dendritic morphology and complete DC function. After stimulating the pDCs with microbial or viral antigen, pDCs produce high amounts of type 1 interferon (IFN) and, based on this, are also known as „natural interferon-producing cell". After activation, they also form dendritic-like protrusions and gain typical DC-like antigen processing and presentation functions. (Liu, 2005)
Conventional DCs (cDC) are fully differentiated cells and show a dendritic morphology and fully-operational DC functions under steady state conditions. When they are newly differentiated, they show high endocytic activity and low surface expression of MHC class I and II molecules. After stimulation of cDCs, the cytoplasm is reorganized and MHC class I and II molecules as well as co-stimulatory molecules are upregulated. cDCs can be further subdivided into migratory DCs and lymphoid tissue-resident DCs. Migratory DCs are the classical textbook DCs which have a high capacity of antigen sampling. They migrate through the lymphatic system to the lymph node where

they can activate T cells. Examples for migratory cDCs are Langerhans cells in the epidermis, dermal DCs located in the dermis or interstitial DCs from the lamina propria of the mucosa. On the other hand, lymphoid tissue-resident DCs are stationary in the lymphoid organs and do not migrate within the lymphatics, but they do collect and present antigen in lymphoid organs themselves. In the mouse system $CD8^+$ and $CD8^-$ cDCs can be further distinguished.

A third major DC subset are the inflammatory DCs that cannot be found under steady state conditions. These cells first arise after infection or inflammation and can develop into TipDCs (tumour-necrosis factor (TNF) / inducible nitric oxide synthase (iNOS)-producing DCs) that produce high amounts of TNF and iNOS (Segura and Amigorena, 2013).

1.4 Working Hypothesis

The emergence, activation and expansion of autoreactive $CD4^+$ T cells are considered crucial events in the development and progression of MS and EAE. Generally, CD4 T^+ cells are activated by APCs such as DCs and macrophages. The classical way of processing and presenting antigen to $CD4^+$ T cells is the MHC class II pathway. But recent studies have identified autophagy as an alternative pathway that shuttles intracellular antigens into MIIC for recognition by $CD4^+$ T cells. Furthermore, constitutive autophagosome formation in MHC class II-positive cells, including DCs, B cells and epithelial cells was demonstrated. In these cells, autophagosomes continuously fused with MHC class II-loading compartments and targeting of antigen to autophagosomes strongly enhanced MHC class II presentation to $CD4^+$ T cells. Additionally, other studies have shown the involvement of the autophagic machinery in processing of even extracellular material. It could be shown in two independent studies that autophagy-related proteins are either recruited to latex beads coated with TLR-ligands or to phagocytosed apoptotic cells that promote the processing of this material. But so far it has not been shown if extracellular self-antigen could be processed by involvement of the autophagic machinery. But unpublished data from our laboratory have shown that the formation of $LC3^+$ vesicles is markedly induced in CNS-resident APCs, namely activated microglia, during autoimmune CNS inflammation in MOG-induced EAE.

Thus, we hypothesized that an autophagic machinery-dependent presentation of autoantigens by DCs facilitates the activation of autoreactive $CD4^+$ T cells within the CNS. To address this question we used conditional gene targeting in mice to investigate whether autophagy in DCs influences the development and/or progression of EAE. Furthermore, the antigen-presenting capabilities of mouse APCs of the self-protein MOG were investigated.

2 Material and Methods

2.1 Materials

2.1.1 Chemicals and Reagents

Chemicals and molecular biology reagents were mainly obtained from the companies Sigma-Aldrich™, Fisher Scientific, Becton Dickinson Biosciences, Invitrogen™ and Fermentas unless otherwise mentioned.

2.1.2 Plastic Supplies

Plastic supplies such as multiwell plates, disposable plastic pipettes and plastic reaction tubes were obtained from Becton Dickinson Labware (FALCON®), VWR International®, Costar® and NuncTM.

2.1.3 Bacterial Strains

For the amplification of the plasmid pET-22b(+) ($rmMOG_{1-124}$) chemocompetent Top 10 bacteria and for the overexpression of rmMOG protein, chemocompetent BL21 cells were used that were originally purchased from Invitrogen.

2.1.4 MOG_{35-55} Peptide and $rmMOG_{1-124}$ Protein

The MOG_{35-55} peptide (MOG peptide) was purchased from GenScript, dissolved in PBS at a final concentration of 5 mg/ml, filter-sterilized (0.22 µm) and stored at -80°C. The plasmid pET-22b(+) ($rmMOG_{1-124}$) was kindly provided by Burkhard Becher, University of Zurich, Switzerland and originates from Steve Anderton, University of Edinburgh, GB. $RmMOG_{1-124}$ protein (MOG protein) was expressed and purified as described in chapter 2.2.11.

2.1.5 Buffers and Solutions

2.1.5.1 Commercial Reagents and Kits

Reagent / Kit	Company	Catalog number
ACK Lysing Buffer	Invitrogen	A10492-01
Agarose, LE, analytical grade	Promega	V3125
β-mercaptoethanol	Gibco	31350-010
BCA Protein Assay Kit	Thermo Scientific	23225
BD Cytofix/Cytoperm™ Fixation/ Permeabilization Solution Kit with BD GolgiStop™	BD Biosciences	554715
BD GolgiStop™ (Monensin)	BD Biosciences	554715
BSA, 30%	Sigma	A9576-50ml
CFSE	eBioscience	65-0850-84
Collagenase D	Roche	11088866001
cOmplete Protease Inhibitor Cocktail Tablets	Roche	11873580001
DAPI	Invitrogen	D3571
DMSO	Sigma	D2650
DNA loading dye, 6×	Fermentas	R0611
DNase	Roche	2600105
dNTPs, 10 mM	Qiagen	124108743
ECL Western Blotting Substrate	Thermo Scientific	32106
FIREPol, 5× master mix, 7.5 mM	LucernaChem	04-12-0015
Foxp3 Staining Buffer Set	eBioscience	00-5523
GelRed^{TM} Nucleic Acid Gel Stain, 10000×	Biotium	41003
GeneRuler 100 bp DNA Ladder	Fermentas	SM0243
Ionomycin	Sigma	I3909
LB broth base	Invitrogen	12780-029-2.5 kg
L-Glutamine 200 mM 100×	Gibco	25030
LIVE/DEAD® Fixable Aqua Dead Cell Stain Kit	Invitrogen	L34957
LIVE/DEAD® Fixable Near-IR Dead Cell Stain Kit	Invitrogen	L10119
Normal goat serum	Sigma	G9023
PCR reaction buffer with Mg^{2+}	Roche	1127138001
Penicillin-streptomycin, liquid	Invitrogen	15070-063
Percoll	GE Healthcare	17-0891-01
Pertussis toxin islet activating protein	LuBioscience	180

PMA	Sigma	P1585
ProLong® Gold Antifade Reagent	Invitrogen	P36934
Proteinase K	Roche	3115879001
ReBlot Plus Strong Antibody Stripping Solution, 10x	Millipore	2504
Saponin	Fluka	84510
SDS solution	Fluka	5030 – 500 ml
Taq DNA Polymerase	Roche	11435094001
TaKaRa LA Taq with Mg^{2+} plus buffer	Axonlab	RR002M
Triton™-X100	Sigma	T8532
Triton™-X114	Sigma	X114-100 ml
Trypan blue	Gibco	15250-061
Trypsin-EDTA 0.25%	Gibco	25200-072
Tween® 20	Sigma	P5927

2.1.5.2 General Use Buffers

Biopsies lysing buffer	100 mM Tris, pH8.0
	100 mM NaCl
	10 mM EDTA, pH8.0
	0.2% SDS
	0.2 mg/ml proteinase K (added freshly each time)
Cell lysing buffer,	1% NP-40
for Western blot analysis	1x protease inhibitor cocktail (thawed on ice)
	In PBS
Digest buffer, spleen	0.4 mg/ml collagenase D
	20 µg/ml DNase
	In PBS
	Freshly prepared each time
Digest buffer, CNS	0.2 mg/ml collagenase D
	20 µg/ml DNAse
	In PBS
	Freshly prepared each time

FACS buffer	2% FCS 0.01% NaN_3 In PBS Stored at 4°C
Laemmli buffer	60 mM Tris-Cl, pH6.8 2% SDS 10% glycerol 5% β-mercaptoethanol 0.01% bromophenol blue
MACS buffer	1% FCS 2 mM EDTA In PBS Filter-sterilized with 0.22 μm filter device Stored at 4°C
PBS, pH7.4, 10×	1.37 M NaCl 26.8 mM KCl 16.2 mM $Na_2HPO_4*7H_20$ 14.7 mM KH_2PO_4
Paraformaldehyde, 4%	Kantonsapotheke
PTx diluent	0.015 M Tris 0.5 M NaCl 0.017% Triton X-100 Filter-sterilized with 0.22 μm filter device Stored at 4°C
TBE, 5×	44.5 mM Trizma base, pH8.5 44.5 mM Boric acid 2 mM EDTA

2.1.5.3 Cell Culture Medium

BM-DC medium	RPMI 1640 10% heat inactivated FCS 1x penicillin-streptomycin 1x L-glutamine 50 μM β-mercaptoethanol X-63-GM-CSF cell line supernatant (1 part into 10 parts) Filter-sterilized with 0.22 μm filter device
DMEM cell culture medium	DMEM medium 10% heat inactivated FCS 1x penicillin-streptomycin
Freezing medium	10% DMSO In FCS
Medium for primary cells	RPMI 1640 medium 10% heat inactivated FCS 1x penicillin-streptomycin 1x L-glutamine 50 μM β-mercaptoethanol
RPMI cell culture medium	RPMI 1640 medium 10% heat inactivated FCS 1x penicillin-streptomycin

2.1.5.4 Buffers for Immunofluorescence Microscopy

Blocking buffer	10% normal goat serum 1% BSA In PBS
Dilution buffer	10% normal goat serum 1% BSA 0.1% saponin In PBS

Fixation buffer	3% PFA In PBS
Permeabilization buffer	0.1% Triton X-100 In PBS
Washing buffer	0.01% Saponin In PBS

2.1.5.5 Buffers for Purification of MOG Protein

Volumes in brackets indicate approximate amount needed for each purification procedure.

Arginine buffer (250 ml)	50 mM NaH_2PO_4, pH8.0 2 M L-Arginine 300 mM NaCl 50 mM red. glutathione
Dialysis buffer A (2 l)	50 mM NaH_2PO_4, pH8.0 300 mM L-Arginine 300 mM NaCl
Dialysis buffer B (6 l)	50 mM NaH_2PO_4 H, pH8.0 300 mM NaCl
Dialysis buffer C (1× PBS) (10 l)	10 mM Na_2HPO_4, pH7.4 137 mM NaCl 2.7 mM KCl 1.7 mM KH_2PO_4
Elution buffer (50 ml)	250 mM Imidazole In solubilization buffer
Endotoxin-removal buffer (350 ml)	0.1% Triton X-114 In solubilization buffer pH was not adjusted

Lysis buffer (50 ml)	50 mM Tris, pH8.0 300 mM NaCl 25 µg/ml DNAse 1× Roche cOmplete Protease Inhibitor Cocktail Tablet
Solubilization and running buffer (100 ml)	50 mM NaH_2PO_4 , pH8.0 6 M GuHCl 300 mM NaCl 20 mM Imidazole 50 mM β-mercaptoethanol

2.1.5.6 Buffers for Western Blot Analysis

PBS-T buffer	0.1% Tween® 20 In PBS
Running buffer, 10× (1 l)	30.3 g Tris base 144 g Glycine 10 g SDS (Add SDS after pH adjustment) adjust pH to 8.3 (with HCl)
1.5 M Tris pH8.8 (150 ml)	27.23 g Tris base add dH_2O until ~80 ml adjust pH to 8.8 with 6N HCl
1.5 M Tris pH6.8 (100 ml)	18.17 g Tris base Add dH_2O until ~60 ml and adjust pH to 6.8 with 6N HCl
20% SDS solution	Purchased from Fluka (Sigma)
Transfer buffer, 1× 20% methanol	25 mM Tris base 192 mM glycine 20% methanol
Destaining buffer	400 ml H_2O 400 ml methanol 80 ml acetic acid

Coomassie Staining	200 ml methanol
	200 ml H_2O
	40 ml acetic acid
	1 spoontip of Coomassie brilliant blue R250

2.1.6 General Use Material

Material	Company	Catalog Number
Amicon Ultra-15 Centrifugal Filter Units	Millipore	UFC900324
CD4 (L3T4) MicroBeads, mouse	Mylteni	130-049-201
CD11c MicroBeads, mouse	Mylteni	130-052-001
Cell culture slide	SPL	30108
Cell freezing container	Nalgene	-
ECL films	GE Healthcare/VWR	28-9068-37
Ni-NTA Superflow	Qiagen	30410
Polymer microspheres 3.87 µm	Bangs laboratories	PS05N/6749
PureYield™ Plasmid Miniprep System	Promega (HELIX)	A1223
PVDF membrane	GE Healthcare	RPN303F
Spectra/Por 3 Dialysis Tubing, 3.5K MWCO	VWR	734-0686
QIAprep Spin Miniprep Kit	Qiagen	27104
Whatman blotting papers 3 mm CHR	VWR international	588-3186

2.1.7 Cytokines

Material	Company	Catalog Number
GM-CSF	Self-made (chapter 2.2.8.5)	-
Mouse IL-23 recombinant protein	eBioscience	14-8231

2.1.8 PCR Primers

Primer	Target	Sequence (5'-3')
CS003	$Atg5^{flox/flox}$	GAATATGAAGGCACACCCCTGAAATG
CS004	$Atg5^{flox/flox}$	GTACTGCATAATGGTTTAACTCTTGC
CS005	$Atg5^{flox/flox}$	ACAACGTCGAGCACAGCTGCGCAAGG
CS006	$Atg5^{flox/flox}$	CAGGGAATGGTGTCTCCCAC
CS007	CD11c-Cre-GFP	GCGGTCTGGCAGTAAAAACTATC
CS008	CD11c-Cre-GFP	GTGAAACAGCATTGCTGTCACTT

CS009	CD11c-Cre-GFP (positive control 1)	CTAGGCCACAGAATTGAAAGATCT
CS010	CD11c-Cre-GFP (positive control 2)	GTAGGTGGAAATTCTAGCATCATCC
CS011	B6-GFP-LC3	ATAACTTGCTGGCCTTTCCACT
CS012	B6-GFP-LC3	CGGGCCATTTACCGTAAGTTAT
CS013	B6-GFP-LC3	GCAGCTCATTGCTGTTCCTCAA
CS014	$Atg7^{flox/flox}$	TGGCTGCTACTTCTGCAATGATGT
CS015	$Atg7^{flox/flox}$	CAGGACAGAGACCCATCAGCTCCAC
CS016	$Atg7^{flox/flox}$	TTAGCACAGGGAACAGCGCTCATGG

2.1.9 Antibodies

2.1.9.1 FACS Antibodies

2D2 genotyping

Antigen	Fluorochrome	Clone	Dilution	Company
CD4	APC	GK1.5	1:1000	BioLegend
CD8	PE-Cy7	53-6.7	1:800	BD
TCR Vb11	PE	RR3-15	1:400	BD

BM-DC time course

Antigen	Fluorochrome	Clone	Dilution	Company
CD11c	PE	HL3	1:200	BD
$H2\text{-}A^b$	Pacific Blue	M5/114.15.2	1:800	BioLegend
$H\text{-}2D^b$	APC	KH95	1:200	BioLegend

Cre leakage

Antigen	Fluorochrome	Clone	Dilution	Company
CD4	APC	GK1.5	1:1000	BioLegend
CD8	PE-Cy7	53-6.7	1:800	BD
CD11b	APC-Cy7	M1/70	1:400	BD

DC:T cell co-culture

Antigen	Fluorochrome	Clone	Dilution	Company
CD4	Pacific Blue	RM4-5	1:1000	BioLegend

DC subset analysis

Antigen	Fluorochrome	Clone	Dilution	Company
CD8a	Brilliant violett 570	53-6.7	1:200	BioLegend
CD11b	APC-Cy7	M1/70	1:400	BD
CD11c	PE-Cy7	N418	1:400	eBioscience
CD45.2	Pacific Blue	104	1:800	BioLegend
CD86	Alexa Fluor® 700	PO3	1:200	BioLegend
F4/80	APC	BM8	1:200	BioLegend
H2-A^b	Biotinylated	AF6-120.1	1:800	BD
Ly6c	PercCP-Cy5.5	HK1.4	1:200	BioLegend
Siglec-H	PE	eBio440c	1:800	eBioscience
Streptavidin	Qdot800	-	1:800	Invitrogen

ICS

Antigen	Fluorochrome	Clone	Dilution	Company
CD4	APC-Cy7	GK1.5	1:500	BioLegend
CD8	PerCP-Cy5.5	53-6.7	1:500	BD
CD11b	APC-Cy7	M1/70	1:400	BD
CD45	Pacific Blue	30-F11	1:800	BioLegend
IFN-γ	PE-Cy7	XMG1.2	1:250	BioLegend
GM-CSF	PE	MP1-22E9	1:250	BD
IL-17A	Alexa Fluor® 647	TC11-18H10.f	1:200	eBioscience

Treg analysis

Antigen	Fluorochrome	Clone	Dilution	Company
CD4	Pacific Blue	RM4-5	1:800	BioLegend
CD25	APC	PC61	1:500	BD
CD45	APC-Cy7	30-F11	1:400	BD
FoxP3	PE	FJK-16s	1:100	eBioscience

2.1.9.2 Anti CD3 and CD28 Antibodies (Co-Culture)

Antigen	Clone	Final Concentration	Company
CD3	145-2C11	5 µg/ml	BD
CD28	37.51	5 µg/ml	BD

2.1.9.3 Antibodies for Immunofluorescence Cytochemistry

All antibodies used for immunofluorescence cytochemistry were diluted in dilution buffer as indicated in the table below. The diluted antibodies were spun for five minutes at 13000 rpm to remove precipitated antibodies.

Antibody	Company	Catalog number	Dilution
1° Antibody Rabbit anti-LC3 polyclonal, MBL	LabForce	PM036	1:100
2° Antibody Goat anti-rabbit IgG (H+L), Alexa Fluor® 488	Invitrogen	A-11008	1:500

2.1.9.4 Antibodies for Western Blot Analysis

Antibody	Company	Catalog number	Dilution
β-actin antibody [AC-15] HRP-conjugated	Abcam	ab49900-100	1:50000
Atg5 and Atg5-Atg12 complex	Biomol	0262-100/ATG5-7C6	1:400
Atg8/LC3	Biomol	0231-100/LC-3-5F10	1:1000
Goat anti-mouse IgG, HRP	BioRad	170-6516	1:10000

2.1.10 Mice

Female or male B6 mice were purchased from Janvier or Zuchtbetrieb Fuellinsdorf, Switzerland. C57 Bl/6J-Tg(Itgax-cre-EGFP)4097Ach/J were purchased from Charles River. $Atg5^{flox/flox}$ mice were a kind gift of Noboru Mizushima (University of Tokyo, Japan). To generate conditional knockout (KO) mice lacking macroautophagy in $CD11c^{+}$ APCs CD11c-Cre-$EGFP^{+/-}$ mice were bred with $Atg5^{flox/flox}$ mice to generate $Atg5^{flox/flox}$ CD11c-Cre-$EGFP^{+/-}$ mice (designated DC^{Atg5KO} mice). For a more detailed breeding scheme see chapter 3.1.

MOG-specific TCR transgenic mice C57BL/6-Tg(Tcra2D2,Tcrb2D2)1Kuch/J (designated 2D2) were a kind gift from Burkhard Becher (University of Zurich, Switzerland). $Atg7^{flox/flox}$ mice were a kind gift of Masaaki Komatsu (University of Tokyo, Japan). To generate conditional KO mice lacking Atg7 in $CD11c^{+}$ APCs, CD11c-Cre-$EGFP^{+/-}$ mice were bred with $Atg7^{flox/flox}$ mice to generate $Atg7^{flox/flox}$ CD11c-Cre-$EGFP^{+/-}$ mice (designated DC^{Atg7KO} mice). DC^{Atg5KO}, DC^{Atg7KO} and 2D2 mice were bred in-house under specific pathogen-free conditions. Animal experiments were approved by the Swiss Veterinary Office (134/2011) and were carried out according to federal and institutional guidelines.

2.2 Methods

2.2.1 Genotyping

2.2.1.1 Preparation of DNA Samples for Genotyping

Biopsies were taken from either ear or tail (0.3-0.6 cm) and transferred to 1.5 ml tubes. 100 µl of tail digestion buffer, which had been completed with proteinase K, was added to each biopsy. The digest was performed at 550 rpm, 56°C for four to six hours or overnight. When the digest was completed 300 µl of H_20 was added to 100 µl of digest buffer. The sample was centrifuged for ten minutes at maximum speed in a tabletop centrifuge to pellet cell debris. The supernatant was transferred to a fresh tube containing 500 µl of isopropanol and mixed well. The sample was centrifuged as described above and the supernatant was removed. The DNA pellet was washed with 200 µl of ice-cold (-20°C) ethanol 70%. At this step, the DNA was not resuspended, but only rinsed with ethanol 70%. Another centrifugation step was performed and the supernatant was discarded. The DNA was air-dried for a maximum of 15 minutes. Finally, the DNA was resuspended in 100 µl of H_20 and used for the genotyping PCR.

2.2.1.2 Genotyping PCR Protocols

Depending on the allele that had to be screened for, different PCRs were performed. They differed in their master mix as well as in the PCR program applied. For further details see protocols below. The PCR products were analyzed on a 1% agarose gel in TBE buffer.

$Atg5^{flox/flox}$ Genotyping Protocol

Regarding the genotyping for the $Atg5^{flox/flox}$ allele either the *Taq* DNA Polymerase System or the FIREPol 5× Master Mix 7.5 mM Ready to Load were used. The expected PCR products were 650 base pairs (bp) for the Atg5flox allele and 350 bp for the Atg5 wild type (wt) allele. The components of the master mix and the PCR program are shown below.

Standard master mix (1×)

Reagent	**Volume (µl)**
DNA	5.0
10× buffer + $MgCl_2$	5.0
Primer CS 003, 10 µM	1.0
Primer CS 004, 10 µM	1.0
Primer CS 005, 10 µM	1.0
Primer CS 006, 10 µM	1.0
Taq DNA polymerase	0.4
dNTPs	1.0
H_2O	34.6
Total Volume	**50.0**

FIREPol master mix (1×)

Reagent	**Volume (µl)**
DNA	2.0
5× FIREPol mix	4.0
Primer CS 003, 10 µM	0.5
Primer CS 004, 10 µM	0.5
Primer CS 005, 10 µM	0.5
Primer CS 006, 10 µM	0.5
H_2O	12.0
Total Volume	**20.0**

PCR program (standard reaction)

Temperature	Time	
95°C	3 min	
95°C	30 sec	×35
60°C	30 sec	
72°C	1 min	
72°C	10 min	
12°C	∞	

PCR program (FIREPol reagents)

Temperature	Time	
95°C	10 min	
95°C	30 sec	×35
60°C	30 sec	
72°C	1 min	
72°C	10 min	
12°C	∞	

Atg7$^{flox/flox}$ Genotyping Protocol

For the genotyping of the Atg7flox allele the TaKaRa PCR products were used. The expected PCR products were 0.5 kilobase pairs (kb) for the Atg7flox allele and 1.5 kb for the Atg7 wild type allele. The components of the master mix and the PCR program are shown below.

Standard master mix (1×)

Reagent	Volume (µl)
DNA	2.0
10× buffer	2.0
Primer CS014	0.2
Primer CS015	0.2
Taq DNA polymerase	0.2
dNTPs	3.2
H_2O	12.2
Total Volume	**20.0**

PCR program

Temperature	Time	
94°C	5 min	
94°C	30 sec	×30
65°C	30 sec	
68°C	90 sec	
72°C	10 min	
12°C	∞	

CD11c-Cre Genotyping Protocol

Regarding the genotyping for the Cre allele either the *Taq* DNA Polymerase System or the FIREPol "FIREPol 5× Master Mix 7.5 mM Ready to Load were used. The expected PCR products of the Cre transgene is 100 bp and those of the internal positive control 324 bp long. Note, that this PCR

reaction will not discriminate heterozygous from homozygous transgenic animals. The components of the master mix and the PCR program are shown below.

Standard master mix (1×)

Reagent	**Volume (µl)**
DNA	2.0
10× buffer + $MgCl_2$	2.5
Primer CS 007, 10 µM	1.0
Primer CS 008, 10 µM	1.0
Primer CS 009, 10 µM	1.0
Primer CS 010, 10 µM	1.0
dNTPs	1.0
Taq DNA polymerase	0.25
H_2O	15.25
Total Volume	**25.0**

FIREPol master mix (1×)

Reagent	**Volume (µl)**
DNA	2.0
5× FIREPol Mix	4.0
Primer CS 007, 10 µM	0.5
Primer CS 008, 10 µM	0.5
Primer CS 009, 10 µM	0.5
Primer CS 010, 10 µM	0.5
H_2O	12.0
Total Volume	**20.0**

PCR program (standard protocol)

Temperature	**Time**	
94°C	3 min	
94°C	30 sec	
58°C	1 min	×35
72°C	1 min	
72°C	10 min	
10°C	∞	

PCR program (FIREPol protocol)

Temperature	**Time**	
94°C	3 min	
94°C	30 sec	
63°C	1 min	×35
72°C	1 min	
72°C	5 min	
12°C	∞	

2D2 Genotyping Protocol

2D2 mice that are MOG-specific TCR transgenic mice were genotyped by flow cytometry analysis. For this analysis 50 µl of blood were used. The blood was taken by cutting the tip of the tail and 50 µl of blood were withdrawn and mixed with 5 µl of Heparin. The mixture was transferred to FACS tubes and 900 µl of ACK lysing buffer was added. The red blood cell lysis was performed for three minutes at room temperature. The cells were washed with PBS and spun for three minutes at 400 × g at room temperature. The red blood cell lysis was repeated until all red blood cells had been lysed. The cells were finally washed with PBS and subsequently stained with antibody solution (CD4 Pacific Blue, CD8a FITC, Vβ11 PE) for 30 minutes on ice. The cells were washed twice with 4 ml of PBS and fixed with 2% PFA in PBS for ten minutes at room temperature. A final wash with 4 ml of PBS was performed and the cells were resuspended in 200 µl of PBS. If cell clumps had been formed, cells were filtered prior to flow cytometry analysis.

2.2.2 Induction and Scoring of EAE

2.2.2.1 Induction of Active EAE

For the induction of EAE at least nine week old mice were used. EAE was either induced with $MOG_{35–55}$ peptide (MOG peptide) or MOG_{1-124} protein (MOG protein). The MOG peptide or MOG protein were prepared in the same way and the preparation is exemplarily described for the $MOG_{35–55}$ peptide. Initially, a mixture of $MOG_{35–55}$ peptide with CFA was prepared and the final concentration of MOG peptide was 0.5 µg/µl. If necessary the peptide was diluted in PBS and subsequently mixed at a 1:1 ratio with CFA. For the preparation of the MOG peptide:CFA mixture, the two fractions were pooled in a 5 ml polypropylene tube with snap caps. The mixture was vortexed for 30 minutes at room temperature at medium speed. The MOG peptide:CFA homogenate was sonicated on ice five times for 15 seconds each at a power level of 18. Each sonification step was interrupted with breaks of 45 seconds. The homogenate was transferred to a 1 ml syringe and for the injection a 24G×1'' needle was used. Finally, at day 0, the mice were immunized with 200 µl of the MOG peptide:CFA mixture subcutaneously in the left lateral abdomen. At day 7 the injection was repeated, but this time the MOG peptide:CFA mixture was applied to the right abdomen. Additionally, the mice were injected with 300 ng of PTx. 300 ng of PTx was diluted in 100 µl of PTx diluent and was administered intra peritoneally (i.p.) on day zero and two. After induction of EAE mice were observed daily for weight loss, disability and availability of feed and water.

2.2.2.2 Induction of EAE by Adoptive Transfer of Autoreactive $CD4^+$ T Cells

At least nine week old mice were used. The MOG peptide:CFA emulsion was prepared as described above and the final MOG peptide concentration was adjusted to a final concentration of 1 mg/ml. At day zero donor mice (either wt or 2D2) were immunized subcutaneously with 100 µl of MOG-CFA emulsion into both flanks. Thus, in total each mouse received 200 µl of MOG-CFA emulsion. On the same day 300 ng of PTx in 100 µl of PTx diluent was administered i.p. On day seven mice were sacrificed and spleens as well as draining axillary lymph nodes were removed.

Lymphocytes were isolated from spleen and lymph nodes as described in chapter 2.2.3. After the isolation of lymphocytes, cells were counted and the cell number was adjusted to $8\text{-}10\times10^6$ cells/ml in culture medium. Culture medium was additionally supplemented with 20 ng/ml of recombinant IL-23 and 20 µg/ml of MOG $peptide_{35–55}$. Cells were transferred to a 10 cm tissue culture-treated Petri dish and cultured for two days at 37°C and 5% CO_2 in humid atmosphere. Cell blasts were visible under the microscope after two days of culture. One day before the transfer of the cells, the recipient mice were irradiated with 550 rad (cesium source). At day nine the cultured cells were washed with PBS twice and the cell number was adjusted to the desired concentration of 5×10^6 cells/400 µl (2D2 as donor) or $10\text{-}15\times10^6$ cells/ 400 µl (wt as donor). 400 µl of this cell suspension

was injected intraperitoneally into the recipient mice. No additional injection of Ptx was performed. After induction of EAE mice were observed daily for weight loss, disability and availability of feed and water. The disease onset was expected to be two days later than in the active immunization procedure.

2.2.2.3 EAE Scoring and Analysis

After onset of EAE symptoms mice were scored according to the following scoring criteria by a grid test: 0: no detectable signs of EAE, 0.5: distal limp tail weakness, 1.0: complete limp tail, 1.5: limp tail and hind limb weakness, 2.0: unilateral partial hind limb paralysis, 2.5: bilateral partial hind limb paralysis, 3.0: complete bilateral hind limb paralysis, 3.5: complete bilateral hind limb paralysis and partial forelimb paralysis, 4.0: moribund (mouse completely paralyzed), score 5.0: dead. With an EAE score of 1.0 feed and water needed to be provided to guarantee well-being of the mice. Mice were sacrificed if they showed a score of 3.0 for more than seven constitutive days or a score of 3.5 for more than three constitutive days, and immediately if they showed a score of 4.0. Furthermore, mice needed to be sacrificed if they lost more than 30% of their maximum body weight. For the analysis, the average day of onset, mean clinical scores and mean maximal scores were determined.

2.2.3 Lymphocyte Isolation and Preparation

2.2.3.1 Lymphocyte Isolation from Mouse Spleen and Lymph Nodes

T cells and DCs were purified from spleen and/or lymph nodes. For the preparation of DCs from organs, a single-cell suspension was prepared by enzymatic disaggregation with collagenase D and DNase. On the other hand, for the preparation of T cells this disaggregation step can be omitted. Organs were removed from mice, transferred to PBS and kept on ice until further proceeding. In a next step, the respective organ was chopped with scissors and digested with spleen digest buffer at 37°C (5% CO_2 in humid atmosphere) for 30 minutes. Afterwards, the tissue was meshed through a 70 µm nylon mesh by using a syringe punch. The nylon mesh was rinsed with 40 ml of PBS, the cells were centrifuged for five minutes at 400 × g and the supernatant was discarded. Additionally, a red blood cell lysis was performed by adding 1 ml of ACK red blood cell lysing buffer followed by thorough resuspension of the cells. After an incubation time of three minutes at room temperature, the cells were washed with PBS as described above.

2.2.3.2 Lymphocyte and Microglia Isolation from Mouse CNS

Mice were sacrificed with CO_2 and perfused with 30-50 ml of ice-cold PBS. The spinal cord was flushed out with a 24G×1'' needle and the brain was removed. The organs were transferred to ice-

cold PBS and all following steps were performed on ice unless otherwise mentioned. The organs were chopped with scissors and digested with 5 ml of digest buffer per brain. The digest was performed for 30 minutes at 37°C and mixed every ten minutes with a 1 ml pipette. To stop the reaction 10 mM of EDTA was added and incubated for another five minutes at 37°C. The digested tissue was meshed through a 70 µm nylon mesh using a syringe punch. The mesh was rinsed with 40 ml of PBS and the cells were spun for 5 minutes at 400 × g at 4°C. The supernatant was discarded and the pellet was resuspended in a 30% percoll solution. The suspension was transferred to 16 ml centrifuge tubes and spun at 10'8000 rpm for 30 minutes at 4°C. To not disturb the gradient, the centrifuge brakes were set to an acceleration of nine and a disacceleration of one. The myelin was sucked off and discarded. The remaining fraction, but not the red blood cells, was transferred to a fresh 50 ml tube und filled up with PBS. The cells were spun at 400 × g for five minutes at 4°C. The supernatant was discarded and the pellet was resuspended in 1 ml of PBS. At the end the cells were counted and used for the desired experiment.

2.2.3.3 Magnetic Activated Cell Sorting

DCs or T cells were purified by magnetic activated cell sorting (MACS) by using CD11c and CD4 MicroBeads, respectively, according to MACS Miltenyi Biotec's recommendations. The procedure is briefly summarized here:

A single-cell suspension was obtained from spleen as described in chapter 2.2.3. Generally, for the performance of MACS separation the cells were kept cold during the entire procedure and all solutions were pre-cooled. To avoid cell clumps, the suspension was filtered through a 70 µm nylon mesh before usage.

Cells were magnetically labeled by using either CD11c MicroBeads (100 µl of CD11c MicroBeads and 400 µl of MACS buffer per 1×10^8 cells) or CD4 MicroBeads (10 µl of CD4 MicroBeads and 90 µl of MACS buffer per 1×10^7 cells). The cells and reagents were mixed thoroughly by pipetting and incubated for 15 minutes at 4°C. The cells were washed with MACS buffer (2 ml per 1×10^7 cells) and centrifuged. The cell pellet was resuspended in MACS buffer (500 µl per 1×10^8 cells) and the magnetic separation was performed with the autoMACS^{TM} separator using the "PosselD" program. The expected percentage of $CD4^+$ T cells in the spleen is around 20% of total cells, whereas the expected number of DCs in the spleen is around 1%.

2.2.4 Flow Cytometric Techniques

2.2.4.1 Flow Cytometry

All flow cytometric analyses were performed in PBS without supplements. A list of used antibodies and their respective dilution is shown in table 2.1.9.1. The used antibody combinations are mentioned with the respective experiment (see results section). For all experiments antibody

staining and live/dead staining by use of the LIVE/DEAD® Fixable Aqua Dead Cell Stain Kit were performed in parallel. All centrifugation steps were performed for five minutes at 400 × g unless otherwise mentioned.

Generally, 30 to 50 µl of antibody mixture were used to stain roughly 1×10^6 cells. The cells were carefully resuspended and incubated for 20 to 30 minutes at 4°C. The cells were washed twice with PBS and centrifuged. The supernatant was discarded and the cells were resuspended in 100 to 200 µl of PBS, depending on the cell number used. Cells were subsequently analyzed via flow cytometry.

2.2.4.2 IFN-γ, IL-17 and GM-CSF Intracellular Cytokine Staining

A lymphocyte suspension was prepared as described in chapter 2.2.3. To perform an intracellular cytokine staining (ICS), $1\text{-}2\times10^7$ cells per condition were used. The needed cells were resuspended in 1 ml of cell culture medium and transferred to sterile FACS tubes. The cells were stimulated *in vitro* by using 50 ng/ml of phorbol ester (PMA) and 500 µg/ml of ionomycin. In order to block the intracellular transport processes, additionally, BD GolgiStop™ (Monensin) was added to the cells. The subsequent time period of incubation depended on the respective cytokine production (GM-CSF: 6 hours, IFN-γ: 4-5 hours). The cells were incubated at 37°C for 5 hours.

In a next step, the surface staining of the cells was performed according to the standard flow cytometry staining procedure (chapter 2.2.4.1). After staining for cell surface markers, the cells were resuspended with 300 µl of PBS. To stain for intracellular antigens, the cells were fixed and permeabilized by use of the BD Cytofix/Cytoperm™ Plus Solution. The cells were pulse vortexed after the last washing step and 200 µl of BD Cytofix/Cytoperm™ Buffer was added per sample (only 100 µl were used when ICS was performed in a 96-well plate format) and thoroughly vortexed again. The cells were incubated for 20 minutes at 4°C and 1 ml of 1× BD Permeabilization/Wash Buffer was added. The cells were centrifuged for three minutes at 500 × g and the supernatant was discarded. Optionally, the staining procedure was stopped at this step and the cells were stored in either 1× BD Permeabilization/Wash Buffer or in FACS buffer at 4°C overnight. In a next step, the cell pellet was resuspended in 30 to 50 µl of properly diluted antibody solution that was diluted in 1× BD Permeabilization/Wash Buffer. The cells were incubated for 20 minutes at 4°C and 1 ml of 1× BD Permeabilization/Wash Buffer was added. Finally, the cells were centrifuged for three minutes at 500 × g and the supernatant was discarded. The cells were resuspended in PBS and subsequently analyzed via flow cytometry.

2.2.4.3 Intracellular Staining for Murine FoxP3$^+$ Regulatory T cells

The Foxp3 Staining Buffer Set from eBioscience was used to perform the intracellular FoxP3 staining for flow cytometry analysis. Prior to the staining, the eBioscience

Fixation/Permeabilization Concentrate (1 part) was diluted into the eBioscience Fixation/Permeabilization Diluent (3 parts) which resulted in the so-called eBioscience Fixation/Permeabilization Working Solution (Fix/Perm solution).

A single cell suspension was prepared as described in chapter 2.2.3 and 1×10^6 cells in 100 µl were used per condition. The surface molecules CD4, CD8 and CD25 were stained according to the general flow cytometry procedure (chapter 2.2.4.1). Cells were washed with PBS and the cell pellet was resuspended with 500 µl of freshly prepared Fix/Perm solution. In a next step, cells were pulse vortexed and incubated at 4°C between 30 minutes and 18 hours in the dark. After this incubation time, cells were washed twice by adding 1 ml of 1× eBioscience Permeabilization Buffer (Perm buffer) followed by centrifugation and aspiration of the supernatant. 10 µl of anti-FoxP3 antibody diluted in 1× Perm buffer was added to the cells. Cells were then incubated at 4°C for at least 30 minutes in the dark. At the end, cells were washed twice with 2 ml of 1× Perm buffer and resuspended in an appropriate volume of PBS and subsequently analyzed by use of flow cytometry.

2.2.4.4 Fluorescent Activated Cell Sorting

Single cell suspensions were prepared as described in chapter 2.2.3 and the final cell number was adjusted to 2×10^7 cells/ml. DCs were purified by fluorescence activated cell sorting (FACS) based on the following markers: $CD45^+$, $CD11c^{high}$ and $H2\text{-}A^{b\ high}$ and the desired cell population was sorted into 5 ml of complete cell culture medium in 15 ml tubes. The FACS was performed at the FACS Aria cell sorter by the technical staff of the Center for Microscopy and Image Analysis at the University of Zurich, Switzerland.

2.2.4.5 Flow Cytometry Analysis

Flow cytometry analyses were either performed on FACSCantoII or LSRII Fortessa provided by the Institute of Experimental Immunology, Zurich, Switzerland. Flow cytometry analysis data were analyzed by Diva or FlowJo software.

2.2.5 CFSE Labeling

To uniformly label the cells with carboxyfluorescein succinimidyl ester (CFSE), it was ensured that the cells were properly resuspended and not aggregated. The quantity of cells labeled depended on the respective experiment. A single-cell suspension of $CD4^+$ T cells was prepared in PBS/0.1% BSA at a final concentration of 5×10^7 cells/ml. CFSE was added to the cells at a final concentration of 1 µM and the cells were incubated for 10 minutes at 37°C. In a next step, the cells were quenched by adding 5 volumes of ice-cold cell culture medium followed by five minutes incubation on ice. Finally, the cells were washed three times with cell culture medium.

2.2.6 DC:T Cell Co-Culture

Isolated (chapter 2.2.3) and MACS-enriched (chapter 2.2.3.3) $CD4^+$ T cells were CFSE-labeled (chapter 2.2.5) and co-cultured with FACS-sorted DCs (chapter 2.2.4.4) in RPMI cell culture medium supplemented with β-mercaptoethanol. The co-culture was performed in a 96-well round-bottom plate at a 1:3 effector to target cell ratio (30000 DCs: 100000 T cells). Depending on the conditions to be tested either MOG peptide, MOG protein, or beads coated with MOG protein were added to the cells in cell culture medium. To control for unspecific proliferation of $CD4^+$ T cells, the following negative controls were included: T cells only and DCs plus T cells without further additives. As positive control $CD4^+$ T cells were cultured in the presence of an anti-CD3 and anti-CD28 antibody. The wells were coated with 5 µg/ml of anti-CD3 and anti-CD28 antibody each in PBS for five hours at room temperature or overnight at 4°C. Finally, the cells were incubated for four days at 37°C and 5% CO_2 in a humid atmosphere. To check for CFSE dilution, cultured cells were washed twice with PBS and spun at 400 × g for five minutes. The cells were stained with anti-CD4 and the LIVE/DEAD® Fixable Near-IR Dead Cell Stain Kit was used. CFSE dilution was analyzed via flow cytometry analysis and assessed by CFSE dilution. For the analysis of T cell proliferation, only those samples were analyzed that showed 1% live cells ($AmCyan^-$ cells) of the starting cell number (starting cell number 100000 T cells). Furthermore, all $CFSE^{dim/low}$ cells were considered as proliferated T cells and the percentage of this cell number was used.

2.2.7 Coating of Polystyrene Beads with MOG Protein

The coating procedure of polystyrene beads is based on recommendations form Technote 204 from Bangs laboratories. The polystyrene beads were coated with 50 µg of MOG protein per 1×10^8 beads. For the coating, 1×10^8 beads were taken and washed with 1 ml of PBS. In a next step, beads were centrifuged at 600 × g for five minutes and the supernatant was discarded. The washing step was repeated once more and the beads were resuspended in 950 µl of PBS. The beads were added to 50 µl of MOG protein (stock 1 mg/ml) and mixed by pipetting. The coating was performed for one to two hours at room temperature and, additionally, overnight in the cold room on a rotator. On the next day, the beads were washed 5 times with PBS and counted. In the experimental setup of a co-culture experiment (chapter 2.2.6), the beads were used at a bead to DC ratio of 8:1, 4:1, 2:1 and 1:1.

2.2.8 Cell Culture

All cell lines or primary cells were cultured at 37°C in a humid atmosphere of 5% CO_2 in air. The different cell lines were cultured in medium specifically designed for their respective nutritional and survival factor characteristics. Glass bottles, pipette tips, PBS and endotoxin-free Milli-Q water were sterilized by autoclaving before usage. Culture plates, flasks and further plastic supplies used

for cell culture were purchased from SPL Life Sciences. Cell culture work was performed under sterile conditions in a biological safety cabinet. All centrifugation steps of cells were performed with the Multipurpose Centrifuge 5810 R from Eppendorf ® at 400 × g for five minutes at 4°C, unless otherwise mentioned.

2.2.8.1 Determination of Cell Concentration

Cells were counted by using a Neubauer-counting chamber (Fisher Scientific), also known as hemocytometer. To distinguish viable from dead cells, a trypan blue staining was performed by mixing the cell suspension and trypan blue at a 1:1 ratio. Dead cells are stained by trypan blue whereas live cells do not take up the trypan blue dye. The viability and cell numbers were determined by use of a Leica DMIL microscope.

2.2.8.2 Cell Passaging of Adherent Cells

Adherent cells were kept at a cell density of 20-90%. For detachment of cells, cell medium was removed and cells were rinsed with PBS. Trypsin-EDTA 0.25% was added to the cells and incubated for one minute at room temperature to assure a quick and efficient detachment of the cells. During the incubation time the flask was frequently tapped to facilitate detachment. The cells were washed with PBS and resuspended in complete cell culture medium and plated into new tissue culture flasks. If Trypsin was to be avoided, adherent cells were detached by use of a cell scraper instead.

2.2.8.3 Freezing and Thawing of Cells

Cells to be frozen were washed with medium and resuspended in freezing medium. Cells were transferred to cryo tubes and and slowly frozen using a cell freezing container. On the next day, cells were transferred to liquid nitrogen for long-term storage.

To thaw cells, a frozen aliquot of cells was thawed quickly in a 37°C water bath and cells were immediately transferred to complete medium to dilute the DMSO and minimize osmotic shock. Cells were spun, supernatant discarded, and the cell pellet resuspended in fresh complete medium and plated. As soon as the cells appeared healthy and started to grow exponentially they were maintained as normal and could be used for experiments.

2.2.8.4 Culturing of Primary Mouse Cells

Single cell suspensions were obtained as described in chapter 2.2.3. The cells of interest were cultured under general cell culture conditions as described above.

2.2.8.5 Cell Line X-63-GM-CSF

The X-63-GM-CSF cell line is a mouse myeloma cell line served as a source for GM-CSF and the supernatant of the X-63-GM-CSF cell culture was used to generate bone marrow-derived DCs. The cell line X-63-GM-CSF was cultured in complete DMEM medium. To start with, X-63-GM-CSF cells were cultured under selective conditions to select for the GM-CSF gene. The antibiotic G418 was added at a final concentration of 500 µg/ml and G418 selection was performed for 10 to 14 days. After successful selection, the cells were washed and seeded at a final density of 3×10^5 cells/ml of complete medium without G418 in a 10 cm cell culture dish. This equals approximately 6.5×10^6 cells/ per 30 ml in a 175 cm^2 dish. The cells were kept in culture for a week or until the pH indicator in the medium turned yellow indicating acidity. At the end, the medium was harvested and spun at 500 × g for five minutes. The supernatant was kept, sterile filtered with a 0.22 µm mesh, aliquoted and stored at -20°C until further usage.

2.2.8.6 Generation of Bone Marrow-Derived DCs

For isolation of progenitor DCs from the bone marrow (BM), BM-donors were euthanized and skin and muscles from pelvis, femur and tibia were removed. Bones were transferred to PBS and stored on ice. Later on, the bones were cut with scissors in half and flushed with PBS by use of a 30G1/2'' needle. The cells were forced through a 70 µm cell strainer and topped with PBS. In a next step, the cells were centrifuged at 400 × g for five minutes and the supernatant was discarded. For red blood cell lysis, the cell pellet was resuspended in 3 ml of ACK red blood cell lysing buffer and incubated for three minutes at room temperature. The lysis was stopped by adding 50 ml of PBS and the cells were centrifuged. The supernatant was discarded and the cell number was adjusted to a final cell concentration of 2-2.5×10^6 cells/ml in complete BM-DC medium. The cells were finally cultured in a total volume of 10 ml (2-2.5×10^7 total cells) in a 10 cm non-tissue culture treated petri dish. A full medium change was performed every other day by collecting the floating cells, spinning them and resuspending the resulting pellet in fresh BM-DC medium. The cells were then placed back to the original dish. In total, the cells were cultured for eight to ten days to assure proper differentiation into a DC-like phenotype. At the last day of culture, the complete medium was removed and the adherent cells were removed by either trypsinization or scraping them off with a cell scraper. The purity and maturation status of the cells was confirmed by flow cytometry analysis. Generally, a purity of 80% of $CD11c^+$ DCs could be achieved.

2.2.9 Immunofluorescence Microscopy

2.2.9.1 Preparation of Cells for Immunofluorescence Microscopy

To study the localization of $LC3^+$ autophagosomes after the treatment of BM-DCs with MOG protein-coated beads, immunofluorescence microscopy was performed. BM-DCs were generated as

described in chapter 2.2.8.6 and at day ten of culture, BM-DCs were seeded in a cell culture slide and only the adherent BM-DCs were taken for each experiment. In total, 7.5×10^4 BM-DCs were plated into each well of the cell culture slide and cells were left in the chamber slide overnight in order to attach properly. In parallel, the polystyrene beads were coated with MOG protein as described in chapter 2.2.7. On the next day, the BM-DCs were cultured under various conditions for four hours at 37°C.

2.2.9.2 Immunofluorescence Staining for Microscopy

For the immunofluorescence staining, the cells were washed by drawing off the medium with a sucking device and adding 200 µl of PBS to each well. The PBS was left on the cells for three minutes and was then sucked off again. All washing steps described in the following section were performed in this way and all staining steps were performed as room temperature – unless otherwise mentioned. The cells were fixed with 200 µl of 3% PFA per well and incubated for 15 minutes to then be washed twice with PBS. In a next step, the cells were permeabilized with 0.1% Triton-X in PBS. To do so, 200 µl of 0.1% Triton-X in PBS was added to each well and incubated for five minutes. Another washing step was performed and the cells were blocked for 30 minutes with 100 µl of blocking buffer per well. Next, the desired primary antibody was diluted in dilution buffer and 100 µl of the antibody was added to the cells and incubated for one hour. In a next step, the primary antibody was removed and cells were washed twice with washing buffer. The secondary antibody was prepared as described before and 100 µl of secondary antibody was added to the cells for 45 minutes. After the incubation, the cells were washed twice with washing buffer. Finally, the cell nucleus was stained with 200 µl of DAPI (dilution 1:5000 in PBS) for two minutes. The cells were washed twice with washing buffer and once with PBS. Afterwards the slides were mounted with ProLong® Gold Antifade Reagent and the sample was topped with a cover slide (1.5 thickness). To let the mounting medium harden, the slides were let sit for 24 hours in the dark, and were then transfered to 4°C for long-term storage.

2.2.9.3 Analysis of Immunofluorescence Cytochemistry

The analysis of the immunofluorescence cytochemistry stainings was performed using the inverted CLSM Leica SP5 Mid-UV confocal microscope at the ZMB (Zentrum für Mikroskopie und Bildanalyse, University of Zurich, Switzerland). Acquisition of the data was performed using the LAS Leica Application Imaging software and the graphical analysis was performed with ImageJ.

2.2.10 Protein Analysis

2.2.10.1 Cell Lysis for Western Blot

For the entire procedure, the cells were kept on ice to prohibit stress-related responses during the preparation of the cells. The medium of the cells was removed and washed once with PBS. To detach the adherent cells, the cells were either trypsinized or scraped off. The cells were mixed well and a single cell suspension was prepared. The cells were transferred to a 15 ml tube and washed with 10 ml PBS. The cells were spun at 400 × g for five minutes at 4°C, the supernatant was discarded and the cell pellet was resuspended in 1 ml of PBS and transferred to 1.5 ml tubes. The cells were spun another time and the supernatant was completely removed. At this point the cells can be stored at -80°C for later usage. The cell pellet was resuspended in lysis buffer (50 µl lysis buffer per 1×10^6 cells) by pipetting the cells up and down vigorously until the suspension was homogenous. The cells were incubated on ice for 20 minutes and vortexed for 15 seconds. The lysed cells were centrifuged at maximum speed in a table top centrifuge for ten minutes at 4°C to separate cell lysate from cell debris. The supernatant was transferred to a fresh 1.5 ml tube and small aliquots were removed for BCA protein quantification (chapter 2.2.10.2). The cell lysates were snap frozen and stored at -80°C.

2.2.10.2 BCA Assay for Protein Quantification

Protein quantification was performed using the bicinchoninic acid (BCA) Protein Assay Kit according to manufacturer's recommendations. First, a bovine serum albumin BSA standard was prepared in PBS. The final BSA concentration ranged from 2000 µg/ml to 25 µg/ml. The working reagent provided by the BCA Protein Assay Kit was prepared as recommended. Since the sample size was limited, the "microplate procedure" was applied. In this procedure, 10 µl of each sample and standard were used and pipetted into a flat bottom 96-well plate. In a next step, 200 µl of the working reagent were added to each well and was mixed with the sample. The plate was closed with adhesive tape to prevent evaporation of the sample and the mixture was incubated at 37°C for 30 minutes. After this incubation time, the plate was cooled to room temperature and the absorbance was measured at a wavelength of 540 nm on an ELISA plate reader.

2.2.10.3 Western Blot Procedure

Depending on the purpose of the Western blot, different protein samples were analyzed. If not mentioned differently, the samples were prepared according the protocol provided in chapter 2.2.10.1. The samples were prepared in Laemmli buffer and boiled at 95°C for five minutes to denature the proteins. Generally, a 12.5% SDS-PAGE of 0.75 to 1.5 mm thickness was prepared in a BioRad stacking system. The samples were applied to the wells and the gel was run at 85 V for two to three hours or until the protein front reached the very bottom of the gel. The protein transfer

was carried out using a semi-dry blotting system. The Whatman paper was equilibrated with transfer buffer and, in parallel, the PVDF membrane was activated for five minutes with 100% Methanol and then also equilibrated with transfer buffer. The transfer unit was assembled and the transfer was performed for one hour at 10 V. Next, the membrane was blocked with blocking solution for one hour at room temperature while gently shifting. All further steps were also performed at room temperature on a shaker. The primary antibody was added in 5% skimmed milk in PBS-T buffer and incubated for one hour at room temperature or overnight at 4°C. Next, the membrane was washed once for 15 minutes and three times for five minutes with PBS-T. The secondary antibody was prepared in the same way as the primary antibody and the membrane was incubated for one hour. The membrane was washed as described above and a final washing step was performed by washing twice with PBS for five minutes each. The membrane was developed using the Pierce ECL Western Blotting Substrate. Membranes were developed on ECL films for different timings to visualize protein levels. Actin detection was used as a loading control to normalize LC3, Atg5, and Atg7 levels.

2.2.10.4 Stripping of Western Blot Membrane

The PVDF membrane was washed twice for five minutes with PBS-T and twice for five minutes with H_2O. The water was removed and 5 ml of ReBlot System Strong Solution was added. The membrane was incubated for 30 minutes at room temperature while gently shifting on a shaker. To remove residues of the stripping solution, the membrane was washed twice for five minutes with H_2O and in a next step twice with PBS-T. To repeat the detection procedure, the membrane was blocked with 5% skimmed milk powder in PBS-T and the normal detection procedure was continued.

2.2.11 Overexpression and Purification of MOG Protein

2.2.11.1 Transformation of Chemocompetent Bacteria

For the amplification of the plasmid pET-22b(+) ($mMOG_{1-124}$) chemocompetent Top 10 bacteria were transformed. On the other hand, for the overexpression of rmMOG $protein_{1-124}$ chemocompetent BL21 cells were used. Both bacterial strains were transformed by using the following protocol:

Bacteria were thawed on ice and 1 µl of plasmid DNA (stock 40 ng/µl) was added to the bacteria. The bacteria were incubated on ice for 30 minutes and a heat shock was performed for 30 seconds at 42°C. The bacteria were put back on ice for five minutes and 1 ml of LB medium without additives were added. The cells were incubated for 45 minutes at 37°C and 220 rpm. All bacteria were plated on 1 LB Amp^+ plate and incubated overnight at 37°C in inverted position. On the next day, a colony was picked and transferred to 5 ml of LB Amp^+ medium and incubated overnight at

37°C and 220 rpm. A glycerol stock of both bacterial strains was prepared by mixing the bacterial culture and 100% glycerol at a 1:1 ratio. The glycerol stock was transferred to cryo tubes and stored at -80°C.

2.2.11.2 DNA Plasmid Purification and Sequencing

DNA plasmids were purified by a PureYield™ Plasmid Miniprep System from Promega. The bacterial lysate was prepared by adding 600 µl of bacterial culture to a 1.5 ml microcentrifuge tube. 100 µl of Cell Lysis Buffer was additionally added to the tube and mixed by inverting the tube. Furthermore, 350 µl of cold Neutralization Solution was added and mixed by inverting the tube. The suspension was centrifuged at maximum speed in a table-top centrifuge for three minutes. The supernatant was transferred to a PureYield Minicolumn and the column was placed into a fresh tube. Another centrifugation step was performed at maximum speed for 15 seconds. The flow through was discarded and the column was placed back into the same tube. The column was washed by adding 200 µl of Endotoxin Removal Wash and a centrifugation step was performed as described above. After this step, 400 µl of Column Wash Solution was added to the column and centrifuged for 30 seconds. To elute the DNA, the column was transferred to a clean 1.5 ml reaction tube and 30 µl of Elution Buffer or nuclease-free water were directly applied to the column matrix. The column was incubated or one minute at room temperature and was then centrifuged for 15 seconds to elute the plasmid DNA. The eluted plasmid DNA was stored at -20°C.
The plasmid DNA was sequenced by the sequencing service of Microsynth AG, Switzerland.

2.2.11.3 Overexpression of MOG Protein

On the day before the actual overexpression of MOG protein, 50 ml of LB medium supplemented with ampicillin (final concentration 100 µg/ml) were inoculated with the bacterial glycerol stock BL21 $mMOG_{1-124}$. This culture was incubated overnight at 37°C and 220 rpm. On the next day, 2 l of LB medium (supplemented with 100 µg/ml ampicillin, 0.1% glucose and 1 mM $MgCl_2$) were inoculated with ~10 ml of the overnight culture to reach a starting OD_{600} of 0.1. At an OD_{600} of 0.7 the protein overexpression was induced by adding 1 mM of IPTG and incubated for three more hours. The suspension was centrifuged at 3000 × g for 20 minutes at 4°C and the pellets were collected and pooled. The pellet can be stored at -20°C for long-term storage.

2.2.11.4 Purification of MOG Protein

For the purification of MOG protein, all steps were performed at room temperature unless otherwise mentioned. The bacterial pellet was resuspended in 30 ml of lysis buffer and the bacteria were disrupted via French press by applying a pressure of 900-1100 PSI. This step was repeated three to

four times. The bacterial lysate was centrifuged at 30000 × g for 30 minutes at room temperature. The supernatant was decanted and the inclusion body pellet was resuspended in 30 ml of lysis buffer by use of a spatula. This centrifugation step was repeated once more. The pellet was resuspended in ~50 ml of solubilization buffer to solubilize the inclusion bodies. The tube was closed with PARAFILM^{TM} and incubated overnight at room temperature while spinning to entirely dissolve the inclusion body pellet. The solved inclusion bodies were filtered with a 0.45 µm filter device. The Ni-NTA Superflow column (column volume 3 ml) was equilibrated with running buffer and the protein suspension was loaded onto this column. The flow through was reloaded three more times to increase binding efficiency. The column was washed with 20 column volumes (CV) of solubilization buffer and afterwards with 200 CV of endotoxin-removal buffer. The protein was eluted batch-wise with four CV of elution buffer. The protein concentration was determined with the nano drop (chapter 2.2.11.5) and the concentration was adjusted to 3 mg/ml with the solubilization buffer in order to reduce the amount of imidazole before dialysis.

The protein was further diluted 1:3 with arginine buffer and transferred to a 3000 MWCO dialysis membrane tube. The dialysis was performed for 24 hours against dialysis buffer A (15× volume). During the dialysis, the volume increased threefold. A second dialysis was performed for three hours against dialysis buffer B (15x volume). The dialysis against buffer B was repeated for 12 hours (50x volume). To finish, the sample was dialysed three times against 5 l of of dialysis buffer C (125000x volume).

To concentrate the sample, a 3000 MWCO Millipore concentrator was used. The final concentration was adjusted to 1-2 mg/ml. The MOG protein$_{1\text{-}124}$ was snap-frozen in liquid nitrogen and stored at -80°C. To thaw the protein, the solution was thawed quickly at 37°C in order to avoid precipitation of protein.

2.2.11.5 Nanodrop

The Nanodrop ND-1000 (Thermo Scientific) is a microvolume UV-Vis spectrophotometer that can be used to analyze DNA, RNA and proteins. It was used to determine the protein concentration of purified MOG protein. The absorption of purified MOG protein at 280 nm 0.1% (=1 g/l) was 1.344.

2.2.11.6 Statistical analysis

For clinical EAE scores, differences between groups were evaluated by two-way analysis of variance (ANOVA) with Bonferroni's post-test. For cell subsets and cytokine expression, differences between two cell populations were evaluated by the two-tailed Student's *t*-test. *P* values of less than 0.05 were considered significant.

3 Results

We hypothesized that autophagy in CD11c-expressing cells accelerates EAE development and progression due to increased loading of self-antigen onto MHC class II molecules. To test this hypothesis, we generated a knock out (KO) mouse system in which one of the hallmark proteins of autophagy is conditionally deleted in $CD11c^+$ cells by use of the Cre/loxP recombination system. This recombination system enables the targeted deletion of a gene of interest. Principally, in the Cre/loxP recombination system, two recombination sites, called loxP sites, flank the gene of interest. A loxP-flanked DNA sequence is also described as "floxed" (abbreviated as flox or fl). An enzyme, named Cre (cyclization or causes recombination enzyme), catalyzes the homologous recombination between the two loxP sites and, consequently, the floxed gene is removed (Bouvier and Cheng, 2009; Mortensen, 2001). In order to conditionally eliminate autophagy from $CD11c^+$ cells, the Atg5 protein was targeted in a Cre/loxP recombination system. Atg5 is a protein essential for autophagosome formation whose complex with Atg12 and Atg16L mediates ligation of Atg8 to the autophagosomal membrane for vesicle expansion and substrate recruitment. Accordingly, Atg5-deficient cells do not show autophagic activity. Thus, CD11c Cre/loxP-deleter transgenic mice allow us to study the development of EAE in the absence of autophagic activity in $CD11c^+$ APCs, mainly DCs, compared to control (CTRL) littermates.

3.1 Breeding of the Conditional KO Mouse

In order to generate mice that are deficient in Atg5 in $CD11c^+$ cells, multiple breeding steps were necessary (breeding scheme shown in Figure 3.1). The first step was to cross CD11c-$Cre^{-/-}$ $Atg5^{fl/oxflox}$ mice with CD11c-$Cre^{+/-}$ $Atg5^{wt/wt}$ mice. This breeding step produced, amongst others, mice of the CD11c-$Cre^{+/-}$ $Atg5^{flox/wt}$ genotype. These mice, in the next breeding step, were bred to CD11c-$Cre^{-/-}$ $Atg5^{flox/flox}$ mice. In the last step, CD11c-$Cre^{-/-}$ $Atg5^{flox/flox}$ mice were crossed with CD11c-$Cre^{+/-}$ $Atg5^{flox/flox}$ and this, finally, resulted in mice with the genotype of interest. For all experiments, control mice that do not lack the *atg5* gene in $CD11c^+$ cells (CD11c-$Cre^{-/-}$ $Atg5^{flox/flox}$, designated $DC^{Atg5CTRL}$ mice) and mice that conditionally lack the *atg5* gene in $CD11c^+$ cells (CD11c-$Cre^{+/-}$ $Atg5^{flox/flox}$, designated DC^{Atg5KO} mice) were compared.

The desired genotypes were confirmed by genotyping PCR. To screen for Cre and the Atg5floxed transgene, two different genotyping PCRs were performed. The CD11c-Cre genotyping reaction yielded a band of 324 bp, which represents an internal positive control and a band of 100 bp representing the Cre transgene. On the other hand, depending on the genotype of the respective mouse, the Atg5 floxed genotyping PCR reaction was supposed to give a 650 bp band (floxed gene), a band of 350 bp (Atg5 wild type) and a third band of 300 bp (Atg5floxed deleted when Cre is also positive). Exemplarily, one agarose gel depicting a genotyping result is shown in Figure 3.1.

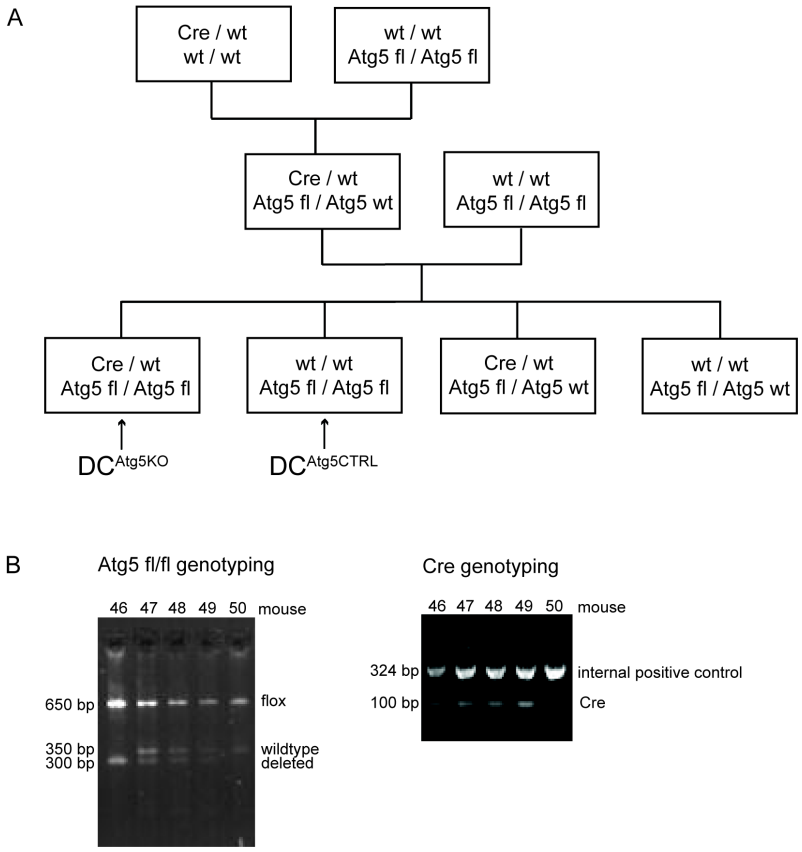

Figure 3.1: Schematic flow sheet representing the breeding strategy for the generation of DC^{Atg5KO} and DC^{Atg5CTRL} mice and representative genotyping results. (A) Breeding was performed according to this scheme. The upper row in each box represents the *cre* allele, and the lower row represents the *atg5* allele. The offspring of interest is CD11c-Cre$^{+/-}$ Atg5$^{flox/flox}$ (DC^{Atg5KO}) and CD11c-Cre$^{-/-}$ Atg5$^{flox/flox}$ (DC^{Atg5CTRL}). **(B)** Agarose gel showing genotyping results of *atg5*floxed and CD11c-Cre genotyping PCR. Left: Results of the *atg5*floxed genotyping. Expected bands: 650 bp=floxed gene, 350 bp=Atg5 wild type, 300 bp=*atg5*floxed deleted when *cre* is also positive. Right: Results of the CD11c-Cre genotyping. Expected bands: 324 bp=internal positive control, 100 bp=*cre* transgene. The results of mice number 46 to 50 are exemplarily shown.

3.2 Characterization of DC^{Atg5KO} and DC^{Atg5CTRL} Mice

The use of the Cre/loxP recombination system implies that most tissue-specific promoters do not work absolutely tissue-specific. This might result in the ectopic expression of Cre and, thus, lead to unintended gene deletion in other cell types. Additionally, the random genomic insertion of Cre is able to cause transgene silencing with uncontrollable effects on cell proliferation and viability and might also show toxic effects on cells *in vitro* and *in vivo*. Furthermore, the targeted promoter needs to reach a high level of activity to ensure a complete excision of the target gene.

In consideration of this knowledge and despite the fact that our mouse system had been already described for even DC migration, activation marker expression and cytokine secretion in DC^{Atg5KO} and DC^{Atg5CTRL} mice (Lee et al., 2010), we wanted to confirm these data with regard to cell frequencies. We evaluated the specific Cre expression and unspecific Cre leakage as well as the frequency of cell subsets such as DCs, macrophages and T cells under steady state conditions.

3.2.1 Cre Expression by CD11c^{+} Cells in DC^{Atg5KO} and DC^{Atg5CTRL} Mice

In order to confirm specific Cre expression in CD11c^{+} cells, cells from spleen and CNS, which derived from either DC^{Atg5KO} or DC^{Atg5CTRL} mice, were analyzed by flow cytometry. Cells were analyzed according to their forward scatter (FSC) and side scatter (SSC) characterictics. And the subsequent analysis was based on their CD45, H2-A^{b} and CD11c expression and the Cre expression on H2-A^{b+} CD11c^{+} double positive cells.

As shown in Figure 3.2, Cre expression was assessed by the relative expression of the conjugate Cre-EGFP and it could be shown that Cre-EGFP is expressed in CD11c^{+} cells from DC^{Atg5KO}, but not from DC^{Atg5CTRL} mice. This result held true for H2-A^{b+} CD11c^{+} cells from both spleen and CNS.

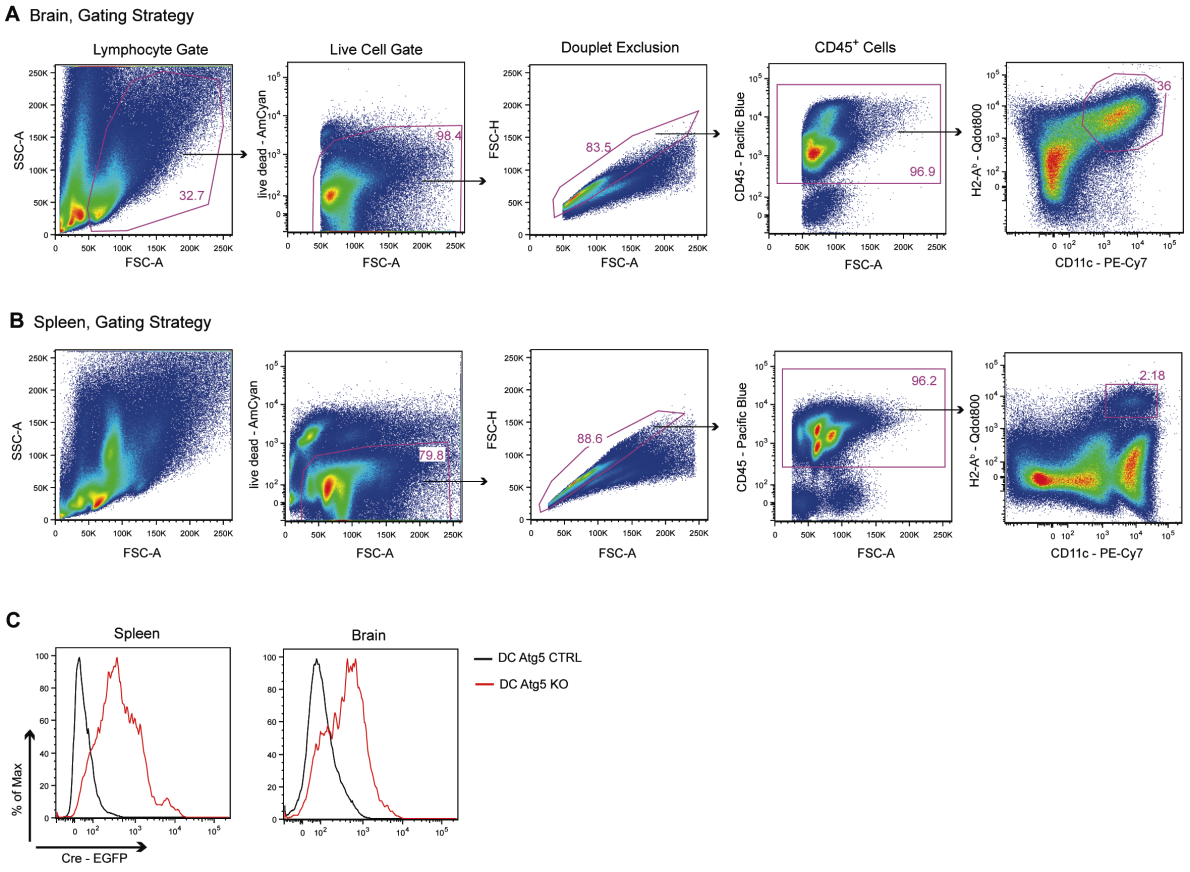

Figure 3.2: Comparison of Cre expression of CD11c^{+} cells originated from spleen and CNS of DC^{Atg5KO} and DC^{Atg5CTRL} mice. Cells from spleen and CNS from DC^{Atg5KO} and DC^{Atg5CTRL} mice were stained with CD45, CD11c and H2-A^{b} antibodies conjugated with fluorochromes. Cells of interest (CD45^{+} CD11c^{+} H2-A^{b+}) were analyzed by flow cytometry and Cre expression levels were assessed by EGFP expression. Gating strategy for the analyses is shown for **(A)** spleen and **(B)** CNS. **(C)** Histogram illustrating Cre expression of CD45^{+} CD11c^{+} H2-A^{b+} cells in spleen and CNS of DC^{Atg5CTRL} (black line) and DC^{Atg5KO} (red line) mice.

3.2.2 Cre Expression in CD4$^+$, CD8$^+$ and CD11b$^+$ Cells

As shown in Figure 3.2, Cre is expressed by H2-A^{b+} CD11c$^+$ cells that were derived from DC^{Atg5KO} mice, but not by H2-A^{b+} CD11c$^+$ cells that were derived from DC^{Atg5CTRL} mice. To further confirm that Cre expression is specific to CD11c$^+$ cells and does not affect unspecifically other cell types, Cre-EGFP expression by CD4$^+$, CD8$^+$ and CD11b$^+$ cells was also assessed by flow cytometry (Figure 3.3). Five DC^{Atg5CTRL} mice and four DC^{Atg5KO} mice were compared to one B/6 wildtype mouse. CD4$^+$, CD8$^+$ and CD11b$^+$ cells do not express Cre-EGFP and, thus, an effect based on Cre leakage into these cell compartments could be excluded in future experiments.

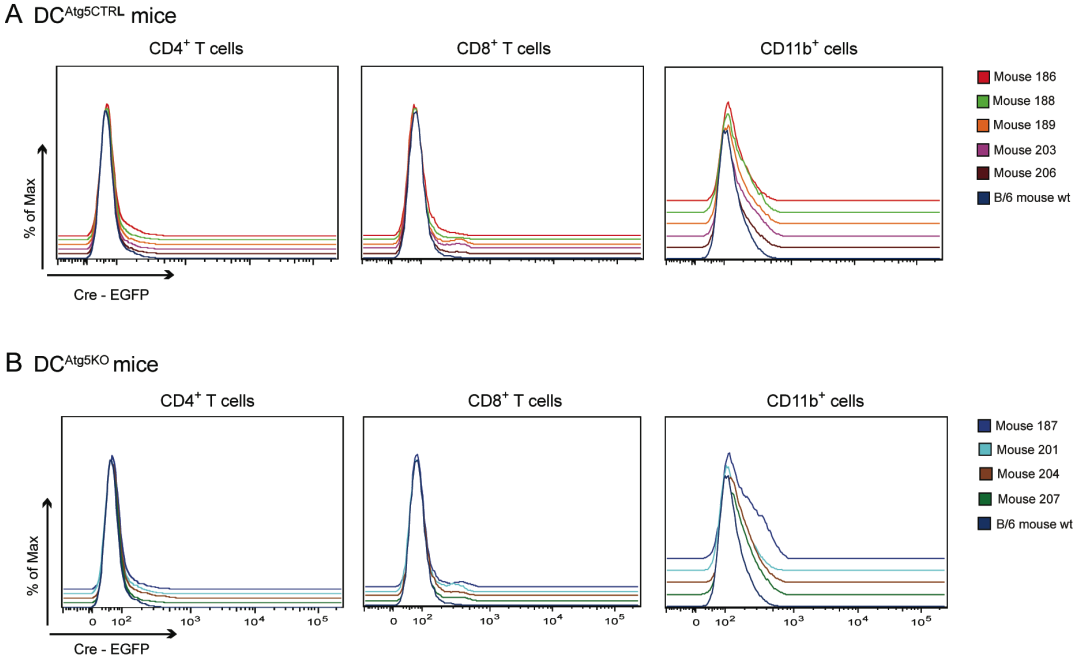

Figure 3.3: Analysis of unspecific Cre-leakage into CD4$^+$, CD8$^+$ and CD11b$^+$ cells. Splenocytes from DC^{Atg5CTRL} and DC^{Atg5KO} mice were stained with CD4, CD8 and CD11b antibodies conjugated with fluorochromes. Cells of interest (CD4$^+$ T cells, CD8$^+$ T cells and CD11b$^+$ cells) were analyzed by flow cytometry and Cre expression levels were assessed by EGFP expression. Flow cytometry analysis of splenic CD4$^+$, CD8$^+$ T cells and CD11b$^+$ cells originated from **(A)** DC^{Atg5CTRL} and **(B)** DC^{Atg5KO} mice.

3.2.3 APC Frequencies in DC^{Atg5CTRL} and DC^{Atg5KO} Mice

Since the Cre/loxP recombination system used in this study targets the CD11c$^+$ cell compartment and, thus, mainly CD11c$^+$ DCs were targeted for Atg5-deficiency, we were eager to investigate the APC frequencies under steady state conditions. In this regard, the splenic frequency of CD11c$^+$ H2-A^{b+} cells, CD11c$^+$ CD8$^+$ CD11b$^+$ CD8 DCs, CD11c$^+$ SiglecH$^+$ pDCs and CD11c$^-$ CD11b$^+$ F4/80$^+$ macrophages was determined under steady state condition. The gating strategy as well as APC frequencies are shown in Figure 3.4. The percentage of CD11c$^+$ H2-A^{b+} was higher in DC^{Atg5CTRL} than in DC^{Atg5KO} mice, but the other APC frequencies did no show a significant difference in DC^{Atg5CTRL} and DC^{Atg5KO} mice. The one outlier seen under almost all conditions goes back to one single mouse.

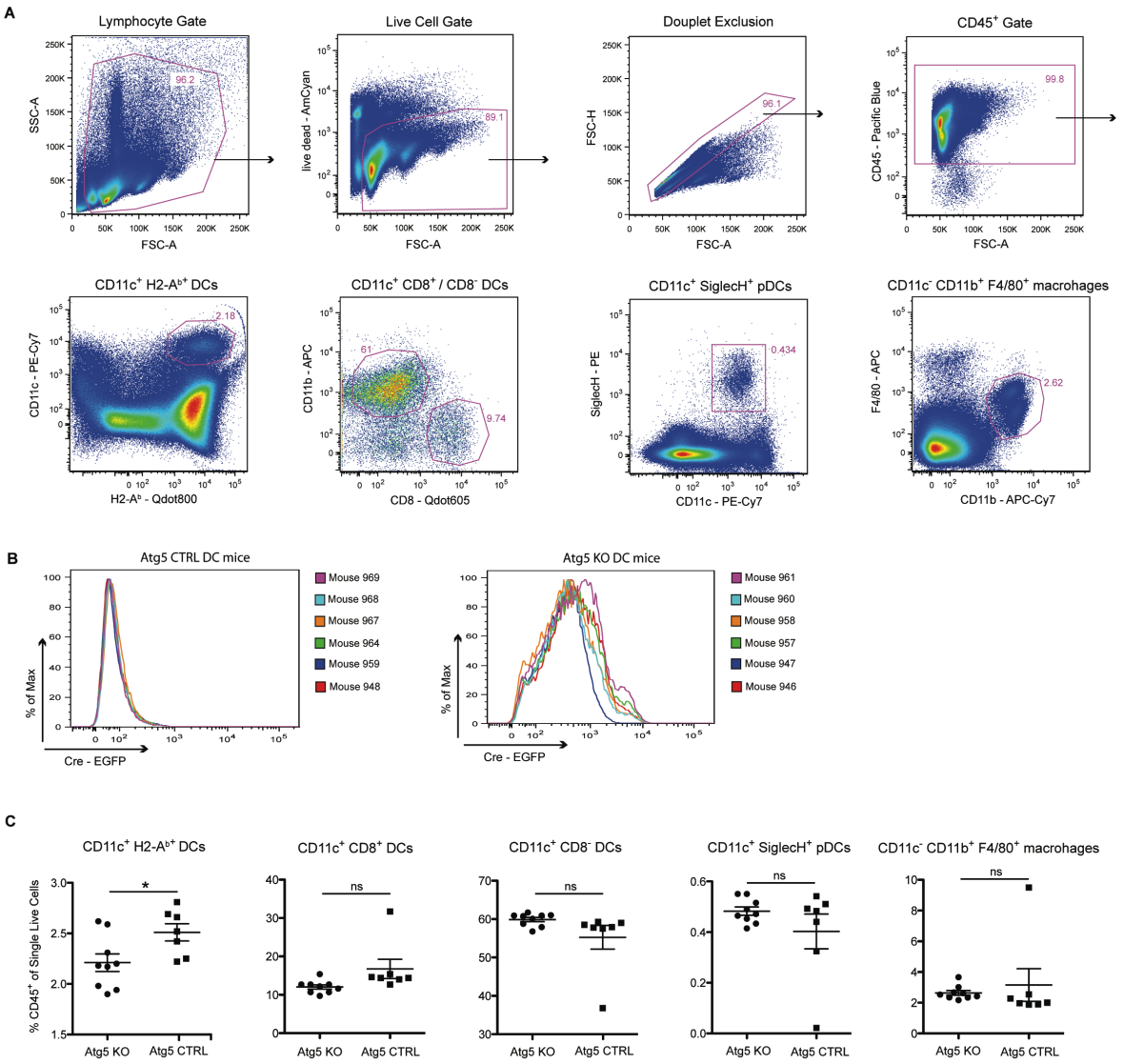

Figure 3.4: APC frequencies in DC^{Atg5KO} and DC^{Atg5CTRL} mice. Splenocytes from DC^{Atg5CTRL} and DC^{Atg5KO} mice were stained with antibodies anti CD45, CD11c, CD11b, H2-A^{b}, SiglecH, CD8, Ly6c, F4/80. Cells were analyzed by flow cytometry based on their FSC and SSC characteristics as well as for APC-specific markers. **(A)** Top row: Gating strategy of flow cytometry analysis is exemplarily shown. Bottom row: Scatter plots to illustrate percentage of CD11c^{+} H2-A^{b+} cells, CD11c^{+} CD8^{+} CD11b^{+} CD8 DCs, CD11c^{+} SiglecH^{+} pDCs and CD11c^{-} CD11b^{+} F4/80^{+} macrophages. **(B)** Assessment of Cre expression levels by EGFP expression in CD11c^{+} H2-A^{b+} splenocytes originated from DC^{ATG5KO} and DC^{ATG5CTRL} mice. **(C)** Percentage of single, live CD45^{+} APC subsets. Each symbol represents one mouse, and horizontal lines indicate the mean with SEM.

3.2.4 T Cell Frequencies in DC^{Atg5KO} and DC^{Atg5CTRL} Mice

Next, T cell frequencies in DC^{Atg5KO} and DC^{Atg5CTRL} mice were investigated. Hence, splenocytes originating from each mouse strain were analyzed by flow cytometry for T cell markers such as CD4 and CD8, but also more specifically for the production of IFNγ (Th1 cells), IL-17 (Th17 cells) and GM-CSF (GM-CSF-producing Th cells) after PMA/ionomycin treatment.

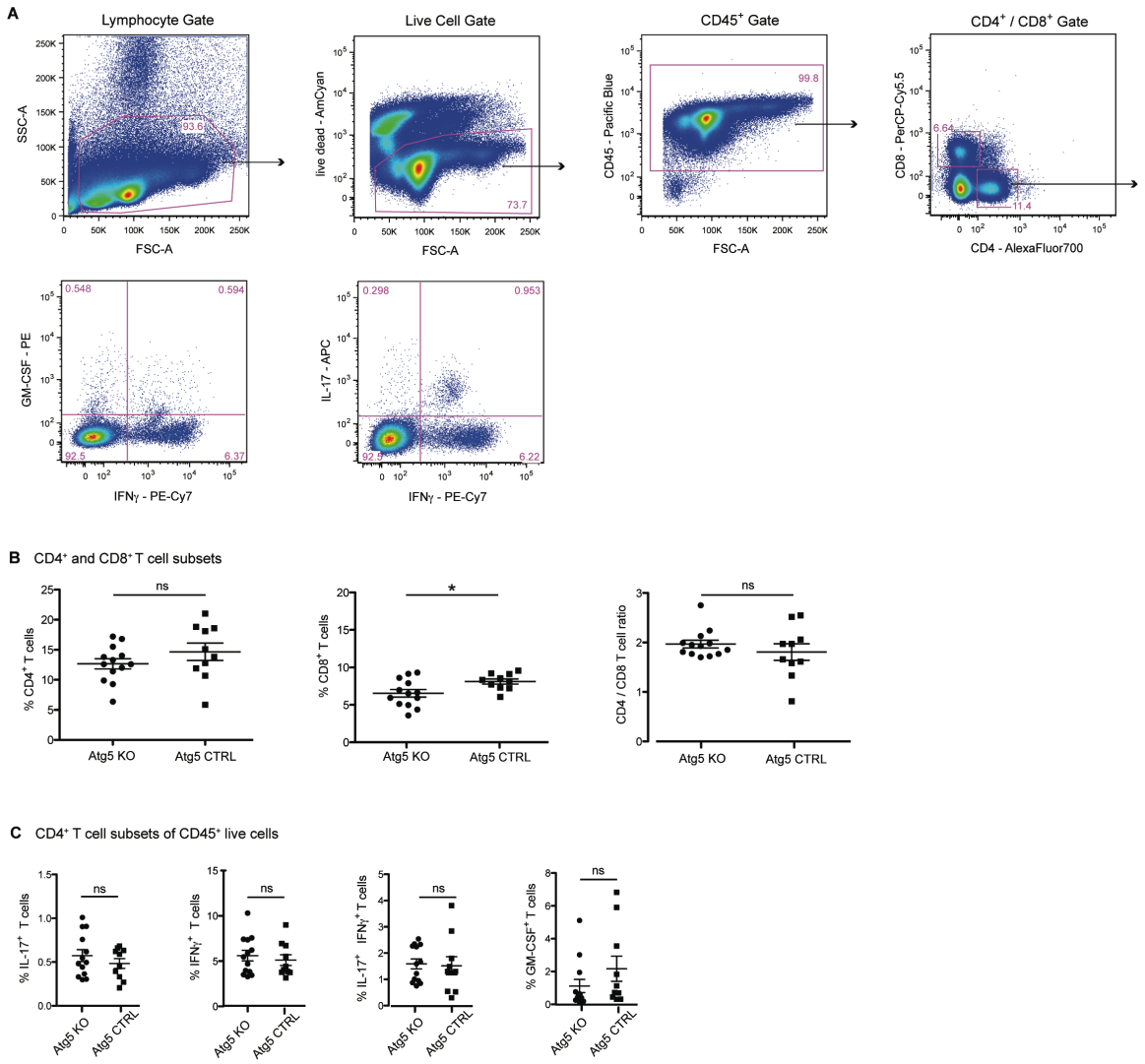

Figure 3.5: Investigation of CD4$^+$ and CD8$^+$ T cell fractions in DC^{Atg5KO} and DC^{Atg5CTRL} mice. Splenocytes from DC^{Atg5CTRL} and DC^{Atg5KO} mice were stained with CD45, CD8, CD4, IFNγ, IL-17 and GM-CSF antibodies. Cells were analyzed by flow cytometry based on their FSC and SSC characteristics as well as for T cell-specific markers. **(A)** Gating strategy of flow cytometry analysis is exemplarily shown. Scatter plots to illustrate percentage of **(B)** CD4$^+$ T cells, CD8$^+$ T cells and CD4/CD8 ratio and **(C)** IL-17, IFN-γ and GM-CSF-producing CD4$^+$ T cells. **(B+C)** Each symbol represents one mouse, and horizontal lines indicate the mean with SEM.

Splenocytes were analyzed according to their FSC and SSC characterictics, as well as to their CD45, CD4 and CD8 expression. The gating strategy applied to analyze these cell subsets is shown in Figure 3.5A. The percentage of CD4$^+$ and CD8$^+$ T cells is shown in Figure 3.5B, whereas the percentage of CD4$^+$ T cells that produce IL-17, IFNγ, IL-17 and IFNγ, or GM-CSF is illustrated in Figure 3.5C. Comparing all T cell subsets from DC^{Atg5KO} and DC^{Atg5CTRL} mice, it was shown that the percentage of CD8$^+$ T cells in DC^{Atg5CTRL} mice was increased compared to DC^{Atg5KO} mice. But the percentage of CD4$^+$ T cells and the level of cytokine production, such as IFNγ, IL-17 and GM-CSF, did not yield a significant difference.

As for the analysis of $CD4^+$ and $CD8^+$ T cells, a similar analysis was performed with regard to the frequency of Tregs in DC^{Atg5KO} and $DC^{Atg5CTRL}$ mice. In this context, Tregs were defined as $CD4^+$ $CD25^+$ and $Foxp3^+$ and were analyzed by flow cytometry.

The gating strategy in the context of this experimental setup and the percentage of Tregs in the spleen of DC^{Atg5KO} and $DC^{Atg5CTRL}$ mice is shown in Figure 3.6. It could be shown that there was no difference in Treg frequencies between DC^{Atg5KO} and $DC^{Atg5CTRL}$ mice. Contrary the results shown in Figure 3.5, in this independent experiment, no statistical difference in the percentage of $CD8^+$ T cells could be demonstrated.

Since the statistical significance of $CD8^+$ T cells in the first experiment was rather low (*P* value 0.0244) and there was no statistical difference in the second experiment, it was concluded the analyzed T cell subsets under steady state conditions show a similar percentage in both groups and that it should not be of any influence during the functional studies performed.

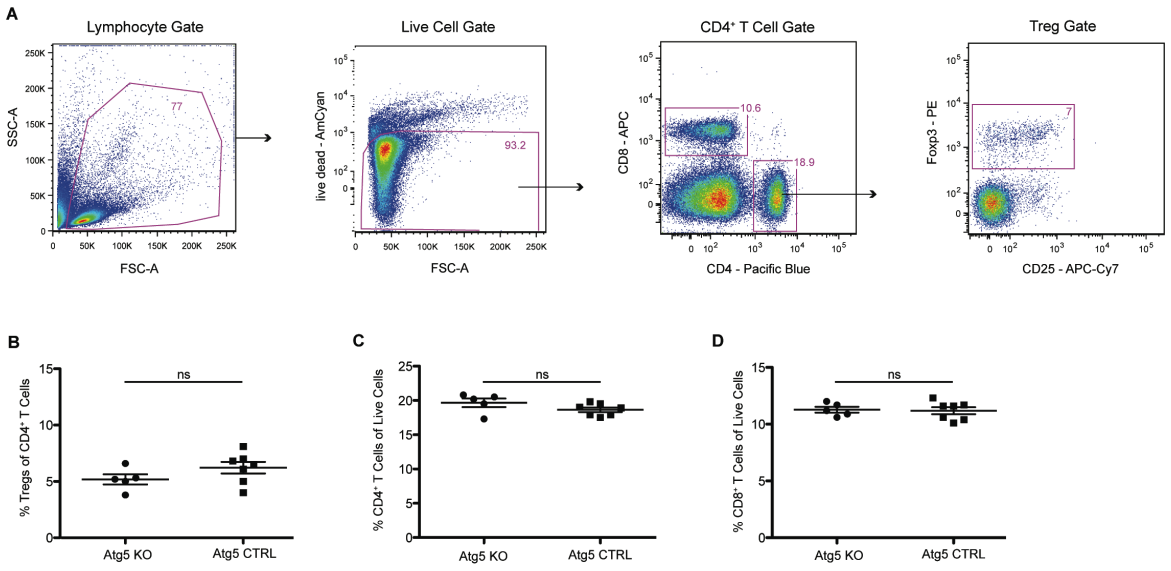

Figure 3.6: Investigation of the percentage of Tregs in DC^{Atg5KO} and $DC^{Atg5CTRL}$ mice. Splenocytes from $DC^{Atg5CTRL}$ and DC^{Atg5KO} mice were stained with CD8, CD4, CD25 and Foxp3 antibodies. Cells were analyzed by flow cytometry based on their FSC and SSC characteristics. Splenic Tregs ($CD4^+$ $CD25^+$ $Foxp3^+$) were analyzed by flow cytometry analysis. **(A)** Gating strategy of flow cytometry analysis is exemplarily shown. Percentage of **(B)** Tregs, **(C)** $CD4^+$ T cells and **(D)** $CD8^+$ T cells are shown as scatter plots. **(B-D)** Each symbol represents one mouse, and horizontal lines indicate the mean with SEM.

3.3 Active EAE in DC^{Atg5KO} and $DC^{Atg5CTRL}$ Mice

3.3.1 Induction of Active EAE with MOG Peptide

In order to investigate the susceptibility and disease severity in DC^{Atg5KO} mice in comparison to $DC^{Atg5CTRL}$ mice, EAE was actively induced in these two mouse strains. Mice were injected subcutaneously with 100 µg of MOG_{35-55} peptide (MOG peptide) in an emulsion with CFA at days 0

and 7. Additionally, PTx was applied at day 0 and 2 intraperitoneally. In total, three independent experiments were performed and each of them is shown in Figure 3.7.

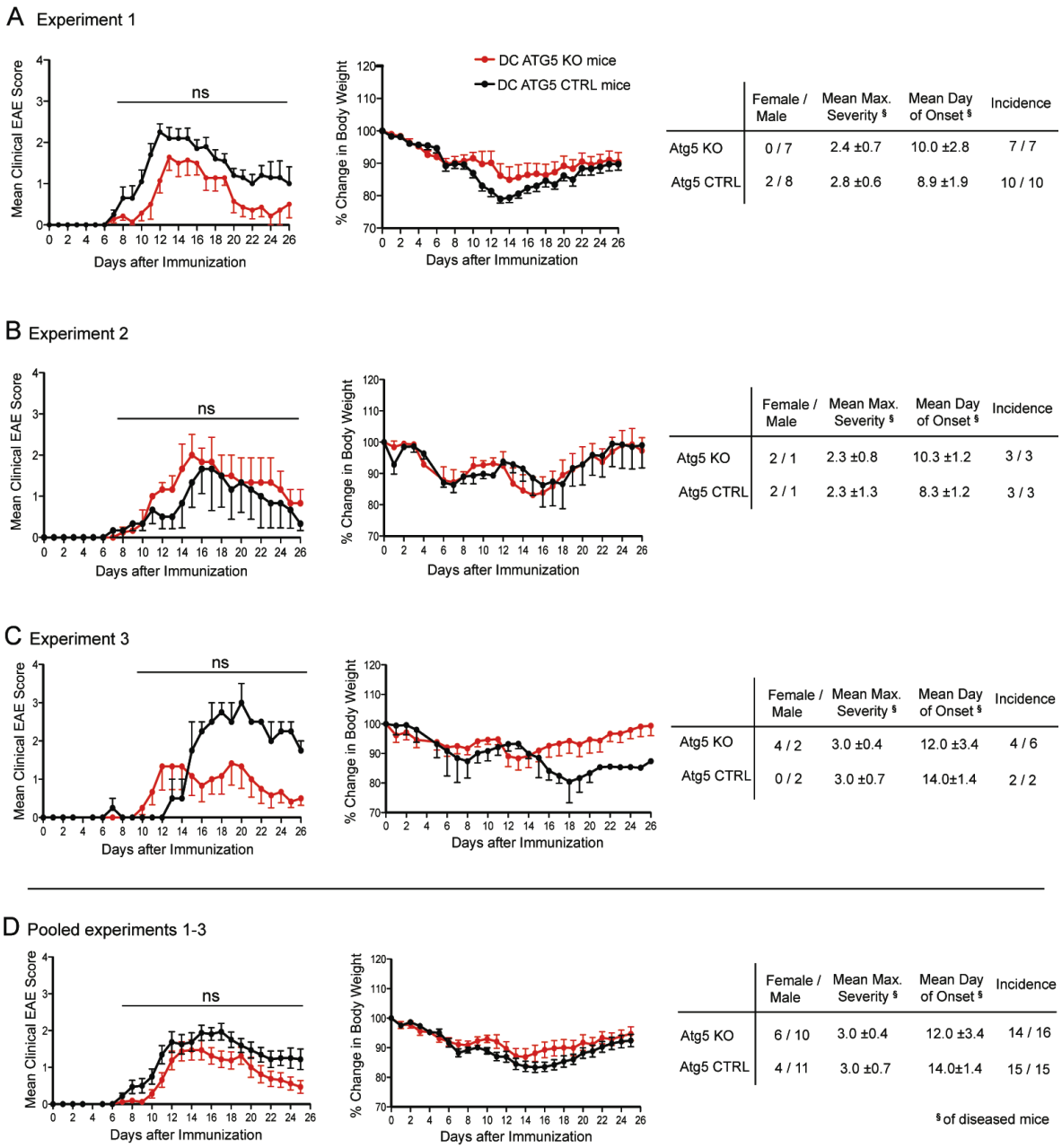

	Female / Male	Mean Max. Severity §	Mean Day of Onset §	Incidence
Atg5 KO	0 / 7	2.4 ±0.7	10.0 ±2.8	7 / 7
Atg5 CTRL	2 / 8	2.8 ±0.6	8.9 ±1.9	10 / 10

	Female / Male	Mean Max. Severity §	Mean Day of Onset §	Incidence
Atg5 KO	2 / 1	2.3 ±0.8	10.3 ±1.2	3 / 3
Atg5 CTRL	2 / 1	2.3 ±1.3	8.3 ±1.2	3 / 3

	Female / Male	Mean Max. Severity §	Mean Day of Onset §	Incidence
Atg5 KO	4 / 2	3.0 ±0.4	12.0 ±3.4	4 / 6
Atg5 CTRL	0 / 2	3.0 ±0.7	14.0±1.4	2 / 2

	Female / Male	Mean Max. Severity §	Mean Day of Onset §	Incidence
Atg5 KO	6 / 10	3.0 ±0.4	12.0 ±3.4	14 / 16
Atg5 CTRL	4 / 11	3.0 ±0.7	14.0±1.4	15 / 15

§ of diseased mice

Figure 3.7: MOG peptide-induced EAE in DC^{Atg5KO} and DC^{Atg5CTRL} mice. Mice were immunized with double injections of 100 µg of MOG peptide. In total three independent experiments were performed **(A-C)** and the pooled data of these experiments are shown in **(D)**. Black dots represent DC^{Atg5CTRL} and red dots DC^{Atg5KO} mice. For each experiment female/male ratio, mean maximum severity, mean day of onset and disease incidence are summarized in table form. § Mean maximum severity and mean day of onset are based on diseased mice. Statistical analysis: ns = not significant, *P < 0.05, **P < 0.01 and ***P < 0.001 two-way analysis of variance (ANOVA) with Bonferroni's post-test. Clinical disease was monitored daily and mice were scored according to the guidelines specified in the material and methods section.

Comparing the clinical EAE course of the three independent experiments, heterogenous results were observed. DC^{Atg5KO} mice showed a more severe disease course than $DC^{Atg5CTRL}$ mice in two experiments, whereas in one experiment the opposite trend was documented. Overall, no difference in EAE score could be shown. For all experiments, the clinical disease course was correlated to the percentage of body weight change. In each experiment a clear correlation between disease course and weight loss could be shown. This reflects the observed EAE scores.

3.3.2 Induction of Active EAE with MOG Protein

No difference in disease severity could be seen when EAE was induced with MOG peptide in $DC^{Atg5CTRL}$ and DC^{Atg5KO} mice. Since it might be that MOG peptide bypasses the requirement for antigen processing, it was reasoned that EAE induction with MOG protein instead of MOG peptide might require the LAP machinery. Accordingly, we hypothesized, that LAP would not be induced in DC^{Atg5KO} mice by the induction of EAE with MOG protein, which might be reflected in a difference in EAE course. To proof this hypothesis, EAE was induced as described above, but with MOG protein instead of MOG peptide. The clinical disease course of three independent experiments as well as the pooled data are depicted in Figure 3.8.

Evaluating the EAE data shown in Figure 3.8, inconsistent results were obtained. In two experiments DC^{Atg5KO} mice showed a more severe disease course than $DC^{Atg5CTRL}$ mice, where in one experiment the opposite trend could be seen. In summary, also under these conditions, no difference in EAE severity could be shown. These results were reflected by the change of body weight.

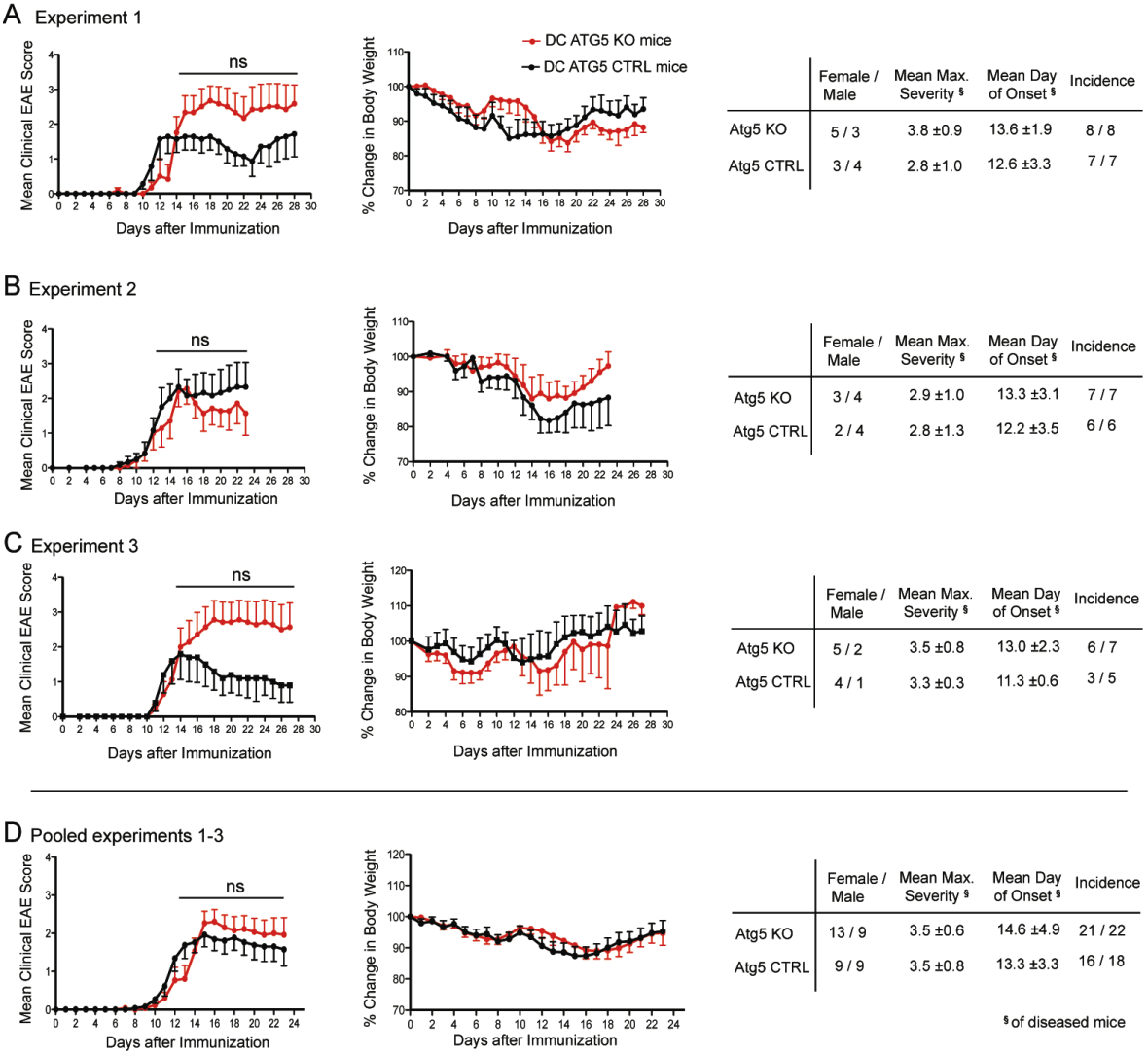

	Female / Male	Mean Max. Severity §	Mean Day of Onset §	Incidence
Atg5 KO	5 / 3	3.8 ±0.9	13.6 ±1.9	8 / 8
Atg5 CTRL	3 / 4	2.8 ±1.0	12.6 ±3.3	7 / 7

	Female / Male	Mean Max. Severity §	Mean Day of Onset §	Incidence
Atg5 KO	3 / 4	2.9 ±1.0	13.3 ±3.1	7 / 7
Atg5 CTRL	2 / 4	2.8 ±1.3	12.2 ±3.5	6 / 6

	Female / Male	Mean Max. Severity §	Mean Day of Onset §	Incidence
Atg5 KO	5 / 2	3.5 ±0.8	13.0 ±2.3	6 / 7
Atg5 CTRL	4 / 1	3.3 ±0.3	11.3 ±0.6	3 / 5

	Female / Male	Mean Max. Severity §	Mean Day of Onset §	Incidence
Atg5 KO	13 / 9	3.5 ±0.6	14.6 ±4.9	21 / 22
Atg5 CTRL	9 / 9	3.5 ±0.8	13.3 ±3.3	16 / 18

§ of diseased mice

Figure 3.8: MOG protein-induced EAE in DC^{Atg5KO} and $DC^{Atg5CTRL}$ mice. Mice were immunized with double injections of 100 µg of MOG protein. In total three independent experiments were performed **(A-C)** and the pooled data of these experiments are shown in **(D)**. Black dots represent $DC^{Atg5CTRL}$ and red dots DC^{Atg5KO} mice. For each experiment female/male ratio, mean maximum severity, mean day of onset and disease incidence are summarized in table form. § Mean maximum severity and mean day of onset are based on diseased mice. Statistical analysis: ns = not significant, $*P < 0.05$, $**P < 0.01$ and $***P < 0.001$ two-way ANOVA with Bonferroni's post-test. Clinical disease was monitored daily and mice were scored according to the guidelines specified in the material and methods section.

3.3.3 Induction of Active EAE with Different Concentrations of MOG protein

When EAE was induced with either MOG peptide or MOG protein, no difference in disease course or severity could be shown when $DC^{Atg5CTRL}$ and DC^{Atg5KO} mice were compared (Figure 3.7 and 3.8). Based on these results, it was assumed that the high amount of MOG peptide or MOG protein and CFA might have caused such a strong immune response that potential differences between the two experimental groups were masked. Accordingly, it was considered that a decrease in antigenic load might lead to a better-controlled immune response that might result in more consistent results.

In the experimental setup, DC^{Atg5KO} and $DC^{Atg5CTRL}$ mice were injected with either 50 µg or 20 µg of MOG protein. The amount of CFA was kept at a constant level and only the amount of MOG protein was decreased.

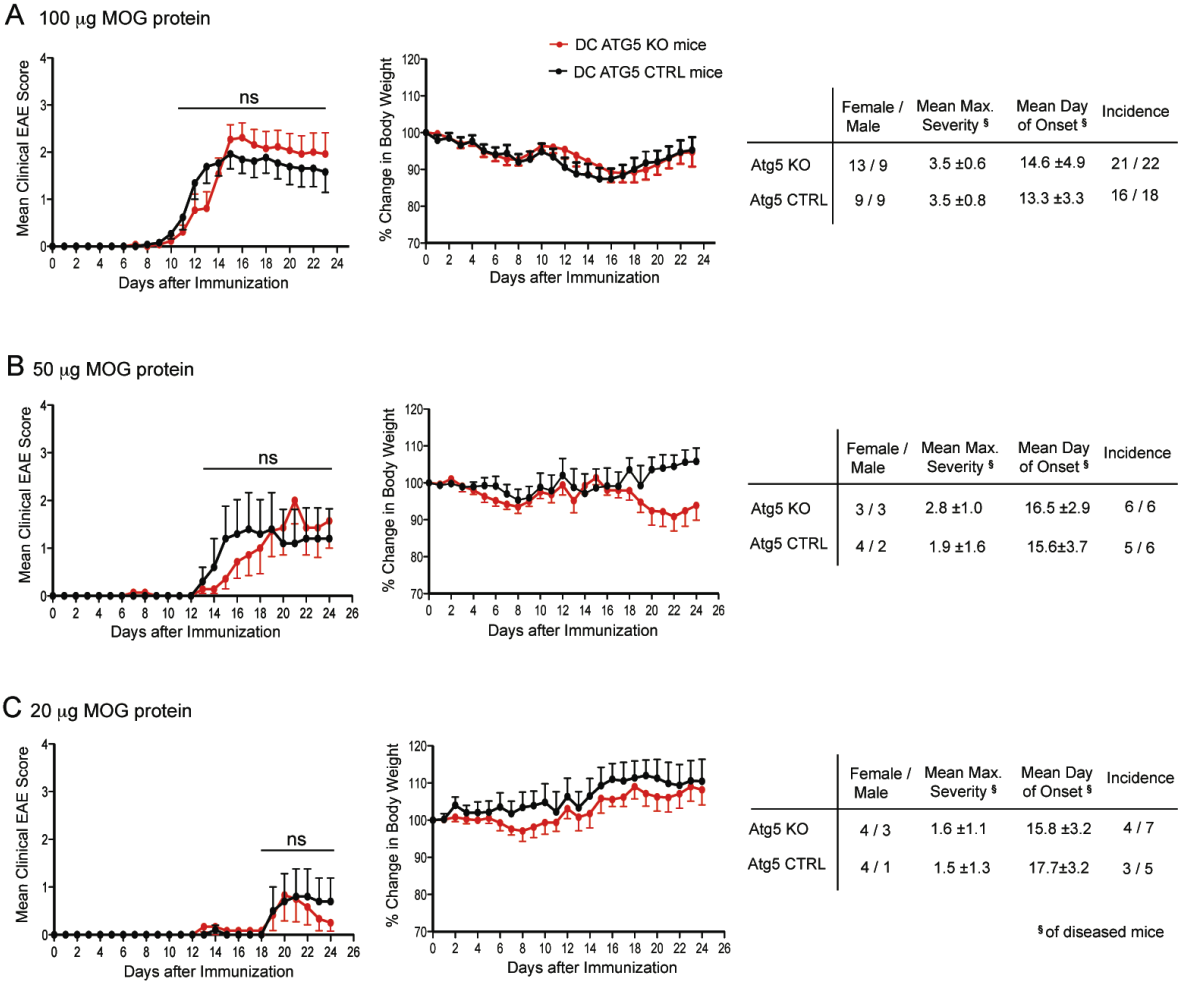

	Female / Male	Mean Max. Severity §	Mean Day of Onset §	Incidence
Atg5 KO	13 / 9	3.5 ±0.6	14.6 ±4.9	21 / 22
Atg5 CTRL	9 / 9	3.5 ±0.8	13.3 ±3.3	16 / 18

	Female / Male	Mean Max. Severity §	Mean Day of Onset §	Incidence
Atg5 KO	3 / 3	2.8 ±1.0	16.5 ±2.9	6 / 6
Atg5 CTRL	4 / 2	1.9 ±1.6	15.6±3.7	5 / 6

	Female / Male	Mean Max. Severity §	Mean Day of Onset §	Incidence
Atg5 KO	4 / 3	1.6 ±1.1	15.8 ±3.2	4 / 7
Atg5 CTRL	4 / 1	1.5 ±1.3	17.7±3.2	3 / 5

§ of diseased mice

Figure 3.9: Titration of MOG protein during the induction of active EAE in DC^{Atg5KO} and $DC^{Atg5CTRL}$ mice. Active EAE was induced with double injections of **(A)** 100 µg, **(B)** 50 µg or **(C)** 20 µg of MOG protein. Results are shown in line graphs where black dots represent $DC^{Atg5CTRL}$ mice and red dots DC^{Atg5KO} mice. For each experiment female/male ratio, mean maximum severity, mean day of onset and disease incidence are summarized in table form. § Mean maximum severity and mean day of onset are based on diseased mice. Statistical analysis: ns = not significant, $*P < 0.05$, $**P < 0.01$ and $***P < 0.001$ two-way ANOVA with Bonferroni's post-test. Clinical disease was monitored daily and mice were scored according to the guidelines specified in the material and methods section.

When DC^{Atg5KO} and $DC^{Atg5CTRL}$ mice were injected with different amounts of MOG protein, it could be shown that disease incidence decreases with lower amounts of MOG protein injected. The lower disease incidence is reflected in a lower clinical EAE score. This holds true for both experimental groups and no difference between groups could be shown.

3.3.4 Induction of Active EAE in DC^{Atg7KO} and $DC^{Atg7CTRL}$ Mice with MOG protein

In one of the intermediate steps of autophagosomal formation, Atg12 is first ligated to Atg5 by assistance of the E1-like enzyme Atg7. In a next step, this conjugate forms a complex with Atg16L1 which results in a complex named Atg5-Atg12/Atg16L1. This protein complex is essential for the ligation of Atg8 to the autophagosomal membrane. Conclusively, Atg5 as well as Atg7 are similarly essential for the formation of the autophagosome. Since Atg5 is also described to be of importance in autophagy-unrelated processes such as regulation of apoptosis, exocytosis and innate antiviral immune signalling (Subramani and Malhotra, 2013), we wanted to control for an autophagy-specific effect in our model by using a control mouse strain, namely $Atg7^{flox/flox}$ CD11c-$Cre^{-/-}$ ($DC^{Atg7CTRL}$ mice) and $Atg7^{flox/flox}$ CD11c-$Cre^{+/-}$ (DC^{Atg7KO} mice). This mouse system is based on the same principal as for the Atg5 KO system, but lacks Atg7 instead of Atg5 in the $CD11c^{+}$ cell compartment. To control for the autophagy-specific effect in the EAE model, DC^{Atg7KO} and $DC^{Atg7CTRL}$ mice were injected with double injections of 100 µg of MOG protein as described above. The results of three independent experiments are shown in Figure 3.10.

In all three experiments both experimental groups showed a similar course of disease and percentage of body weight change. Furthermore, mean maximmum score and mean day of onset as well as the disease incidence did not differ between groups.

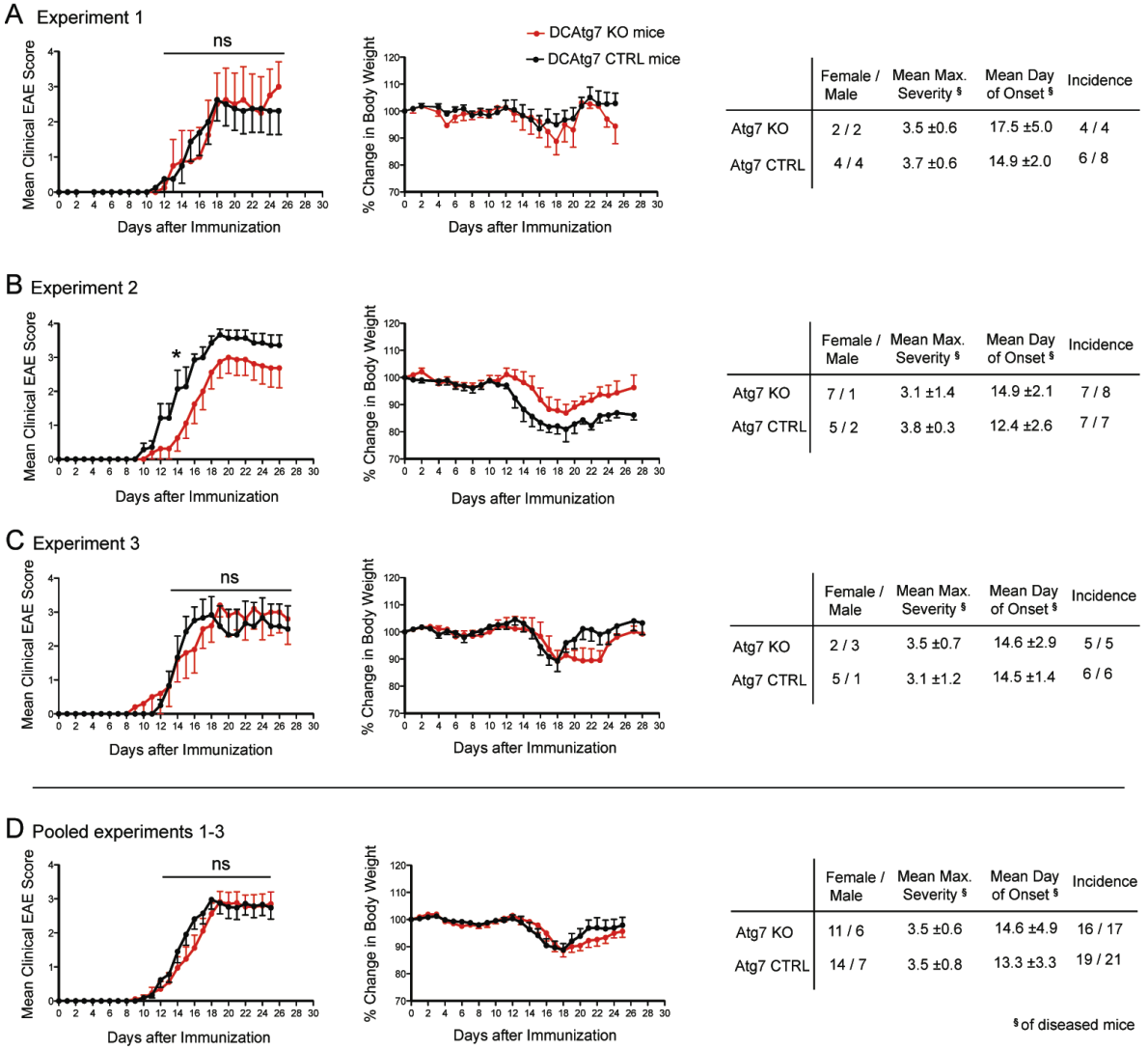

	Female / Male	Mean Max. Severity §	Mean Day of Onset §	Incidence
Atg7 KO	2 / 2	3.5 ±0.6	17.5 ±5.0	4 / 4
Atg7 CTRL	4 / 4	3.7 ±0.6	14.9 ±2.0	6 / 8

	Female / Male	Mean Max. Severity §	Mean Day of Onset §	Incidence
Atg7 KO	7 / 1	3.1 ±1.4	14.9 ±2.1	7 / 8
Atg7 CTRL	5 / 2	3.8 ±0.3	12.4 ±2.6	7 / 7

	Female / Male	Mean Max. Severity §	Mean Day of Onset §	Incidence
Atg7 KO	2 / 3	3.5 ±0.7	14.6 ±2.9	5 / 5
Atg7 CTRL	5 / 1	3.1 ±1.2	14.5 ±1.4	6 / 6

	Female / Male	Mean Max. Severity §	Mean Day of Onset §	Incidence
Atg7 KO	11 / 6	3.5 ±0.6	14.6 ±4.9	16 / 17
Atg7 CTRL	14 / 7	3.5 ±0.8	13.3 ±3.3	19 / 21

§ of diseased mice

Figure 3.10: MOG protein-induced EAE in DC^{Atg7KO} and DC^{Atg7CTRL} mice. Mice were immunized with double injections of 100 µg of MOG peptide. In total three independent experiments were performed **(A-C)** and the pooled data of these experiments are shown in **(D)**. Black dots represent DC^{Atg7CTRL} and red dots DC^{Atg7KO} mice. For each experiment female/male ratio, mean maximum severity, mean day of onset and disease incidence are summarized in table form. § Mean maximum severity and mean day of onset are based on diseased mice. Statistical analysis: ns = not significant, *P < 0.05, **P < 0.01 and ***P < 0.001 two-way ANOVA with Bonferroni's post-test. Clinical disease was monitored daily and mice were scored according to the guidelines specified in the material and methods section.

3.4 Adoptive transfer EAE in DC^{Atg5KO} and DC^{Atg5CTRL} Mice

Actively induced EAE by the injection of either MOG peptide or MOG protein did not yield any differences between DC^{Atg5KO} and DC^{Atg5CTRL} mice in terms of EAE severity (Figure 3.7 and 3.8). As mentioned earlier, a possible reason for the absence of a phenotype could be the fact that MOG peptide and MOG protein might not be processed in the context of LAP or macroautophagy. It was further reasoned that particulate antigen might be necessary to induce this pathway in the context of

EAE since it had been already shown that LAP can be induced by the uptake of dead cells (Martinez et al., 2011) or even live cells by entosis (Florey et al., 2011).

In the adoptive transfer model of EAE, in contrast to the active induction of EAE, transferred myelin-reactive T cells encounter the self-antigen in the recipient mouse for the first time when it is presented by local APCs in the CNS. This self-antigen, in the form of cells or cell debris, needs to be processed and presented. Atg5-deficient $CD11c^{+}$ cells might not be able to process the self-antigen properly and, thus, might not be competent in reactivating infiltrating myelin-reactive T cells. Accordingly, EAE was induced by adoptive transfer of auotreactive T cells in DC^{Atg5KO} and $DC^{Atg5CTRL}$ mice. 2D2 transgenic mice, that carry a MOG-specific TCR, were injected with MOG peptide. Seven days later, splenocytes and cells from axillary and inguinal lymph nodes were isolated, re-stimulated in the presence of MOG peptide and IL-23 and, finally, adoptively transferred to DC^{Atg5KO} and $DC^{Atg5CTRL}$ recipient mice. The results from this experiment are depicted in Figure 3.11.

So far, three independent experiments have been performed. It could be demonstrated that almost none of the DC^{Atg5KO} mice developed EAE symptoms or showed a change in body weight. Whereas, $DC^{Atg5CTRL}$ mice showed a comparable course of disease as in the experiments described above. That means that $DC^{Atg5CTRL}$ mice showed a similar disease onset at day 15.4 (± 2.7 days), mean maximum severity of 3.6 (± 0.7) and a disease incidence of 80.0% when compared to the mice described in earlier experiments (Figure 3.7 and 3.8).

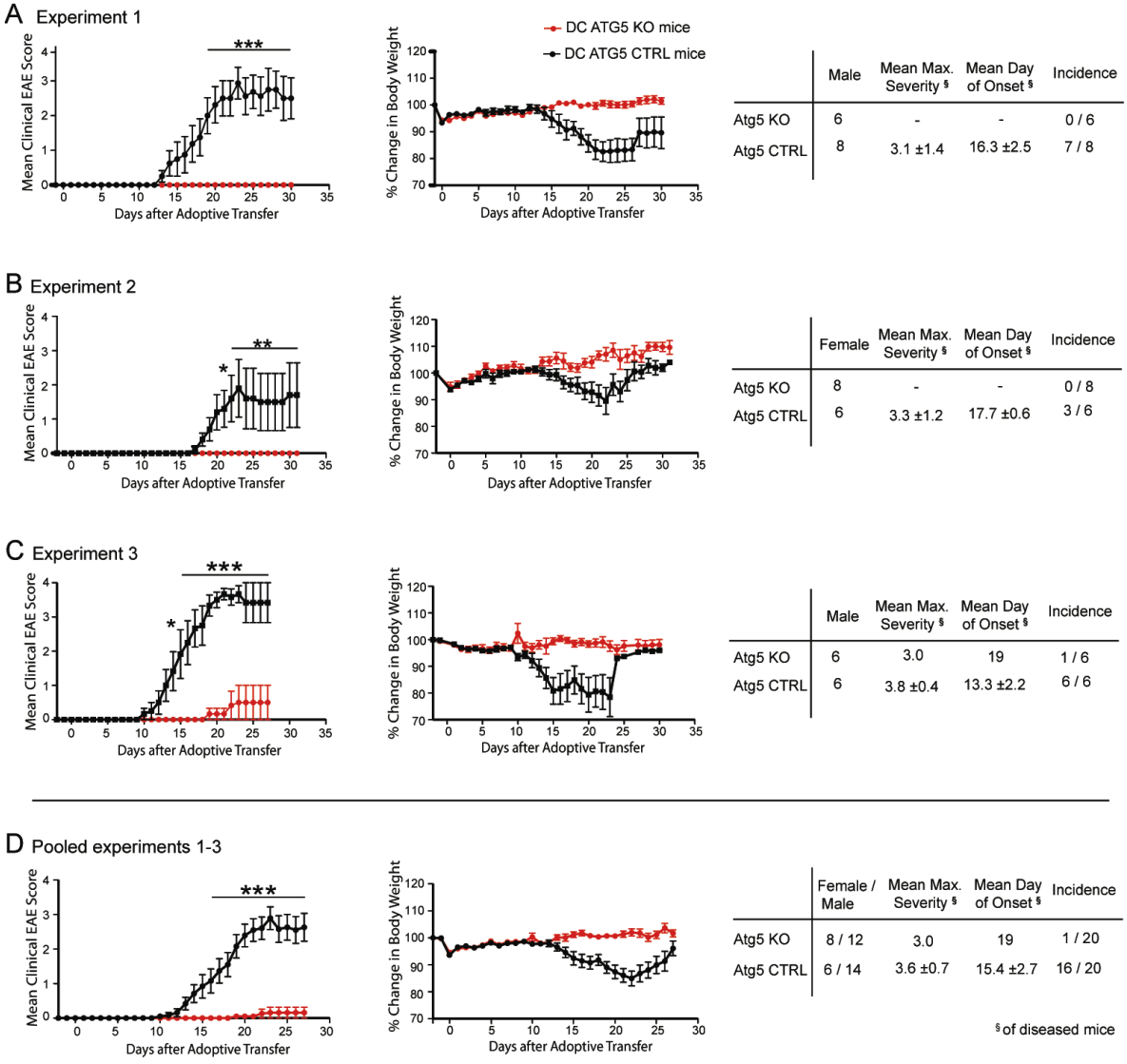

	Male	Mean Max. Severity §	Mean Day of Onset §	Incidence
Atg5 KO	6	-	-	0 / 6
Atg5 CTRL	8	3.1 ±1.4	16.3 ±2.5	7 / 8

	Female	Mean Max. Severity §	Mean Day of Onset §	Incidence
Atg5 KO	8	-	-	0 / 8
Atg5 CTRL	6	3.3 ±1.2	17.7 ±0.6	3 / 6

	Male	Mean Max. Severity §	Mean Day of Onset §	Incidence
Atg5 KO	6	3.0	19	1 / 6
Atg5 CTRL	6	3.8 ±0.4	13.3 ±2.2	6 / 6

	Female / Male	Mean Max. Severity §	Mean Day of Onset §	Incidence
Atg5 KO	8 / 12	3.0	19	1 / 20
Atg5 CTRL	6 / 14	3.6 ±0.7	15.4 ±2.7	16 / 20

§ of diseased mice

Figure 3.11: Adoptive transfer EAE experiment with DC^{Atg5KO} and DC^{Atg5CTRL} mice. 2D2 mice were immunized with MOG peptide and at day seven splenocytes were removed. Splenocytes were cultured for two days in the presence of MOG peptide and IL-23 and then transferred into sublethally irradiated recipient DC^{Atg5KO} and DC^{Atg5CTRL} mice. In total three independent experiments were performed **(A-C)** and clinical EAE score as well as change in body weight are shown. The pooled data of these experiments are shown in **(D)**. Black dots represent DC^{Atg5CTRL} and red dots DC^{Atg5KO} mice. For each experiment gender, mean maximum severity, mean day of onset and disease incidence are summarized in table form. § Mean maximum severity and mean day of onset are based on diseased mice. Statistical analysis: ns = not significant, *P < 0.05, **P < 0.01 and ***P < 0.001 two-way ANOVA with Bonferroni's post-test. Clinical disease was monitored daily and mice were scored according to the guidelines specified in the material and methods section.

3.5 *In Vitro* Studies of Antigen Processing and Presentation

Based on the results of the *in vivo* EAE experiments presented in chapter 3.4, the deficiency of Atg5 in $CD11c^+$ APCs does have an effect on the development and progression of adoptive transfer EAE. In order to investigate the processes that lead to this effect, we were eager to perform *in vitro* studies to define the underlying mechanism.

3.5.1 Antigen Presentation Assay

Antigen processing and presenting capabilities of DCs were assessed by co-cultures with T cells. DCs from spleen of either $DC^{Atg5CTRL}$ or DC^{Atg5KO} mice were isolated by MACS ($CD11c^+$ selection) and FACS ($CD45^+$ $CD11c^+$ H2-A^{b+}). In parallel, MOG-specific $CD4^+$ T cells were isolated from spleen from 2D2 mice by positive MACS isolation ($CD4^+$ selection) and were CFSE-labelled in a final step. DCs and T cells were co-cultured at a ratio of 1:3 in the presence of MOG peptide, MOG protein or polystyrene beads coated with MOG protein. Beads were added to the co-culture at different beads to DC ratios ranging from 0.5:1, 1:1, 2:1, 4:1 to 8:1. Cells were co-cultured for four days and T cell proliferation was assessed by CFSE dilution. As positive control, T cells were incubated with anti CD3 and anti CD28 plate-bound antibodies. As negative control, T cells were cultured alone or in the presence of DCs only.

The pooled results of three independent experiments are shown in Figure 3.12. T cells in presence of CD3/CD28 and T cells co-cultured with DCs in the presence of MOG peptide showed a blasted phenotype based on their FSC and SSC characteristics. In contrast, T cells alone did not blast at all. T cell proliferation was assessed by CFSE dilution.

Because of the variations between experiments in terms of T cell survival and T cell proliferation, each experiment was normalized to the condition Atg5CTRL DCs and T cells in the presence of 1 µM of MOG peptide. T cell proliferation in the presence of DCs derived from either DC^{Atg5KO} or $DC^{Atg5CTRL}$ mice was higher in the presence of Atg5-deficient DCs when MOG protein or beads coated with MOG protein were present. Even under conditions under which statistical difference could not be reached the same trend held true.

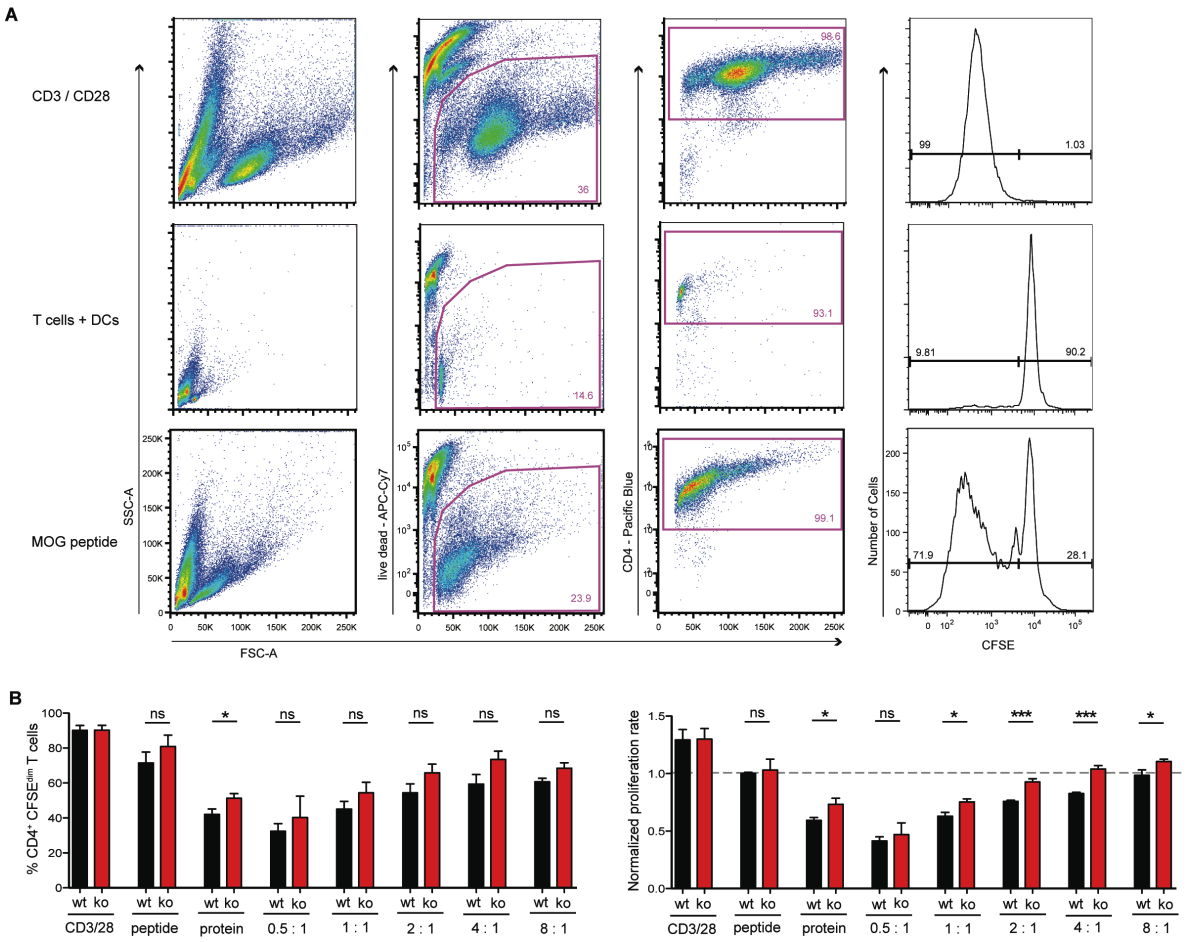

Figure 3.12: DC:T cell co-culture to study the antigen presentation capabilities of primary DCs. Splenic DCs ($CD11c^{+}$ $H2\text{-}A^{b+}$) originated from either $DC^{Atg5CTRL}$ or DC^{Atg5KO} mice were MACS and FACS-isolated and co-cultured with MOG-specific $CD4^{+}$ $CFSE^{+}$ T cells in the presence of antigen for four days. As antigen 1 µM of MOG peptide or protein and beads coated with MOG protein were used. Beads were incubated with the cells at a bead to DC ratio of 0.5:1, 1:1, 2:2, 4:1 and 8:1. As positive control T cells were stimulated by anti-CD3 and CD28 treatment. As a read-out for antigen presentation, T cell proliferation was assessed by a CFSE dilution assay. **(A)** Gating strategy to determine percentage of proliferated T cells ($CD4^{+}$ $CFSE^{low}$). Three experimental setups are shown. Top: CD3/CD28 stimulation as positive control, middle: T cells and DCs withouth stimulus, bottom: T cells and DCs in the presence of 1 µM MOG peptide. **(B)** Left: Percentage of proliferated T cells in the presence of various stimuli (see above). Right: Same experimental setup as on left, but data were normalized. The percentage of $DC^{Atg5CTRL}$ DCs in the 1 µM MOG peptide condition was set to 1. Black symbols: DCs originated from $DC^{Atg5CTRL}$ mice. Red symbols: DCs originated from DC^{Atg5KO} mice. Pooled data of three independent experiments are shown.

3.5.2 Phagocytosis Assay

3.5.2.1 Characterization of BM-DCs as an *In Vitro* Model

To study phagocytic capabilities of DCs, the *in vitro* model of our choice was bone marrow-derived dendritic cells (BM-DCs). BM-DCs are widely used as a model for APCs and show the classical characteristics of an APC such as antigen processing and presentation competences as well as T cell activating capabilities.

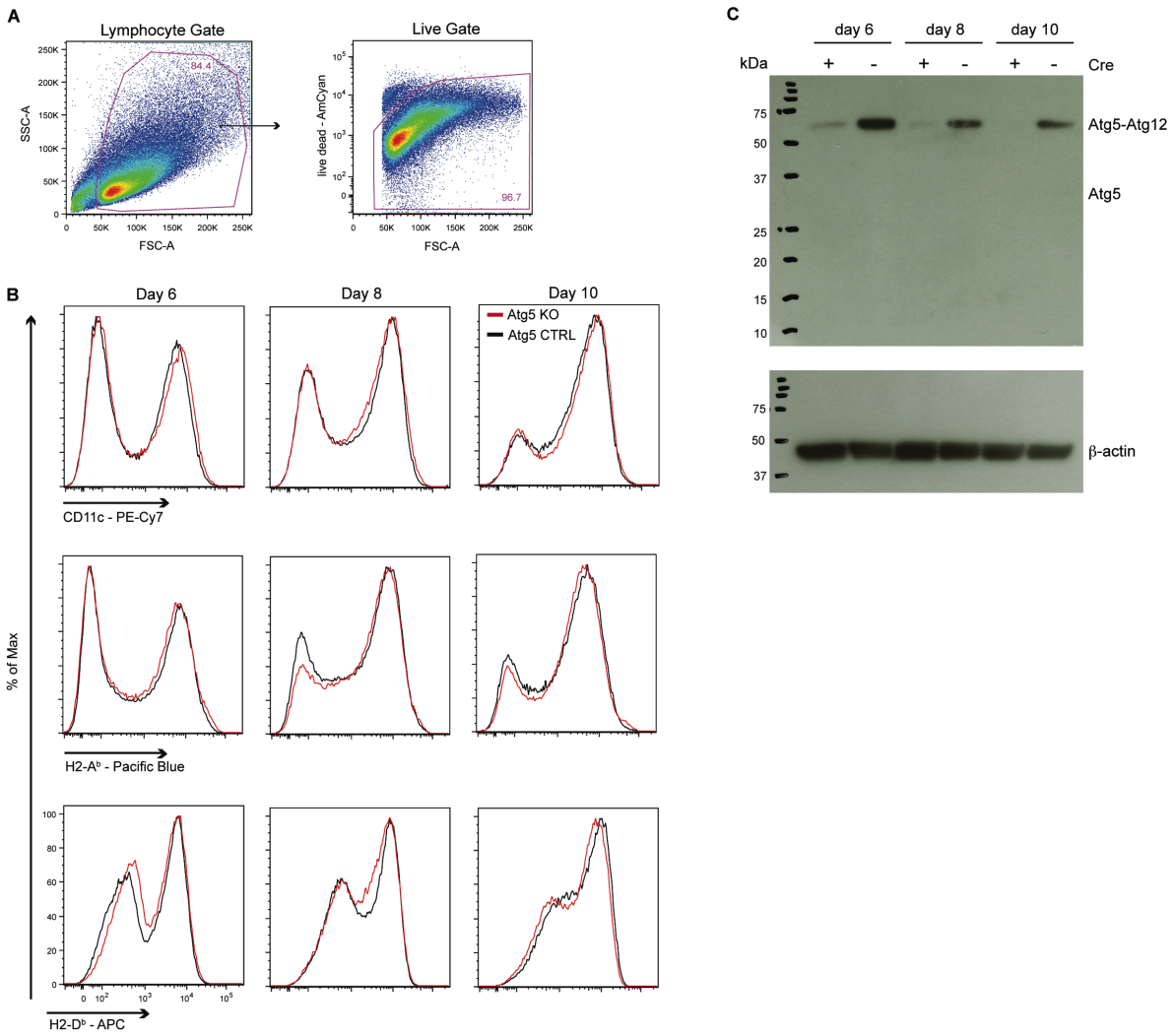

Figure 3.13: Investigation of mouse BM-DCs for CD11c, H2-A^b and H2-K^b expression and Atg5-deficiency in a time-dependent manner. BM-DCs were differentiated from mouse bone marrow of DC^{Atg5CTRL} and DC^{Atg5KO} mice in the presence of GM-CSF. **(A+B)** At day 6, 8 and 10 BM-DCs were stained with CD11c, H2-A^b and H2-K^b antibodies. **(A)** FSC and SSC characteristics of BM-DCS at day 6. **(B)** Analysis of cell surface expression of CD11c, H2-A^b and H2-K^b by flow cytometry at day 6, 8 and 10. **(C)** At day 6, 8 and 10 BM-DCs were also analyzed by anti-Atg5 Western blot for Atg5-deficiency. Anti-β-actin was used as a loading control and Precision Plus Protein Standard from BioRad was used to estimate protein size.

For the purpose of our studies, BM-DCs derived from bone marrow were differentiated in the presence of GM-CSF. It is noted that BM-DCs differentiated in the presence of GM-CSF are distinct from BM-DCs differentiated in the presence of Flt3L. More specifically, BM-DCs differentiated in the presence of GM-CSF resemble the inflammatory or TipDC type, whereas BM-DCs differentiated in the presence of Flt3L show more features of cDCs and pDCs (Harding et al., 2001; Xu et al., 2007b).

BM-DCs originated from either DC^{Atg5CTRL} or DC^{Atg5KO} mice were used. To ensure the same phenotypic features of these two cell lineages, BM-DCs from DC^{Atg5CTRL} and DC^{Atg5KO} mouse origin were analyzed for CD11c, H2-A^b and H2-K^b expression at days 6, 8 and 10 by flow cytometry. Histograms illustrating the relative expression of these cell surface molecules are shown in Figure

3.13B. Furthermore, Atg5-deficiency of these BM-DCs was investigated by anti-Atg5 Western blot. The results of this Western blot are shown in Figure 3.13C.

The cell surface expression of CD11c, H2-A^b and H2-K^b on BM-DCs was documented over time. All three markers were upregulated over time and no differences between cells from $DC^{Atg5CTRL}$ and DC^{Atg5KO} mice were detected. Furthermore, Atg5 expression by theses BM-DCs were checked on day six, seven and ten by Western blot analysis. A decrease of Atg5 in BM-DCs from DC^{Atg5KO} mice was detected over time and reached a total ablation at day ten. In contrast, Atg5 was present in BM-DCs of $DC^{Atg5CTRL}$ mice at all time points tested.

3.5.2.2 Phagocytosis of Beads by BM-DCs

We next investigated the antigen uptake of the self-antigen MOG protein. Classically, small soluble peptides and proteins are taken-up by fluid-phase endocytosis, also known as macropinocytosis (Blum et al., 2013). So far, LAP has been associated with the degradation of intracellular pathogens such as bacteria (Gong et al., 2011; Lam et al., 2013), particles associated with ligands for TLR2, 4 or 6 (Sanjuan et al., 2007), the detection of apoptotic cells by their exposure of phophatidylserine and their recognition by T cell immunoglobulin mucin-4 (TIM-4) (Martinez et al., 2011) as well as the uptake of live cells by entosis (Florey et al., 2011). However, LAP has not been described in the context of macropinocytosis. Conclusively, the soluble self-antigen MOG protein it-self is most likely not targeted by LAP.

In order to study antigen uptake in the context of LAP, we were eager to find a method that induces LAP-associated uptake of self-protein. It had been already shown in other autophagy studies, that extracellular antigen coated to beads can be taken up and degraded in the context of LAP (Sanjuan et al., 2007). Based on those studies and unpublished data from our laboratory (Susana de Freitas Romão, personal communication), MOG protein was coupled to polystyrene beads and incubated with BM-DCs. Beads and BM-DCs were cultured at a ratio of 10:1 for a time span of four hours. In a next step, phagocytic uptake was assessed by fluorescent microscopy where beads were identified as round black wholes with a diameter of roughly 3.9 μm. LAP was visualized by anti-LC3 staining. A representative immunocytochemistry picture is shown in Figure 3.13. No LAP formation could be detected when beads were coated with MOG protein. Since MOG protein is a self-protein and is not supposed to trigger pattern recognition receptors, which are known to induce LAP, it was reasoned to induce LAP by a known trigger. An already described trigger of LAP is Pam3CSK4 - a synthetic triacylated lipoprotein that mimics bacterial lipoproteins (Sanjuan et al., 2007). Accordingly, polystyrene beads were coated with Pam3CSK4 or, in an independent setup, with Pam3CSK4 and MOG protein. The analyses of these experimental setups are summarized in Figure 3.13.

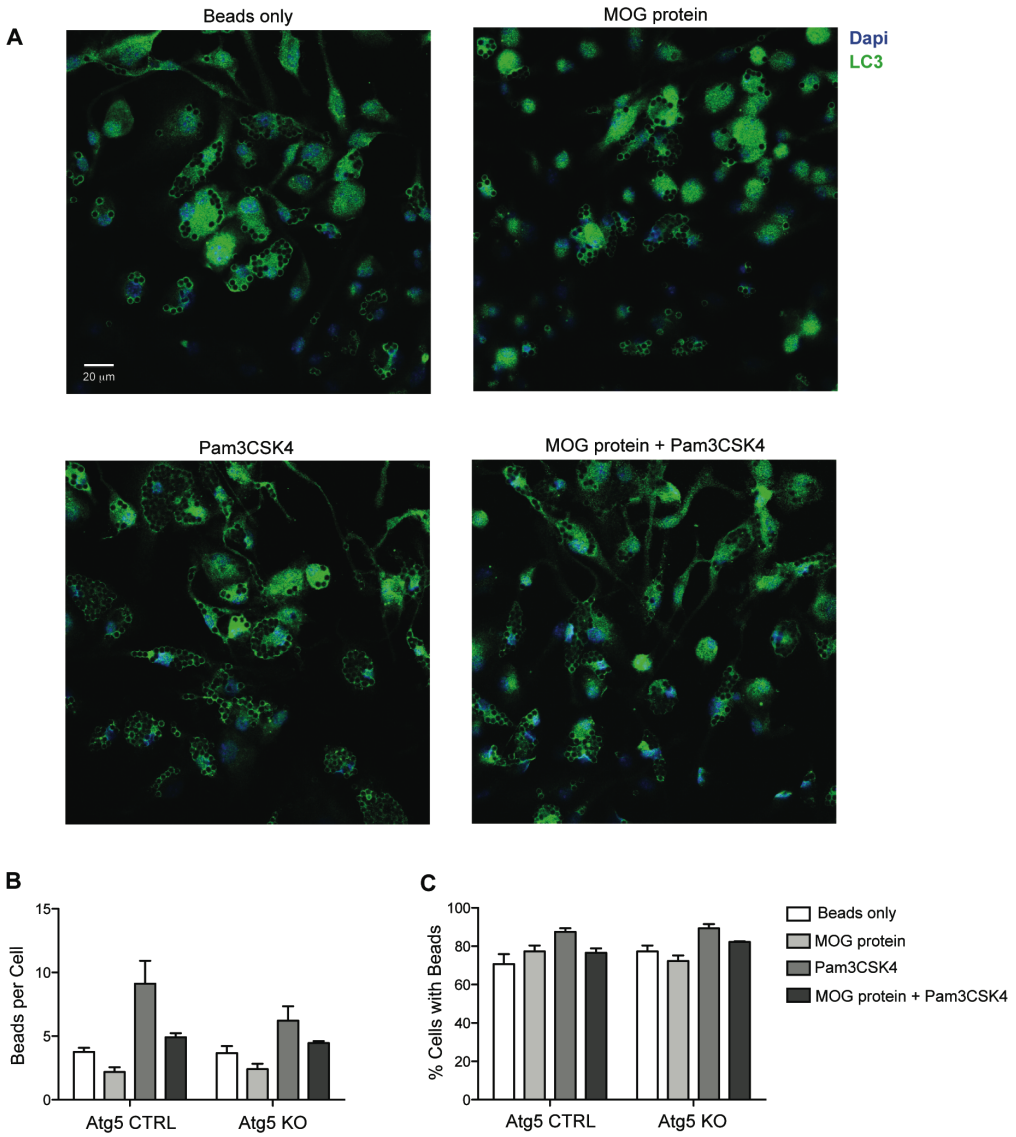

Figure 3.14: Phagocytic uptake of beads by BM-DCs measured by microscopy. BM-DCs were differentiated from DC^{Atg5KO} and $DC^{Atg5CTRL}$ mice in the presence of GM-CSF over a time period of 10 days. At day 10 adherent BM-DCs were harvested and incubated for 4 hours with beads that were coated with the following stimuli: no additive, MOG protein, Pam3CSK4 and MOG protein plus Pam3CSK4. BM-DCs were incubated with coated beads at a ratio of 1:10. **(A)** Representative images of BM-DCs that phagocytosed beads coated with different coatings. Phagocytic capacity was determined by **(B)** counting the number of beads per cell and **(C)** the percentage of cells that phagoytosed beads.

The phagocytic uptake of beads, which were coated with different antigen, by BM-DCs was assessed by fluorescent microscopy. BM-DCs did phagocytose beads, but no unambiguous formation of LC3-associated phagosomes could be detected in any of the conditions tested. To check if there are differences of phagocytic uptake of BM-DCs either derived from $DC^{Atg5CTRL}$ or DC^{Atg5KO} mice, the number of beads per cell was quantified for the conditions “beads only”, “MOG protein”, “Pam3CSK4” and “MOG protein plus Pam3CSK4”. Compared to the condition “beads only”, the number of beads per cell increased when the beads were coated with Pam3CSK4 only, but even decreased when MOG protein was coated on the beads. Furthermore, the supplementation of MOG protein with Pam3CSK4 did not induce LAP - contrary, this supplementation even

decreased the amount of beads in the cell in comparison to the Pam3CSK4 only condition. This might be due to the fact that MOG protein might compete with Pam3CSK4 for binding sides on the beads and, thus, decreases phagocytic uptake. Comparing the phagocytoc capacity of BM-DCs that were either originated from $DC^{Atg5CTRL}$ or DC^{Atg5KO} mice, no difference could be found.

As an alternative read-out, the percentage of cells that contained beads was quantified. A smiliar trend as for the analysis of beads per cells was observed and no difference between Atg5KO BM-DCs and Atg5CTRL BM-DCs could be shown.

4 Discussion

Autoreactive $CD4^+$ T cells are crucial for the development of MS and its animal model EAE. So far, the mechanisms mediating the activation of autoreactive $CD4^+$ T cells in the development of this autoimmune disease are incompletely characterized. We hypothesized that Atg5-dependent presentation of autoantigens by $CD11c^+$ cells facilitates the activation of autoreactive T cells and, conclusively, might have an impact on the development of EAE.

To address this question we investigated whether Atg5-deficiency in $CD11c^+$ cells influences the development of EAE. We showed that Atg5-deficiency in $CD11c^+$ does have an impact on the development of adoptive transfer EAE, but not on the development of active EAE. So far antigen presentation and phagocytosis assays revealed no conclusive results with regard to antigen processing and presenting capabilities of MOG peptide, MOG protein and beads coated with MOG protein by $CD11c^+$ cells or BM-DCs.

4.1 MS, EAE, Autophagy and $CD11c^+$ Cells – The Rationale

4.1.1 The Role of $CD4^+$ T Cells in the Development of MS

MS is an inflammatory autoimmune disease that affects the myelin sheath around the axons in the CNS (Sospedra and Martin, 2005). The exact etiology of this disease is still under debate, but genetic as well as environmental factors are considered crucial for the development of MS. Also the starting point of inflammation, which, eventually, leads to first disease symptoms, is still incompletely understood. Environmental factors such as viral infections are the most favourable suspects that cause initiation of the disease (Ascherio et al., 2012).

MS and EAE are considered mainly $CD4^+$ T cell-driven diseases. The strongest genetic risk factor that determines the susceptibility to suffer from MS is associated with the HLA-DRB1*1501 allele (Schmidt et al., 2007). The HLA-DRB1*1501 allele encodes for MHC class II molecules and, thus, mediates presentation of antigens to $CD4^+$ T cells. This allele is known to increase the risk of developing MS by threefold in heterozygous carriers and by sixfold in homozygous carriers (Sadovnick, 2012). During the course of MS, the main lymphocytic infiltrates comprise of $CD4^+$ and $CD8^+$ T cells and both cell types are ascribed pathogenic functions during the development of MS and EAE (Fletcher et al., 2010). A diversity of immunotherapeutic drugs has been approved and was shown to reduce disease activity and progression (Buck and Hemmer, 2011).

4.1.2 Antigen Processing during CNS Autoimmunity

Antigen processing and presentation is an essential step during the activation process of $CD4^+$ T cells. Antigens need to be taken up by an APC, degraded by the lysosomal machinery and loaded onto MHC class II molecules for presentation to $CD4^+$ T cells. There are two main pathways that

are ascribed to the processing and presentation of antigen on MHC class II molecules – namely, the classical MHC class II antigen processing pathway (Neefjes et al., 2011) and the autophagic pathway (Levine and Deretic, 2007). There is a third, but lesser known, pathway that also contributes antigens to the MHC class II pathway - namely LAP. In the context of EAE or MS, there have been no studies that investigated which one of these pathways is exactly responsible for the processing and presentation of extracellular material in order to stimulate encephalitogenic $CD4^+$ T cells.

Since DCs are known to play the major role in antigen presentation in the priming and restimulation phase of EAE (Greter et al., 2005), we were eager to investigate which role autophagy or LAP might play in the presentation of extracellular self-antigen. We made use of a Cre/loxP-deleter transgenic mouse system in which Atg5 was conditionally deleted in $CD11c^+$ APCs which mainly include DCs. Atg5 is a protein essential for autophagosome formation whose complex with Atg12 and Atg16L1 mediates ligation of Atg8 to the autophagosomal membrane for vesicle expansion and substrate recruitment. Conclusively, if Atg5 is missing in $CD11c^+$ cells neither autophagosomes nor LC3-associated phagosomes can be formed and both of theses pathways are abolished. With this mouse system we were able to study the development of EAE in the absence of Atg5 in $CD11c^+$ APCs compared to control littermates. According to our aims, we hypothesized that autophagy in CD11c-expressing cells accelerates EAE development and progression due to increased loading of self-antigen onto MHC class II molecules.

4.1.3 Potential Role of Autophagy in Autoimmune Diseases

Autophagy has been described to be involved in the pathogenesis of various autoimmune diseases. Generally, there are different roles of autophagy that are ascribed to cause autoimmunity (Lleo et al., 2007). For instance, autophagy is known to eliminate intracellular pathogens (Kuballa et al., 2012) which might lead to presentation of autoantigens on the cell surface or to molecular mimicry. But not only pathogen-related antigens are processed via autophagy, also intracellular self-antigens are presented via MHC class II molecules which might lead to the activation of autoreactive $CD4^+$ T cells (Dengjel et al., 2005).

Autophagy is associated with the most frequent form of inflammatory bowel diseases, namely Crohn's disease. In the context of this disease a defect in autophagy leads to an increase in IL1-β secretion and, consequently, to the generation of an inflammatory milieu. For more information regarding the connection between polymorphisms in autophagy genes and Crohn's disease see (Plantinga et al., 2012). Furthemore, genetic studies have shown that polymorphisms in genes encoding the autophagy-regulating protein IRGM and the Atg16L1 protein, that is part of the Atg5-Atg12/Atg16L1 complex, provide evidence that autophagy is related to Crohn's disease. Even though a functional link between autophagy and the susceptibility to Crohn's disease has not been

established, it is hypothesized that autophagy plays a role in an uncontrolled immune response against commensal gut bacteria or a deficiency in removing of bacteria (Levine and Deretic, 2007). Furthermore, autophagy and SLE are potentially interconnected since it was shown that some autophagic genes, such as genes encoding for Atg5 and Beclin-1, are known to be involed in the removal of dead bodies. A model for the connection of autophagy and SLE envisions that the lack of Atg5 and Beclin-1 results in the absence of "eat me signals" such as the exposure of phosphatidylserine on the cell surface or the deficient release of the "come-get-me" signal lysophosphatidylcholine. These circumstances might lead to an impaired clearance of dead cells and, finally, to the production of autoantibodies against cell debris (Pierdominici et al., 2012).

4.1.4 Potential Role of Autophagy in the Development of MS and EAE

Amongst other characteristics, autophagy is involved in the cellular degradation of unnecessary or dysfunctional cellular components such as protein aggregates. Studies of spinal cords of mice with EAE revealed an increased level of oxidized protein aggregates that went along with a reduced level of LC3. Latter was accounted to be the reason for the accumulation of aggresomes, even though a functional mechanism between the presence of aggresome and disease was not shown (Dasgupta et al., 2013). Furthermore, LC3 level in spinal cord of EAE mice at day 21 post EAE induction was increased in comparison to sham controls. It was concluded that autophagy may be beneficial for the removal of degraded or damaged intracellular organelles within the spinal cord during EAE (Choi et al., 2013). Alirezaei *et al.* investigated if Atg5 levels are modified in T cells in a T cell-mediated autoimmune disease. In this context, a correlation between Atg5 expression in T cells and disease severity could be shown by quantitative PCR and Western blot analysis of blood from mice with EAE and individuals with active RR-MS in comparison to heathly controls. It was concluded that increased levels of Atg5 might promote T cell survival and proliferation during disease progression (Alirezaei et al., 2009). And finally, investigating the role of autophagy in CNS-resident APCs, such as microglia, revealed an upregulation of $LC3^{+}$ puncta at the peak of disease (unpublished data).

4.2 Effect of Atg5-Deficiency in $CD11c^{+}$ Cells on EAE Development

4.2.1 Breeding and Characterization of DC^{Atg5KO} Mice

In order to study the role of LAP in the development and progression of EAE, $DC^{Atg5CTRL}$ (CD11c-$Cre^{-/-}$ $Atg5^{flox/flox}$ genotype) and DC^{Atg5KO} mice (CD11c-$Cre^{+/-}$ $Atg5^{flox/flox}$ genotype) were generated. Due to the known side-effects of the Cre/loxP-deleter transgenic mouse system, such as unspecific activity of promotors (Cre leakage), gene silencing due to random genomic inserton of Cre or incomplete excision of the target gene, a basic characterization of the DC^{Atg5KO} and $DC^{Atg5CTRL}$ mouse was performed. First of all, Cre-EGFP expression was demonstrated in $CD11c^{+}$ H2-A^{b+} cells

originated from either CNS or spleen of DC^{Atg5KO} mice in comparison to $DC^{Atg5CTRL}$ mice. The unspecific Cre expression in $CD4^+$, $CD8^+$ and $CD11b^+$ cells was excluded by flow cytometry and only a low level of unspecific Cre expression was observed in one out of four DC^{Atg5KO} mice in the $CD11b^+$ compartment.

Atg5 is known to also have autophagy-unrelated functions such as negative regulation of innate antiviral immune signals or pro-apoptotic functions (Subramani and Malhotra, 2013). To ensure an uneffected T cell and DC subset repertoire in both $DC^{Atg5CTRL}$ and DC^{Atg5KO} mice, the percentage of $CD4^+$ and $CD8^+$ T cell and Treg fractions as well as DC subsets was investigated. A similar percentage of all afore mentioned cell types was shown by flow cytometry analysis.

4.2.2 Induction of Active EAE with MOG Peptide or Protein

For the induction of EAE, autoreactive $CD4^+$ T cells need to be activated by myelin-specific antigen that is presented by APCs. In the model of active EAE, this self-antigen is given to the mice by injection of a MOG peptide/protein:CFA emulsion. APCs take up the antigen by endocytosis and transport it to the lysosome for degradation and loading onto MHC class II molecules. The exact route of the self-antigen from the phagosome to the MIIC has not been described yet and it could traffic via the classical MHC class II presentation pathway, the LAP pathway or an alternative, so far undescribed, pathway.

In order to study Atg5-dependent antigen processing in the context of EAE development, we induced active EAE in DC^{Atg5KO} and $DC^{Atg5CTRL}$ mice by the injection of MOG peptide in three independent experiments. The pooled data of theses experiments showed no difference between DC^{Atg5KO} and $DC^{Atg5CTRL}$ mice in terms of clinical EAE score or body weight change. One potential explanation for the absence of a phenoytpe might be that MOG peptide can bind to empty MHC class II molecules on the cell surface without being processed. This scenario is rather unlikely since the HLA-DM molecule is responsible for the peptide editing process during which loosely bound peptides are removed. This way it is ensured that only stable peptide:MHC class II molecules exist on the cell surface (Neefjes et al., 2011). Despite these precautions, it might happen that empty MHC class II molecules occur on the cell surface. But, since these empty MHC class II molecules are unstable in their conformation, they aggregate immediately, are internalised and degraded which, again, prevents the binding of unwanted peptides on the cell surface. An alternative explanation for the absence of a phenoytpe might be that MOG peptide does not trigger LAP due to its minor size of 20 amino acids.

To investigate if the injection of MOG protein causes a difference between groups, EAE was actively induced by the injection of MOG protein in CFA. Also under these conditions no difference in disease course or severity could be shown. Consequently, it was considered if MOG protein might also be able to bind onto MHC class II molecules without beeing processed or via bypassing the LAP pathway. Classically, proteins need to be processed before being loaded onto

MHC class II molecules. But, actually, quite contrary views on the necessity of myelin antigen processing were found. For example, Cross *et al.* showed that both, MBP and peptide, need to be processed for antigen presentation (Cross et al., 1990). In contrast, Friedman *et al.* claims that even unprocessed MBP can induce the proliferation of T cell lines and, additionally, that MBP-activated T cell lines are able to induce EAE in recipient mice (Friedman et al., 1992). The former study is supported by newer investigations that demonstrated that antigen processing and presentation is necessary when EAE is elaborated in C57BL/6 mice by MOG peptide injection (Slavin et al., 2001; Tompkins et al., 2002).

Additionally, it was considered that the active induction of EAE in the presence of the strong adjuvant CFA might cause such a strong immune response that a potentially minor effect due to the absence of Atg5 in $CD11c^+$ cells on EAE development might be mimicked. In order to reduce this rather harsh treatment, MOG protein and CFA were diluted. But also under these conditions no difference between experimental groups could be found.

To ensure LAP-specific effects and exclude non-canonical autophagy related functions of Atg5, the same experiments were performed with $DC^{Atg7CTRL}$ and DC^{Atg7KO} mice. The active immunization protocol, with injection of MOG peptide and MOG protein, resulted in no differences between the two experimental groups.

4.2.3 Impact of Atg5-Deficiency in $CD11c^+$ Cells on Adoptive Transfer EAE

The induction of active EAE did not yield a difference between experimental groups, and it could not be determined as to which extend MOG peptide or protein were processed by the Atg5-dependent antigen processing pathway. Therefore we made use of the adoptive transfer EAE model. The main difference between these two models is that in the adoptive transfer model, already primed autoreactive $CD4^+$ T cells encounter the self-antigen in the recipient mouse the first time when presented by local APCs in the CNS. This ensures that CNS antigen needs to be phagocytosed and presented by local APCs.

Furthermore, the adoptive transfer EAE model is considered being a less strong immune activator - due to the absence of the strong adjuvant CFA and PTx. For reasons already elucidated above, adoptive transfer EAE might be beneficial in revealing minor differences. Contrary to the results gained with the active immunization model, in the adoptive transfer EAE model DC^{Atg5KO} mice did not develop any EAE symptoms whereas $DC^{Atg5CTRL}$ mice developed normal EAE symptoms.

4.3 Role of APCs During the Priming and Effector Phase

4.3.1 Priming of Autoreactive $CD4^+$ T cells

Active EAE is induced by subcutaneous injection of CFA and MOG antigen. In order to induce EAE, MOG antigen needs to be processed by APCs and presented to autoreactive T cells. It has

long been accepted that DCs play an important role in linking innate and adoptive immune responses, that they are the main players in raising primary T cell responses and that other professional APCs contribute less to this process (Inaba et al., 1990; Macatonia et al., 1989). Even though DCs are the model APC, unambigous studies showing their role in the first priming of peripheral autoreactive $CD4^+$ T cells during EAE development are still missing. For this reason different types of APCs and their role in peripheral activation of autoreactive $CD4^+$ T cells will be discussed below.

One type of APC that resides in the skin and could be responsible for the antigenic uptake during active EAE are migratory DCs. Migatory DCs belong to the class of cDCs and can be further subdivided into Langerhans cells ($CD11c^+$ $CD207^+$ $CD103^-$) and dermal DCs ($CD11b^-$ $CD103^+$ or $CD11b^+$ $CD103^-$ dermal DCs) (Ginhoux et al., 2007; Henri et al., 2010). One study making use of the model antigen chicken ovalbumin (OVA) showed that migratory and lymphoid-resident DCs are required to initiate T cell responses after subcutaneous injection of OVA antigen (Allenspach et al., 2008). Further studies by King *et al*. supported those data by demonstrating that $CD103^+$ dermal DCs are of major importance for the development of EAE since they are responsible for the priming of encephalitogenic $CD4^+$ T cells (King et al., 2010). Nevertheless, these data were challenged by a study demonstrating that $Batf3^{-/-}$ mice, which lack all peripheral $CD11b^-$ $CD103^+$ DCs (Edelson et al., 2010), show a similar course of disease as C57BL/6 wildtype mice (Edelson et al., 2011). Batf3 is a transcription factor that is required for the development of lymphoid-tissue resident $CD8a^+$ cDCs and $CD103^+$ non-lymphoid DCs as well as dermal $Langerin^+$ $CD103^+$ DCs. In a third study, the role of migratory DCs in inducing tolerance was investigated. The self-antigen MOG was targeted to cell surface receptors on specific DC populations and the tolerogenic effect was studied *in vivo* by use of the EAE model. Migratory DCs were shown to generate Tregs and alleviate EAE symptoms (Idoyaga et al., 2013). Even though these results might be conflictive with the data shown by King *et al*., the authors argue that, under steady state conditions, migratory DCs promote Tregs and peripheral tolerance, whereas, under inflammatory conditions, they promote effector Th1 and Th17 cells (Idoyaga et al., 2013).

Another question still being unanswered is if DCs alone are sufficient to raise an immune response. In a mouse study in which MHC class II expression was restricted to DCs only, mice showed a milder course of disease when EAE was actively induced with MOG protein but not with MOG peptide. This indicates that DCs alone are not sufficient in inducing EAE (Wu et al., 2011). Two recent papers rolled up the field of DC immunology and claimed that DCs are completely dispensable for EAE development (Isaksson et al., 2012; Yogev et al., 2012). Isaksson *et al.* made use of a CD11c-DTR system in which $CD11c^{high}$ DCs can be conditionally deleted by the injection of diphteria toxin, but not pDCs, macrophages and B cells (Jung et al., 2002). Successful DC depletion was estimated by FACS analysis and it could be shown that dermal $Langerin^-$ DCs and $CD11c^{high}$ MHC class II^+ mDCs from skin-draining LNs and spleen were efficiently depleted

whereas 50% of CD11c^{int} MHC class II^{+} inflammatory DCs could not be deleted successfully. And, at peak of disease a large amount of mDCs as well as inflammatory DCs were present in the so-called DC-deficient mice as well as control mice. Using these mice it was demonstrated that priming of encephalitogenic T cells and the development of EAE were not affected in this CD11c-DTR system (Isaksson et al., 2012). In an independent study two different mouse models were used to conditionally ablate DCs and to study their *in vivo* functions during EAE development – namely, the inducible diphtheria toxin receptor (iDTR) model (Buch et al., 2005) and CD11c-DTR mice (Jung et al., 2002). Also in this study DCs were not absolutely depleted and there were always DCs remaining. Despite this flaw, it was claimed that ablation of DCs did not lead to an impairment but actually worsening of EAE symptoms (Yogev et al., 2012). Even though results from both studies go into the same direction, it remains questionable if the remaining DCs might be sufficient in priming autoreactive T cells as it was shown that a low number of peptide:MHC complexes can trigger a high number of TCRs (Valitutti et al., 1995).

But if it was true that DCs are not necessary in priming of T cells, another cell subsets needs to be determined for being responsible. Aside from DCs, the group of professional APCs also includes B cells and macrophages. But also monocytes that differentiate into inflammatory/monocyte-derived DCs (moDCs) might be potential candidates for professional APC functions.

B cells have a diversity of known functions that contribute to the pathogenesis of EAE – namely, secretion of autoantibodies that activate complement and cause demyelination (Lassmann et al., 1988; Linington and Lassmann, 1987; Schluesener et al., 1987), presentation of myelin antigens (Morlacchi et al., 2011) and release of cytokines (Fillatreau et al., 2002; Matsushita et al., 2008). It is noted that not only pathogenic features are ascribed to B cells, but also regulatory functions (Mann et al., 2012). Even though a clear role for B cells in EAE has been demonstrated, it seems as if they were redundant for EAE induction since even B cell-deficient mice develop a severe form of EAE (Dittel et al., 2000; Hjelmström et al., 1998; Wolf et al., 1996).

Despite latter data, Yogev *et al.* investigated the role of B cells in the priming phase of EAE. Mice were immunized with beads that had been treated with CFA, and, in a next step, cells from lymph nodes were checked for uptake of beads. It was shown that both, B cells and macrophages were able to ingest the beads. To further invest the role of B cells, B cells and DCs were ablated in parallel, but no effect on EAE development was shown. Yogev *et al.* suggested that macrophages might be the primarily responsible cell type to prime autoreactive T cells (Yogev et al., 2012). The potential role of macrophages in the development of EAE was investigated by deletion of peripheral macrophages by Cl_2MDP-mnL (mannosylated liposomes containing dichloromethylene diphosphonate) injection (Tran et al., 1998) or by the inhibition of macrophage activation and proinflammatory cytokine production by injection of a therapeutic called CNI-1493 (Martiney et al., 1998). In both studies it could be shown that the absence of macropahges prevented EAE and it indicates that at least peripheral macrophages are essential for the development of EAE.

Monocytes, which are classically defined as the progenitors of macrophages, can also differentiate into inflammatory/monocyte-derived DCs (moDCs; defined as beeing $CD11c^{int}$, MHC II^{+}, $CD11b^{+}$, $Ly6C^{+}$, $CCR5^{+}$) (Domínguez and Ardavín, 2010). In the context of Leishmania and respiratory fungal infection models, it could be shown that moDCs do have the capability of T cell priming (Hohl et al., 2009; León et al., 2007). In a study describing the fate of $Ly6C^{high}$ monocytes during EAE, it was shown that theses cells are recruited to the spinal cord and differentiate into iNOS-producing cells that might be an equivilant to TipDCs (King et al., 2009), but it has not been investigated if these cells are also present during the initial priming phase of T cells. Due to the intermediate expression of CD11c by moDCs and their fast turnover rate, it might be that moDCs during the peripheral inflammation in the skin might not be Atg5-deficient. Conclusively, moDCs might be fully capable of MOG peptide and protein presentation to autoreactive $CD4^{+}$ T cells. Assuming that moDCs were the driving force in active EAE development and Atg5 was still present, no difference in EAE symptoms is to be expected.

Considering the diversity of cell types that have the capability to present self-antigens during the priming phase of EAE, it might very well be that other $CD11c^{-}$ APCs might counterbalance the potential effect of Atg5-deficiency in $CD11c^{+}$ cells during active EAE and that the Atg5-deficiency in $CD11c^{+}$ cells has no effect on EAE development in active EAE.

4.3.2 Brain Resident Cells and Their Potential Role in EAE

Once autoreactive $CD4^{+}$ T cells are present in the periphery, they migrate to the CNS where they need to be reactivated by local APCs (Slavin et al., 2001). Principally, there are two anatomical locations where T cells can encounter their endogenous antigen. Firstly, myelin debris might accumulate in peripheral lymphoid organs such as spleen and deep cervical lymph nodes (de Vos et al., 2002; Ling et al., 2003). Secondly, myelin antigen is presented by resident local APCs in the CNS itself.

Neuroglia, or also called glia cells, are all non-neuronal cells present in the CNS. Neuroglia are responsible for the maintenance of the CNS and functionally there are different responsibilities assigned to them: support and protection of neurons, supply of the neurons with nutrients and oxygen, insulation of neurons and the removal of pathogens and dead cells. In the mammalian system, neuroglia are subclassified into peripheral nervous system (PNS) glia and CNS glia. The CNS neuroglia cells include macroglia (astroglia, oligodendroglia, NG2 glia) and microglia, whereas the PNS neuroglia cells include Schwann cells, olfactory ensheathing cells, satellite glial cells and enteric cells.

Oligodendrocytes have cellular portrusions that form the myelin sheath around the axons of nerve cells to insulate latter and support the conduction of electonical signals. During the course of EAE oligodendrocytes are the main target of the imune attack against myelin components. But since they do not express MHC class II molecules (Lee and Raine, 1989; Wong et al., 1984) they cannot serve

as local APC for the reactivation of T cells.

Astrocytes form the majority of glial cells in the CNS. Their main functions are the provision of neurons with nutrients, maintenance of extracellular ion balance, maintenance of the BBB and repair and scarring processes in the brain. Astrocytes are described to express MHC class II molecules and to activate $CD4^+$ T cells in the context of EAE (Becher et al., 2000; Chastain et al., 2011; Fierz et al., 1985).

Microglia are the macrophage-like cells of the CNS and reside in the parenchymal tissue (Raivich and Banati, 2004). They act as APC, belong to the arm of the innate immune system and detect pathological events in the CNS. Since the CNS is considered as an immune-priviliged organ, mature resident microglia provide surveillance of the CNS – they respond to tissue injury, recognize and eliminate pathogenic substances and are important defenders against a diversity of neurodegenerative diseases (Kreutzberg, 1996). Due to their location in the CNS and the fact that microglia do not only have homeostatic functions, but are also able to interact with cells of the immune system, microglia are thought to play a key role in the initiation of immune responses in the CNS during EAE in mice and MS in humans where they could be found at inflammatory loci (Carson, 2002; Raivich and Banati, 2004). It was further shown that in EAE, under inflammatory conditions, microglia upregulated cell surface markers such as CD45, MHC class II and CD11c which gave them a macrophage and/or DC-like phenotype (Ponomarev et al., 2005). Thus, the role of microglia in the development of EAE in Atg5-deficient mice might also be taken into consideration.

Which one of the two cell types, microglia or DCs, are the major player during the CNS inflammation, still needs to be determined. In this context, one study showed that the abolishment of microglia cells leads to attenuation of EAE disease symptoms (Heppner et al., 2005) whereas two other studies favoured DCs to be the main APC for T cell activation (Greter et al., 2005; McMahon et al., 2005; Platten and Steinman, 2005). It was concluded that CNS-resident DCs are the most important APCs in the reactivation of transferred myelin-specific $CD4^+$ T cells and that resident microglia or infiltrating macrophages are negligible. In newer studies, researchers' attention was turned to the role of monoctyes during EAE since they are recruited to the CNS under inflammatory condtions. Once in the inflamed CNS, monocytes differentiate into moDCs and might function as the main APC during CNS inflammation (King et al., 2009; Mildner et al., 2009).

But, for microglia as well as for moDCs, it remains elusive if these cell subsets are immediately Atg5-deficient after upregulation of CD11c. Studies, investigating the half-life of proteins involved in autophagy, revealed that Atg5 has an approximate half-life of 48 hours after small interfering RNA (siRNA) transfection (Deretic, 2010). Additionally, we have shown that Atg5-deficiency during BM-DC differentiation is most efficient after 10 days of culture. Hence, microglia and moDCs might not be Atg5-deficient when reactivating myelin-specific $CD4^+$ T cells.

This suggests that, in the adoptive transfer EAE model, CNS-resident $CD11c^+$ APCs are the main

players in reactivating transferred myelin-specific $CD4^+$ T cells and that Atg5-deficient $CD11c^+$ APCs are not able to successfully present myelin antigen due to the absence of the Atg5-dependent antigen processing machinery. Whereas, in active EAE this effect is masked since other $CD11c^-$ APCs might overrule the reactivation process of $CD4^+$ T cells in presence of the pronounced proinflammatory milieu during active EAE.

4.4 Potential Role of Atg5 in Antigen Presentation During EAE

4.4.1 Antigen Presentation Capabilities of Atg5-Deficient DCs

The antigen presentation capabilities of Atg5-deficient DCs were first assessed in a co-culture setup. Splenic primary DCs originating from $DC^{Atg5CTRL}$ or DC^{Atg5KO} mice were co-cultured with MOG-specific $CD4^+$ T cells in the presence of MOG peptide, MOG protein or polystyrene beads coated with MOG protein. Antigen presentation capabilities were studied by assessing $CD4^+$ T cell proliferation by means of a CFSE dilution assay. In this experimental setup, $CD4^+$ T cells proliferated more in the presence of Atg CTRL DCs than in the presence of Atg5 KO DCs. This is in contrast to the *in vivo* data that demonstrated that EAE symptoms are almost completely abolished when Atg5-dependent antigen processing pathways are blocked – indicating that reactivation of autoreactive $CD4^+$ T cells by Atg5-deficient $CD11c^+$ cells is impaired. In order to further investigate these findings, an additional phagocytosis assay was performed and will be discussed in the next section.

4.4.2 TLR-Dependent Atg5-Associated Phagocytosis

The question arises if MOG peptide/protein or MOG protein-coated beads can soleyly trigger LAP or if additional triggers are necessary. For instance, classical autophagy was described to be triggered by PAMPs and danger-associated molecular pattern (DAMPs) (Tang et al., 2012), whereas LAP was described to be triggered by receptor mediated signaling pathways such as TLRs (Sanjuan et al., 2007), FcRs (Henault et al., 2012) and PtdSerR (Martinez et al., 2013) or even by the uptake of live cells (entosis) (Florey et al., 2011).

To address this question and the issue raised in the latter chapter, the phagocytic capacity of Atg5-deficient BM-DCs in comparison to control DCs was studied in a bead phagocytosis assay in the presence of Pam3CSK4. Pam3CSK4 is a synthetic bacterial triacylated lipopeptide (LP) and interatcs with TLR1 and TLR2. In this experiment, beads were coated with MOG protein, Pam3CSK4 or MOG protein plus Pam3CSK4 and added to BM-DCs for four hours. The phagocytic uptake was estimated by determining the number of beads per cell or, alternativley, as the percentage of cells that phagocytosed any number of beads. Even in the presence of a TLR agonist, no LC3-associated phagosomes could be detected and no difference in the phagocytic uptake of beads could be demonstrated. These negative results, even in the presence of Pam3CSK4, might be

attributed to unsuccessful binding of the compounds to the beads, suboptimal incubation time of cells together with beads or a general incapability of mouse BM-DCs to form LC3-associated phagosomes after Pam3CSK4 stimulation.

Since LPS (TLR4 agonist) also induces LAP (Sanjuan et al., 2007), it was reasoned that MOG protein or peptide should be supplemented with LPS to achieve better results. It needs to be taken into consideration that the recombinant MOG protein used in our assays was purified by use of a crude preparation procedure after which a high amount of endotoxin was still present (data not shown). Consequently, the purified recombinant MOG protein, which was most likely associated with LPS, was used in the above-mentioned assays and it was not sufficient to induce LAP.

Alternatively, zymosan, which is a β-glucan mannan-rich particle found on the cell surfaces of yeast and interacts with TLR2, could be added to the *in vitro* cultures. But since zymosan is expressed by yeast cells and yeast is not known to be of influence during EAE or MS, it might be far-fetched to set zymosan into the context of CNS autoimmunity. Furthermore, zymosan has an ameliorating effect on the development of EAE (Li et al., 2013), which would argue against the role of zymosan in disease induction.

Investigating other TLRs in the context of EAE, TLR9 (Prinz et al., 2006) and, to some extend, TLR2 signaling mediates the pathogenicity of EAE, whereas TLR1, 4 and 6-deficiency in mice did not have an impact on the development of active EAE (Miranda-Hernandez et al., 2011). Additionally, both studies showed that MyD88 deficiency abrogates disease. For a summary of the role of TLRs in autoimmunity compare (Mills, 2011). Additionally, it was shown that FcγRs are responsible for the internalization of DNA-immuno complexes (DNA-IC) and that this internalization induced the recruitment of TLR9 to the phagosome and the secretion of TNFα. Based on these data, it was proposed by the authors that LAP is responsible for the convergence of the phagocytic and autophagic pathway (Henault et al., 2012). Conclusively, it might be wortwhile to test TLR9 agonists in the context of our *in vitro* studies.

4.4.3 FcR-Mediated Phagocytosis

LAP has been described to be induced by FcR engagement (Henault et al., 2012). Noteworthy, a connection between B cells, plasma cells, and the presence of antibodies against myelin antigen and the development of MS is established. Furthermore, one hallmark for the diagnostic of MS is the presence of oligoclonal Igs and plasma cells in the cerebrospinal fluid (Esiri, 1977; Ziemssen and Ziemssen, 2005). The role of B cells has also been described in the EAE model and pathogenic as well as regulatory functions were attributed to them (Mann et al., 2012). Despite the intense investigation of the role of B cells during EAE, contradictory results were shown. On the one hand it was shown that antibodies have the capacity to promote the phagocytosis of myelin and contribute to the inflammation and demyelination in the CNS (Linington et al., 1988; Morris-

Downes et al., 2002). But on the other hand it was also shown that mice that are deficient in B cells still develop EAE (Dittel et al., 2000; Hjelmström et al., 1998; Wolf et al., 1996). Even though B cells might be dispensable during the development of EAE, it is out of question that B cells do infiltrate into inflammatory lesions and that autoantibodies targeting myelin antigens are released during MS (Genain et al., 1999).

There are different ways of how B cells might exert their effector functions during demyelination (Weber et al., 2011). Amongst various mechanisms, opsonization of target cells and subsequent phagocytosis of the opsonized cells are noteworthy in the context of this study. FcRs, which are expressed on APCs, recognize the opsonized target and phagocytose it, which, finally, leads to destruction of tissue. Generally, the internalization of IgG-opsonized particles by phagocytosis is best described for Fcγ receptors (FcγR) (Flannagan et al., 2012). And, in the context of EAE, it seems as if macrophages play a major role in phagocytosing antibody-opsonized myelin and, eventually, causing demyelination and tissue damage (Sadler et al., 1991; Trotter et al., 1986). But also microglia, the resident "macrophages" within the CNS are associtaed with neuronal damage by phagocytosis (Bauer et al., 1994; Cash et al., 1993; Huizinga et al., 2012). Mouse DCs, which are thought to be the main APC during EAE, express both FcγRIII (activating) and FcγRIIb (inhibitory) on their surface (Regnault et al., 1999). The expression of FcγRIII and FcγRIIb would give DCs the potential to bind to the Fc part of an antibody and phagocytose opsonized myelin-expressing oligodendrocytes. So far there are only few studies describing the role of DCs in the phagocytosis of myelin-antigen or oligodendrocytes. Investigating human MS lesions it was demonstrated that DC-SIGN$^+$ DCs do contain myelin debris when present in the perivascular spaces of active MS lesions (Serafini et al., 2006). In the context of another study, it was investigated how the phagocytosis of human myelin influences the activation state of human moDCs. It was shown that myelin-laden DCs actually suppress the proliferation of T cells, whereas the secretion of TGF-β was increased and the migratory capacity of myelin-treated DCs was decreased (Gredler et al., 2010). These results might argue that DCs play a primary role in controlling immunity and tolerance, but it does not exclude the fact that FcR-mediated phagocytosis of antibody-opsonized oligodendrocytes is important for the development of EAE. And if there was a hypothetical association between FcR-mediated phagocytosis and LAP, the lack of LAP in CNS-resident DCs might lead to an insufficient restimulation of infiltrating autoreactive T cells. This hypothesis would be supported by studies in SLE in which it was shown that DCs preferrably phagocytose apoptotic bodies opsonized by autoantibodies and apoptotic bodies or blebs displaying "eat me signals" (Frisoni et al., 2005).

4.4.4 Phagocytosis of Apoptotic Cells and Self-Antigen

The uptake of dying cells is importat to maintain homeostasis in the body what otherwise might result in SLE (Shao and Cohen, 2011). In this context, LAP was described to be induced by phagocytosis of apoptotic, necrotic, and RIPK3-dependent necrotic cells (Martinez et al., 2011) or, alternatively, by the uptake of live cells (entosis) (Florey et al., 2011). Martinez *et al.* showed that PtdSer on the surface of dying cells is recognized by the PtdSer receptor TIM4 that triggers the recruitment of autophagy-related proteins to the dead cell-containing phagosome (Martinez et al., 2011). Conclusively, it could be that the presence of apoptotic cells might trigger LAP in BM-DCs or primary splenic DCs. To investigate this, target cells like an apoptotic or necrotic MOG-expressing oligodendrocyte cell line could be co-cultured with Atg5-deficient cells to check for phagocytic uptake by the engagement of LAP or T cell stimulation in the CFSE dilution assay.

4.4.5 Non-Antigen Processing-Related Functions of Atg5

The lack of EAE symptoms in the DC^{Atg5KO} mouse group in the adoptive transfer experiments might also go back to non-autophagy related functions of Atg5 (Subramani and Malhotra, 2013). For instance, one non-autophagy related function of Atg5 is that the Atg12-Atg5 complex negatively regulates innate antiviral immune signalling by secluding CARD proteins (Jounai et al., 2007; Takeshita et al., 2008). Additionally, Atg16L1 and Atg5 have a beneficial role in the secretion of antimicrobial peptides through exocytosis by Paneth cells (Cadwell et al., 2008); and Atg5 and Atg7 are necessary for the polarized secretion of cathepsin K by osteclasts at the ruffled border of the cell (DeSelm et al., 2011). Atg5 makes cells more susceptible towards apoptotic stimuli as it was shown that Atg5 cleaved by calpain-mediated caspase activation and, thus, apoptotic cell death (Yousefi et al., 2006).

Regarding the diversity of non-canonical autophagy functions of Atg5, only some of the functions outlined above might be applicable to our model. Firstly, Atg5 negatively regulates type I IFN secretion (Jounai et al., 2007; Takeshita et al., 2008). Type I IFNs are mainly secreted by pDCs after triggerung of TLRs and viral infections (Colonna et al., 2004) and, in the context of EAE, are known to have protective characteristics in MS and EAE (Kalinke and Prinz, 2012). This is in line with the fact that IFN-β KO mice show exacerbated disease symptoms and more severe neurological symptoms compared to the control group (Teige et al., 2003). As per our model, Atg5 is deleted in $CD11c^{+}$ cells and this could theoretically result in more type I IFN secretion and, thus, in a mildened disease course. This would fit the results of the adoptive transfer EAE model, but with regard to the active EAE model, the question arises why this effect is missing – especially, since latter system provides a high amount of TLR agonists in form of CFA and PTx that should lead to an increase in type I IFN secretion.

A second non-canonical autophagy function of Atg5 that might be of importance during EAE development is that Atg5 makes cells more prone to apoptosis (Yousefi et al., 2006). This effect has

only been shown for T cells, so that it is hard to judge how Atg5-deficiency might influence apoptosis in $CD11c^+$ cells. One could assume that Atg5-deficiency in $CD11c^+$ cells would lead to a higher survival rate of $CD11c^+$ cells. Hence, more $CD11c^+$ cells should be present to process and present antigen and, thus, more myelin-specific $CD4^+$ T cells should be activated and should cause more severe EAE symptoms. This is contrary to our observed results, but further investigations will be necessary to ensure the antigen-processing role of Atg5 in our model.

4.5 Active vs. Adoptive Transfer EAE Model

The pathogenic steps of active and adoptive transfer EAE are similar and can be subdivided into distinct phases (Stromnes and Goverman, 2006a; 2006b). Myelin-specific $CD4^+$ T cells that escaped tolerogenic mechanisms are activated in the periphery (Seamons et al., 2003) and migrate via the BBB into the CNS (Brabb et al., 2000; Hickey, 1991; Wekerle et al., 1986). Infiltrating cells are reactivated by local or infiltrating APCs that present myelin antigen on their surface in the context of co-stimulatory molecules (Kawakami et al., 2004; McMahon et al., 2005; Tompkins et al., 2002). This leads to a cascade of inflammatory events during which cytokines are secreted and macrophages and other APCs are recruited. Macrophages secrete additional pro-inflamatory cytokines such as TNF-α and IL-1 which contribute to tissue damage in the CNS (Kuchroo et al., 2002). The tissue damage causes an additional infiltration of T cells, B cells and APCs. By executing their inflammatory effector functions, demyelination is caused and focal plaques in the CNS are formed, which, eventually, results in the emergence of disease symptoms (Sospedra and Martin, 2005). With regard to clinical disease symptoms, adoptive transfer EAE might yield in higher disease severity, a higher rate of incidence and a more synchronous course of disease. But in terms of clinical and histological aspects, both models show the same features and characteristics (Miller et al., 2010).

Despite the similarities between active and adoptive transfer EAE, the adoptive transfer EAE model brings along some advantages. In adoptive transfer EAE, the effector phase is induced exactly at the moment when the already primed autoreactive $CD4^+$ T cells are injected into the recipient mouse. This is of particular interest when the infiltration of cells into the CNS is to be investigated. Additionally, each pathophysiological step, such as $CD4^+$ T cell priming in the donor, activation and expansion of $CD4^+$ T cells *in vitro* and the effector phase in the recipient mouse, can be investigated and manipulated one by one. This progressive analysis enables the separation of induction and effector phases. Depending on the *in vitro* settings used, the effector phenotypes of the different T helper subsets can be dissected, which might be beneficial for the characterization of T cell effector functions in the CNS. Furthermore, cells to be transferred can be labeled *in vitro* and, thus, tracked *in vivo* in order to locate and investigate their activities in the recipient. In adoptive transfer EAE, there is no antigen depot given that might lead to continuos *de novo* activation of

naïve T cells. (McCarthy et al., 2012; Racke, 2001; Rao and Segal, 2012; Stromnes and Goverman, 2006a)

4.5.1 Adjuvant Effect

4.5.1.1 MOG:CFA Antigen Depot

In adoptive transfer EAE, autoreactive $CD4^+$ T cells are primed in a donor mouse, restimulated *in vitro* and transferred to a naïve recipient mouse. From the site of injection, the T cells migrate to the CNS where they are restimulated by local self-antigen presented on MHC class II molecules. During this entire process no peripheral source of CNS antigen is present. On the other hand, in active EAE, a peripheral antigen depot constisting the self-antigen, namely MOG peptide or protein, is present during the entire experiment. This antigen depot potentially enables continuos *de novo* activation of naïve T cells and might even support migration of T cells back and forth from the antigen depot to the CNS. Additionally, the antigen depot allows continuos transport of self-antigen to the lymphatic system.

The antigen depot also contains CFA, which consists of heat-killed *Mycobacterium tuberculosis* that stimulates the innate immune response. CFA is indespensable for the induction of EAE since *Mycobacterium tuberculosis* carries PAMPs that bind TLRs and, in turn, trigger immune responses which finally lead to EAE (Marta et al., 2009). Furthermore, CFA greatly affects APCs, which, in turn, might also affect all other cells of the immune system and which might have an impact on EAE development in this particular mouse system.

4.5.1.2 Presence of *Pertussis* Toxin

Another factor that differs between active and adoptive EAE is the use of PTx in the active EAE model. PTx's exact mechanism of action is still unknown, but it is thought to have an impact on increasing the BBB permeability and, thus, supporting the migration of effector cells into the CNS as it was first described by Linthicum (Linthicum et al., 1982). The theory that PTx may lead to an increased permeability of the BBB is further supported by a recent study that showed that PTx supports angiogenesis in microvascular endothelial cells of the brain (Lu et al., 2008). Additionally, patrolling phagocytes interact with brain capillaries by binding of integrin aM (ITGaM) to intercellular adhesion molecule 1 (ICAM1) which is expressed at low levels on capillary surfaces under steady state conditions, but is upregulated in response to PTx (Richard et al., 2011).

Besides of this classical view of action, PTx has also been described as an inhibitor of lymphocyte recirculation – involving their inability to localize to lymph nodes or Peyer's patches (Spangrude et al., 1984). When PTx is coinjected with an antigen, it strengthens Th1 and Th2 responses, which was shown by increased secretion of IFN-γ and IL-2 by naïve T cells, respectively (Ryan et al., 1998), and also the induction of high frequencies of peptide-specific Th1 cells (Hofstetter et al., 2002). Furthermore, PTx has a negative impact on the induction of peripheral T cell anergy and

even though one might assume that PTx acts as a superantigen, this assumption could be disproven (Kamradt et al., 1991). PTx blocks trafficking of single positive thymocytes via the corticomedullary junction, which, ultimately, leads to a disturbed thymocyte distribution in the thymus (Suzuki et al., 1999). In terms of regulatory mechanisms during the course of EAE, PTx reduces the number of $CD4^+$ $CD25^+$ Tregs and their regulatory capabilities *in vivo* (Cassan et al., 2006; Chen et al., 2006). On the other hand, PTx generates IL-17-producing $CD4^+$ cells in an IL-6-dependent manner (Chen et al., 2007) and promotes the maturation of APCs measured by surface expression of MHC class II, CD80, CD86, CD40, and DEC205 and a higher functional capacity shown by an increased capacity to stimulate T cells proliferation (Hou et al., 2003).

The above-mentioned effects of PTx on the immune system illustrate in how many aspects PTx might influence the outcome of active and adoptive transfer EAE. Nevertheless, it is rather elusive how PTx might mask the effect of Atg5-deficiency in $CD11c^+$ cells in active EAE whereas the effect is so prominent in adoptive transfer EAE.

4.6 Future Investigations

In order to address the question why Atg5-deficiency does have an impact on adoptive transfer EAE, but not on active EAE, further *in vivo* studies need to be performed. To begin with, infiltrating T cells in the CNS need to be investigated. A central question is, if T cells do infiltrate at comparable levels and which T cell effector functions they feature. In case T cells do not infiltrate into the CNS, it might be worth knowing to which organ they do home instead or where they accumulate.

With regard to DCs, it needs to be studied, which DC subsets are present in the CNS, if there is a difference between $DC^{Atg5CTRL}$ and DC^{Atg5KO} mice and if DCs got activated at the same level in the two different strains. Once the percentage of infiltrating DCs is determined, it would be also interesting to specify what their phagocytic and presenting features *ex vivo* might be. In this context, a similar experimental setup as the *in vitro* co-culture experiments is to be considered.

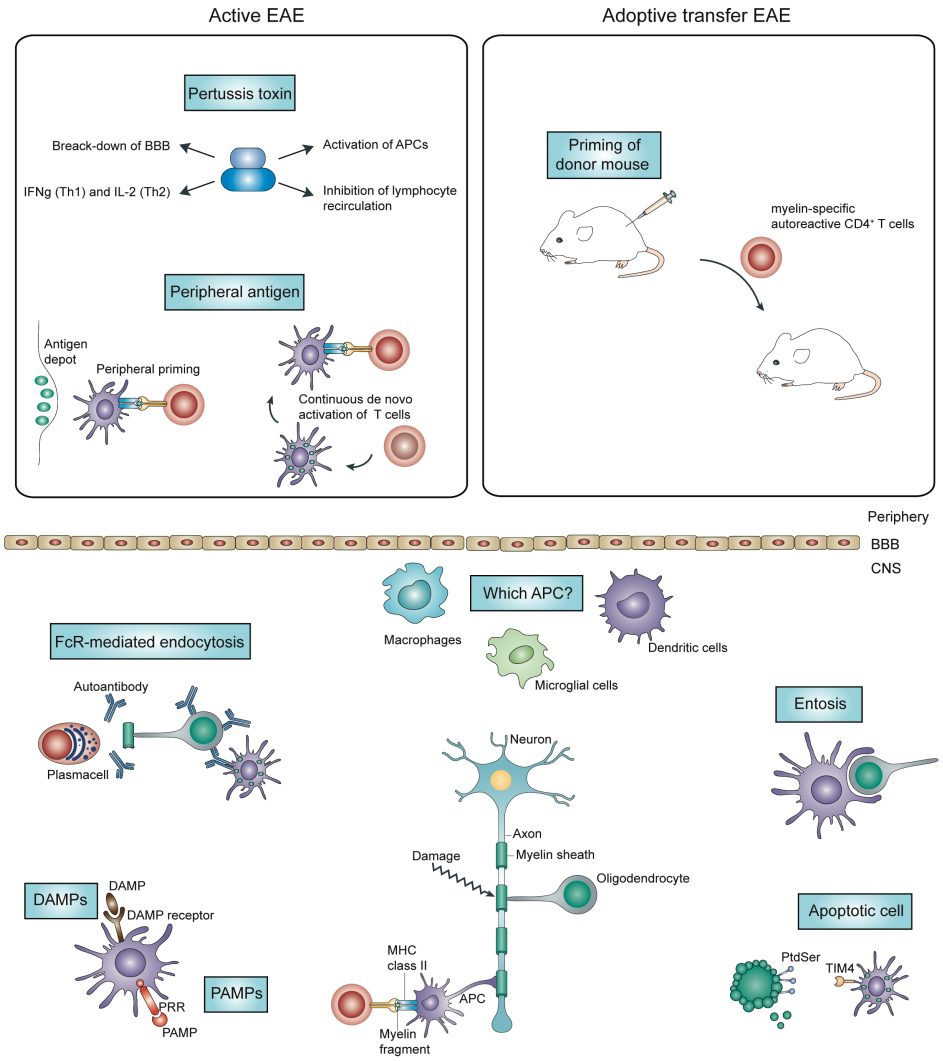

Figure 4.1: Model for the potential role of Atg5 in the development of EAE. Top: Comparison of the factors that differ in the induction of active and adoptive transfer EAE in the periphery. The most prominent factors are the presence of peripheral antigen and the injection of Ptx during the induction of active EAE. In adoptive transfer EAE, donor mice are immunized with MOG peptide and seven days later autoreactive $CD4^+$ T cells are transferred to recipient mice. **Bottom:** Potential mechanisms that might cause the induction of phagocytosis of self-antigen. Processes envolved might be entosis, phagocytosis of apoptotic material, FcR-mediated phagocytosis or PAMP/DAMP-mediated phagocytosis or other non-antigen processing-related functions of Atg5. Figure based on elements from (Steinman, 2009).

5 References

Abele, R., and Tampé, R. (2004). The ABCs of immunology: structure and function of TAP, the transporter associated with antigen processing. Physiology (Bethesda) *19*, 216–224.

Acheson, E.D., Bachrach, C.A., and Wright, F.M. (1960). Some comments on the relationship of the distribution of multiple sclerosis to latitude, solar radiation, and other variables. Acta Psychiatr Scand Suppl *35*, 132–147.

Alirezaei, M., Fox, H.S., Flynn, C.T., Moore, C.S., Hebb, A.L.O., Frausto, R.F., Bhan, V., Kiosses, W.B., Whitton, J.L., Robertson, G.S., et al. (2009). Elevated ATG5 expression in autoimmune demyelination and multiple sclerosis. Autophagy *5*, 152–158.

Allenspach, E.J., Lemos, M.P., Porrett, P.M., Turka, L.A., and Laufer, T.M. (2008). Migratory and lymphoid-resident dendritic cells cooperate to efficiently prime naive CD4 T cells. Immunity *29*, 795–806.

Ascherio, A., and Munger, K.L. (2007). Environmental risk factors for multiple sclerosis. Part II: Noninfectious factors. Ann. Neurol. *61*, 504–513.

Ascherio, A., and Munger, K.L. (2010). Epstein-barr virus infection and multiple sclerosis: a review. J Neuroimmune Pharmacol *5*, 271–277.

Ascherio, A., Munger, K.L., and Lünemann, J.D. (2012). The initiation and prevention of multiple sclerosis. Nat Rev Neurol *8*, 602–612.

Ashford, T.P., and Porter, K.R. (1962). Cytoplasmic components in hepatic cell lysosomes. The Journal of Cell Biology *12*, 198–202.

Atkinson, M.A. (2012). The pathogenesis and natural history of type 1 diabetes. Cold Spring Harb Perspect Med *2*.

Axe, E.L., Walker, S.A., Manifava, M., Chandra, P., Roderick, H.L., Habermann, A., Griffiths, G., and Ktistakis, N.T. (2008). Autophagosome formation from membrane compartments enriched in phosphatidylinositol 3-phosphate and dynamically connected to the endoplasmic reticulum. The Journal of Cell Biology *182*, 685–701.

Bach, J.-F. (2002). The Effect of Infections on Susceptibility to Autoimmune and Allergic Diseases. N. Engl. J. Med. *347*, 911–920.

Bauer, J., Sminia, T., Wouterlood, F.G., and Dijkstra, C.D. (1994). Phagocytic activity of macrophages and microglial cells during the course of acute and chronic relapsing experimental autoimmune encephalomyelitis. J. Neurosci. Res. *38*, 365–375.

Becher, B., Prat, A., and Antel, J.P. (2000). Brain-immune connection: immuno-regulatory properties of CNS-resident cells. Glia *29*, 293–304.

Ben-Nun, A., Wekerle, H., and Cohen, I.R. (1981). The rapid isolation of clonable antigen-specific T lymphocyte lines capable of mediating autoimmune encephalomyelitis. Eur. J. Immunol. *11*, 195–199.

Berger, S.B., Romero, X., Ma, C., Wang, G., Faubion, W.A., Liao, G., Compeer, E., Keszei, M., Rameh, L., Wang, N., et al. (2010). SLAM is a microbial sensor that regulates bacterial phagosome functions in macrophages. Nat Immunol *11*, 920–927.

Bernales, S., McDonald, K.L., and Walter, P. (2006). Autophagy counterbalances endoplasmic reticulum expansion during the unfolded protein response. PLoS Biol. *4*, e423.

Bettelli, E., Pagany, M., Weiner, H.L., Linington, C., Sobel, R.A., and Kuchroo, V.K. (2003). Myelin oligodendrocyte glycoprotein-specific T cell receptor transgenic mice develop spontaneous autoimmune optic neuritis. J. Exp. Med. *197*, 1073–1081.

Bhattacharya, A., and Eissa, N.T. (2013). Autophagy and autoimmunity crosstalks. Front Immunol *4*, 88.

Blum, J.S., Wearsch, P.A., and Cresswell, P. (2013). Pathways of antigen processing. Annu. Rev. Immunol. *31*, 443–473.

Born, W.K., Kemal Aydintug, M., and O'Brien, R.L. (2013). Diversity of γδ T-cell antigens. Cell. Mol. Immunol. *10*, 13–20.

Bouvier, J., and Cheng, J.-G. (2009). Recombineering-based procedure for creating Cre/loxP conditional knockouts in the mouse. Curr Protoc Mol Biol *Chapter 23*, Unit23.13.

Brabb, T., Dassow, von, P., Ordonez, N., Schnabel, B., Duke, B., and Goverman, J. (2000). In situ tolerance within the central nervous system as a mechanism for preventing autoimmunity. J. Exp. Med. *192*, 871–880.

Brocke, S., Gaur, A., Piercy, C., Gautam, A., Gijbels, K., Fathman, C.G., and Steinman, L. (1993). Induction of relapsing paralysis in experimental autoimmune encephalomyelitis by bacterial superantigen. Nature *365*, 642–644.

Brown, A.M., and McFarlin, D.E. (1981). Relapsing experimental allergic encephalomyelitis in the SJL/J mouse. Lab. Invest. *45*, 278–284.

Buch, T., Heppner, F.L., Tertilt, C., Heinen, T.J.A.J., Kremer, M., Wunderlich, F.T., Jung, S., and Waisman, A. (2005). A Cre-inducible diphtheria toxin receptor mediates cell lineage ablation after toxin administration. Nat. Methods *2*, 419–426.

Buck, D., and Hemmer, B. (2011). Treatment of multiple sclerosis: current concepts and future perspectives. J. Neurol. *258*, 1747–1762.

Busch, R., Doebele, R.C., Patil, N.S., Pashine, A., and Mellins, E.D. (2000). Accessory molecules for MHC class II peptide loading. Curr. Opin. Immunol. *12*, 99–106.

Cadwell, K., Liu, J.Y., Brown, S.L., Miyoshi, H., Loh, J., Lennerz, J.K., Kishi, C., KC, W., Carrero, J.A., Hunt, S., et al. (2008). A key role for autophagy and the autophagy gene Atg16l1 in mouse and human intestinal Paneth cells. Nature *456*, 259–263.

Carson, M.J. (2002). Microglia as liaisons between the immune and central nervous systems: functional implications for multiple sclerosis. Glia *40*, 218–231.

Cash, E., Zhang, Y., and Rott, O. (1993). Microglia present myelin antigens to T cells after phagocytosis of oligodendrocytes. Cell. Immunol. *147*, 129–138.

Cassan, C., Piaggio, E., Zappulla, J.P., Mars, L.T., Couturier, N., Bucciarelli, F., Desbois, S., Bauer, J., Gonzalez-Dunia, D., and Liblau, R.S. (2006). Pertussis toxin reduces the number of splenic Foxp3+ regulatory T cells. J. Immunol. *177*, 1552–1560.

Cecconi, F., and Levine, B. (2008). The role of autophagy in mammalian development: cell makeover rather than cell death. Dev. Cell *15*, 344–357.

Chastain, E.M.L., Duncan, D.S., Rodgers, J.M., and Miller, S.D. (2011). The role of antigen presenting cells in multiple sclerosis. Biochim. Biophys. Acta *1812*, 265–274.

Chen, X., Howard, O.M.Z., and Oppenheim, J.J. (2007). Pertussis toxin by inducing IL-6 promotes the generation of IL-17-producing CD4 cells. J. Immunol. *178*, 6123–6129.

Chen, X., Winkler-Pickett, R.T., Carbonetti, N.H., Ortaldo, J.R., Oppenheim, J.J., and Howard, O.M.Z. (2006). Pertussis toxin as an adjuvant suppresses the number and function of CD4+CD25+ T regulatory cells. Eur. J. Immunol. *36*, 671–680.

Chicz, R.M., Urban, R.G., Gorga, J.C., Vignali, D.A., Lane, W.S., and Strominger, J.L. (1993). Specificity and promiscuity among naturally processed peptides bound to HLA-DR alleles. J. Exp. Med. *178*, 27–47.

Choi, B.Y., Jang, B.G., Kim, J.H., Seo, J.-N., Wu, G., Sohn, M., Chung, T.N., and Suh, S.W. (2013). Copper/zinc chelation by clioquinol reduces spinal cord white matter damage and behavioral deficits in a murine MOG-induced multiple sclerosis model. Neurobiol. Dis. *54*, 382–391.

Colonna, M., Trinchieri, G., and Liu, Y.-J. (2004). Plasmacytoid dendritic cells in immunity. Nat Immunol *5*, 1219–1226.

Cree, B.A.C., Rioux, J.D., McCauley, J.L., Gourraud, P.-A.F.D., Goyette, P., McElroy, J., De Jager, P., Santaniello, A., Vyse, T.J., Gregersen, P.K., et al. (2010). A major histocompatibility Class I locus contributes to multiple sclerosis susceptibility independently from HLA-DRB1*15:01. PLoS ONE *5*, e11296.

Cross, A.H., Dolich, S., and Raine, C.S. (1990). Antigen processing of myelin basic protein is required prior to recognition by T cells inducing EAE. Cell. Immunol. *129*, 22–31.

Dasgupta, A., Zheng, J., Perrone-Bizzozero, N.I., and Bizzozero, O.A. (2013). Increased carbonylation, protein aggregation and apoptosis in the spinal cord of mice with experimental autoimmune encephalomyelitis. ASN Neuro *5*, e00111.

De Duve, C. (1963). The lysosome. Sci. Am. *208*, 64–72.

de Vos, A.F., van Meurs, M., Brok, H.P., Boven, L.A., Hintzen, R.Q., van der Valk, P., Ravid, R., Rensing, S., Boon, L., 't Hart, B.A., et al. (2002). Transfer of central nervous system autoantigens and presentation in secondary lymphoid organs. J. Immunol. *169*, 5415–5423.

Deegan, S., Saveljeva, S., Gorman, A.M., and Samali, A. (2013). Stress-induced self-cannibalism: on the regulation of autophagy by endoplasmic reticulum stress. Cell. Mol. Life Sci. *70*, 2425–2441.

Delgado, M.A., Elmaoued, R.A., Davis, A.S., Kyei, G., and Deretic, V. (2008). Toll-like receptors control autophagy. Embo J *27*, 1110–1121.

Dengjel, J., Schoor, O., Fischer, R., Reich, M., Kraus, M., Müller, M., Kreymborg, K., Altenberend, F., Brandenburg, J., Kalbacher, H., et al. (2005). Autophagy promotes MHC class II presentation of peptides from intracellular source proteins.

Deretic, V. (2010). Autophagosome and Phagosome (Humana Press).

Deretic, V., and Levine, B. (2009). Autophagy, immunity, and microbial adaptations. Cell Host Microbe *5*, 527–549.

DeSelm, C.J., Miller, B.C., Zou, W., Beatty, W.L., van Meel, E., Takahata, Y., Klumperman, J., Tooze, S.A., Teitelbaum, S.L., and Virgin, H.W. (2011). Autophagy proteins regulate the secretory component of osteoclastic bone resorption. Dev. Cell *21*, 966–974.

Dittel, B.N., Urbania, T.H., and Janeway, C.A. (2000). Relapsing and remitting experimental autoimmune encephalomyelitis in B cell deficient mice. J. Autoimmun. *14*, 311–318.

Domínguez, P.M., and Ardavín, C. (2010). Differentiation and function of mouse monocyte-derived dendritic cells in steady state and inflammation. Immunol. Rev. *234*, 90–104.

Dongre, A.R., Kovats, S., deRoos, P., McCormack, A.L., Nakagawa, T., Paharkova-Vatchkova, V., Eng, J., Caldwell, H., Yates, J.R., and Rudensky, A.Y. (2001). In vivo MHC class II presentation of cytosolic proteins revealed by rapid automated tandem mass spectrometry and functional analyses. Eur. J. Immunol. *31*, 1485–1494.

Dörfel, D., Appel, S., Grünebach, F., Weck, M.M., Müller, M.R., Heine, A., and Brossart, P. (2005). Processing and presentation of HLA class I and II epitopes by dendritic cells after transfection with in vitro-transcribed MUC1 RNA. Blood *105*, 3199–3205.

Dunn, W.A., Jr, Cregg, J.M., and Kiel, J. (2005). Pexophagy. Autophagy *1:2*, 75–83.

Edelson, B.T., Bradstreet, T.R., KC, W., Hildner, K., Herzog, J.W., Sim, J., Russell, J.H., Murphy, T.L., Unanue, E.R., and Murphy, K.M. (2011). Batf3-dependent CD11b(low/-) peripheral dendritic cells are GM-CSF-independent and are not required for Th cell priming after subcutaneous immunization. PLoS ONE *6*, e25660.

Edelson, B.T., KC, W., Juang, R., Kohyama, M., Benoit, L.A., Klekotka, P.A., Moon, C., Albring, J.C., Ise, W., Michael, D.G., et al. (2010). Peripheral CD103+ dendritic cells form a unified subset developmentally related to CD8alpha+ conventional dendritic cells. Journal of Experimental Medicine *207*, 823–836.

Esiri, M.M. (1977). Immunoglobulin-containing cells in multiple-sclerosis plaques. Lancet *2*, 478.

Fierz, W., Endler, B., Reske, K., Wekerle, H., and Fontana, A. (1985). Astrocytes as antigen-presenting cells. I. Induction of Ia antigen expression on astrocytes by T cells via immune interferon and its effect on antigen presentation. J. Immunol. *134*, 3785–3793.

Fillatreau, S., Sweenie, C.H., McGeachy, M.J., Gray, D., and Anderton, S.M. (2002). B cells regulate autoimmunity by provision of IL-10. Nat Immunol *3*, 944–950.

Flannagan, R.S., Jaumouillé, V., and Grinstein, S. (2012). The cell biology of phagocytosis. Annu Rev Pathol *7*, 61–98.

Fletcher, J.M., Lalor, S.J., Sweeney, C.M., Tubridy, N., and Mills, K.H.G. (2010). T cells in multiple sclerosis and experimental autoimmune encephalomyelitis. Clin. Exp. Immunol. *162*, 1–11.

Florey, O., Kim, S.E., Sandoval, C.P., Haynes, C.M., and Overholtzer, M. (2011). Autophagy machinery mediates macroendocytic processing and entotic cell death by targeting single membranes. Nat. Cell Biol. *13*, 1335–1343.

Friedman, A., Reshef, T., and Cohen, I.R. (1992). Induction of experimental autoimmune encephalomyelitis by native myelin basic protein-activated T lymphocyte lines. Eur. J. Immunol. *22*, 279–282.

Frisoni, L., McPhie, L., Colonna, L., Sriram, U., Monestier, M., Gallucci, S., and Caricchio, R. (2005). Nuclear autoantigen translocation and autoantibody opsonization lead to increased dendritic cell phagocytosis and presentation of nuclear antigens: a novel pathogenic pathway for autoimmunity? J. Immunol. *175*, 2692–2701.

Fritz, R.B., Chou, C.H., and McFarlin, D.E. (1983). Induction of experimental allergic encephalomyelitis in PL/J and (SJL/J x PL/J)F1 mice by myelin basic protein and its peptides: localization of a second encephalitogenic determinant. J. Immunol.

Fujinami, R.S., Herrath, von, M.G., Christen, U., and Whitton, J.L. (2006). Molecular Mimicry, Bystander Activation, or Viral Persistence: Infections and Autoimmune Disease. Clinical Microbiology Reviews *19*, 80–94.

Fujita, N., Itoh, T., Omori, H., Fukuda, M., Noda, T., and Yoshimori, T. (2008). The Atg16L complex specifies the site of LC3 lipidation for membrane biogenesis in autophagy. Mol. Biol. Cell *19*, 2092–2100.

Gaipl, U.S., Sheriff, A., Franz, S., Munoz, L.E., Voll, R.E., Kalden, J.R., and Herrmann, M. (2006). Inefficient clearance of dying cells and autoreactivity. Curr. Top. Microbiol. Immunol. *305*, 161–176.

Gale, C.R., and Martyn, C.N. (1995). Migrant studies in multiple sclerosis. Progress in Neurobiology *47*, 425–448.

Genain, C.P., Cannella, B., Hauser, S.L., and Raine, C.S. (1999). Identification of autoantibodies associated with myelin damage in multiple sclerosis. Nature Medicine *5*, 170–175.

Ginhoux, F., Collin, M.P., Bogunovic, M., Abel, M., Leboeuf, M., Helft, J., Ochando, J., Kissenpfennig, A., Malissen, B., Grisotto, M., et al. (2007). Blood-derived dermal langerin+ dendritic cells survey the skin in the steady state. Journal of Experimental Medicine *204*, 3133–3146.

Gold, R., Linington, C., and Lassmann, H. (2006). Understanding pathogenesis and therapy of multiple sclerosis via animal models: 70 years of merits and culprits in experimental autoimmune encephalomyelitis research. Brain *129*, 1953–1971.

Gong, L., Cullinane, M., Treerat, P., Ramm, G., Prescott, M., Adler, B., Boyce, J.D., and Devenish, R.J. (2011). The Burkholderia pseudomallei type III secretion system and BopA are required for evasion of LC3-associated phagocytosis. PLoS ONE *6*, e17852.

Goverman, J., Woods, A., Larson, L., Weiner, L.P., Hood, L., and Zaller, D.M. (1993). Transgenic mice that express a myelin basic protein-specific T cell receptor develop spontaneous autoimmunity. Cell *72*, 551–560.

Gredler, V., Ebner, S., Schanda, K., Forstner, M., Berger, T., Romani, N., and Reindl, M. (2010). Impact of human myelin on the maturation and function of human monocyte-derived dendritic cells. Clin. Immunol. *134*, 296–304.

Greter, M., Heppner, F.L., Lemos, M.P., Odermatt, B.M., Goebels, N., Laufer, T., Noelle, R.J., and Becher, B. (2005). Dendritic cells permit immune invasion of the CNS in an animal model of multiple sclerosis. Nature Medicine *11*, 328–334.

Guce, A.I., Mortimer, S.E., Yoon, T., Painter, C.A., Jiang, W., Mellins, E.D., and Stern, L.J. (2013). HLA-DO acts as a substrate mimic to inhibit HLA-DM by a competitive mechanism. Nat. Struct. Mol. Biol. *20*, 90–98.

Guéguen, M., and Long, E.O. (1996). Presentation of a cytosolic antigen by major histocompatibility complex class II molecules requires a long-lived form of the antigen. Proc. Natl. Acad. Sci. U.S.a. *93*, 14692–14697.

Hanada, T., Noda, N.N., Satomi, Y., Ichimura, Y., Fujioka, Y., Takao, T., Inagaki, F., and Ohsumi, Y. (2007). The Atg12-Atg5 conjugate has a novel E3-like activity for protein lipidation in autophagy. J. Biol. Chem. *282*, 37298–37302.

Harding, C.V., Canaday, D., and Ramachandra, L. (2001). Choosing and Preparing Antigen-Presenting Cells (Hoboken, NJ, USA: John Wiley & Sons, Inc.).

He, C., and Klionsky, D.J. (2009). Regulation mechanisms and signaling pathways of autophagy. Annu. Rev. Genet. *43*, 67–93.

Hemmer, B., Archelos, J.J., and Hartung, H.-P. (2002). New concepts in the immunopathogenesis of multiple sclerosis. Nat. Rev. Neurosci. *3*, 291–301.

Henault, J., Martinez, J., Riggs, J.M., Tian, J., Mehta, P., Clarke, L., Sasai, M., Latz, E., Brinkmann, M.M., Iwasaki, A., et al. (2012). Noncanonical autophagy is required for type I interferon secretion in response to DNA-immune complexes. Immunity *37*, 986–997.

Henri, S., Poulin, L.F., Tamoutounour, S., Ardouin, L., Guilliams, M., de Bovis, B., Devilard, E., Viret, C., Azukizawa, H., Kissenpfennig, A., et al. (2010). CD207+ CD103+ dermal dendritic cells cross-present keratinocyte-derived antigens irrespective of the presence of Langerhans cells. Journal of Experimental Medicine *207*, 189–206.

Heppner, F.L., Greter, M., Marino, D., Falsig, J., Raivich, G., Hövelmeyer, N., Waisman, A., Rülicke, T., Prinz, M., Priller, J., et al. (2005). Experimental autoimmune encephalomyelitis repressed by microglial paralysis. Nature Medicine *11*, 146–152.

Hernán, M.A., Jick, S.S., Logroscino, G., Olek, M.J., Ascherio, A., and Jick, H. (2005). Cigarette smoking and the progression of multiple sclerosis. Brain *128*, 1461–1465.

Hickey, W.F. (1991). Migration of Hematogenous Cells Through the Blood-Brain Barrier and the Initiation of CNS Inflammation - Hickey - 2008 - Brain Pathology - Wiley Online Library. Brain Pathology.

Hjelmström, P., Juedes, A.E., Fjell, J., and Ruddle, N.H. (1998). B-cell-deficient mice develop experimental allergic encephalomyelitis with demyelination after myelin oligodendrocyte glycoprotein sensitization. J. Immunol. *161*, 4480–4483.

Hofstetter, H.H., Shive, C.L., and Forsthuber, T.G. (2002). Pertussis toxin modulates the immune response to neuroantigens injected in incomplete Freund's adjuvant: induction of Th1 cells and experimental autoimmune encephalomyelitis in the presence of high frequencies of Th2 cells. J. Immunol. *169*, 117–125.

Hogquist, K.A., Baldwin, T.A., and Jameson, S.C. (2005). Central tolerance: learning self-control in the thymus. Nat Rev Immunol *5*, 772–782.

Hohl, T.M., Rivera, A., Lipuma, L., Gallegos, A., Shi, C., Mack, M., and Pamer, E.G. (2009). Inflammatory monocytes facilitate adaptive CD4 T cell responses during respiratory fungal infection. Cell Host Microbe *6*, 470–481.

Hou, W., Wu, Y., Sun, S., Shi, M., Sun, Y., Yang, C., Pei, G., Gu, Y., Zhong, C., and Sun, B. (2003). Pertussis toxin enhances Th1 responses by stimulation of dendritic cells. J. Immunol. *170*, 1728–1736.

Huang, J., Canadien, V., Lam, G.Y., Steinberg, B.E., Dinauer, M.C., Magalhaes, M.A.O., Glogauer, M., Grinstein, S., and Brumell, J.H. (2009). Activation of antibacterial autophagy by NADPH oxidases. Proc. Natl. Acad. Sci. U.S.a. *106*, 6226–6231.

Huizinga, R., van der Star, B.J., Kipp, M., Jong, R., Gerritsen, W., Clarner, T., Puentes, F., Dijkstra, C.D., van der Valk, P., and Amor, S. (2012). Phagocytosis of neuronal debris by microglia is associated with neuronal damage in multiple sclerosis. Glia *60*, 422–431.

Hunt, D.F., Michel, H., Dickinson, T.A., Shabanowitz, J., Cox, A.L., Sakaguchi, K., Appella, E., Grey, H.M., and Sette, A. (1992). Peptides presented to the immune system by the murine class II major histocompatibility complex molecule I-Ad. Science *256*, 1817–1820.

Huotari, J., and Helenius, A. (2011). Endosome maturation. Embo J *30*, 3481–3500.

Ichimura, Y., Kirisako, T., Takao, T., Satomi, Y., Shimonishi, Y., Ishihara, N., Mizushima, N., Tanida, I., Kominami, E., Ohsumi, M., et al. (2000). A ubiquitin-like system mediates protein lipidation. Nature *408*, 488–492.

Idoyaga, J., Fiorese, C., Zbytnuik, L., Lubkin, A., Miller, J., Malissen, B., Mucida, D., Merad, M., and Steinman, R.M. (2013). Specialized role of migratory dendritic cells in peripheral tolerance induction. The Journal of Clinical Investigation.

Imboden, J.B. (2009). The Immunopathogenesis of Rheumatoid Arthritis. Annu Rev Pathol *4*, 417–434.

Inaba, K., Metlay, J.P., Crowley, M.T., and Steinman, R.M. (1990). Dendritic cells pulsed with protein antigens in vitro can prime antigen-specific, MHC-restricted T cells in situ. J. Exp. Med. *172*, 631–640.

International Multiple Sclerosis Genetics Consortium (IMSGC), Beecham, A.H., Patsopoulos, N.A., Xifara, D.K., Davis, M.F., Kemppinen, A., Cotsapas, C., Shah, T.S., Spencer, C., Booth, D., et al. (2013). Analysis of immune-related loci identifies 48 new susceptibility variants for multiple sclerosis. Nat. Genet.

Isaksson, M., Lundgren, B.A., and Ahlgren, K.M. (2012). Conditional DC depletion does not affect priming of encephalitogenic Th cells in EAE. Eur. J. Immunol. *42*, 2555–2563.

Itakura, E., and Mizushima, N. (2010). Characterization of autophagosome formation site by a hierarchical analysis of mammalian Atg proteins. Autophagy *6*, 764–776.

Joffre, O.P., Segura, E., Savina, A., and Amigorena, S. (2012). Cross-presentation by dendritic cells. Nat Rev Immunol *12*, 557–569.

Johansen, T., and Lamark, T. (2011). Selective autophagy mediated by autophagic adapter proteins. Autophagy *7*, 279–296.

Jounai, N., Takeshita, F., Kobiyama, K., Sawano, A., Miyawaki, A., Xin, K.-Q., Ishii, K.J., Kawai, T., Akira, S., Suzuki, K., et al. (2007). The Atg5 Atg12 conjugate associates with innate antiviral immune responses. Proc. Natl. Acad. Sci. U.S.a. *104*, 14050–14055.

Jung, C.H., Ro, S.-H., Cao, J., Otto, N.M., and Kim, D.-H. (2010). mTOR regulation of autophagy. FEBS Letters *584*, 1287–1295.

Jung, S., Unutmaz, D., Wong, P., Sano, G.-I., De los Santos, K., Sparwasser, T., Wu, S., Vuthoori, S., Ko, K., Zavala, F., et al. (2002). In vivo depletion of CD11c+ dendritic cells abrogates priming of CD8+ T cells by exogenous cell-associated antigens. Immunity *17*, 211–220.

Kakalacheva, K., Münz, C., and Lünemann, J.D. (2011). Viral triggers of multiple sclerosis. Biochimica Et Biophysica Acta (BBA) - Molecular Basis of Disease *1812*, 132–140.

Kalinke, U., and Prinz, M. (2012). Endogenous, or therapeutically induced, type I interferon responses differentially modulate Th1/Th17-mediated autoimmunity in the CNS. Immunol. Cell Biol. *90*, 505–509.

Kamradt, T., Soloway, P.D., Perkins, D.L., and Gefter, M.L. (1991). Pertussis toxin prevents the induction of peripheral T cell anergy and enhances the T cell response to an encephalitogenic peptide of myelin basic protein. J. Immunol. *147*, 3296–3302.

Kasai, M., Tanida, I., Ueno, T., Kominami, E., Seki, S., Ikeda, T., and Mizuochi, T. (2009). Autophagic compartments gain access to the MHC class II compartments in thymic epithelium. J. Immunol. *183*, 7278–7285.

Kaushik, S., and Cuervo, A.M. (2012). Chaperone-mediated autophagy: a unique way to enter the lysosome world. Trends Cell Biol. *22*, 407–417.

Kawakami, N., Lassmann, S., Li, Z., Odoardi, F., Ritter, T., Ziemssen, T., Klinkert, W.E.F., Ellwart, J.W., Bradl, M., Krivacic, K., et al. (2004). The activation status of neuroantigen-specific T cells in the target organ determines the clinical outcome of autoimmune encephalomyelitis. J. Exp. Med. *199*, 185–197.

Kerfoot, S.M., Long, E.M., Hickey, M.J., Andonegui, G., Lapointe, B.M., Zanardo, R.C.O., Bonder, C., James, W.G., Robbins, S.M., and Kubes, P. (2004). TLR4 contributes to disease-inducing mechanisms resulting in central nervous system autoimmune disease. J. Immunol. *173*, 7070–7077.

Kim, D.-H., Sarbassov, D.D., Ali, S.M., King, J.E., Latek, R.R., Erdjument-Bromage, H., Tempst, P., and Sabatini, D.M. (2002). mTOR interacts with raptor to form a nutrient-sensitive complex that signals to the cell growth machinery. Cell *110*, 163–175.

Kim, I., Rodriguez-Enriquez, S., and Lemasters, J.J. (2007). Selective degradation of mitochondria by mitophagy. Archives of Biochemistry and Biophysics *462*, 245–253.

King, I.L., Dickendesher, T.L., and Segal, B.M. (2009). Circulating Ly-6C+ myeloid precursors migrate to the CNS and play a pathogenic role during autoimmune demyelinating disease. Blood *113*, 3190–3197.

King, I.L., Kroenke, M.A., and Segal, B.M. (2010). GM-CSF-dependent, CD103+ dermal dendritic cells play a critical role in Th effector cell differentiation after subcutaneous immunization. Journal of Experimental Medicine *207*, 953–961.

Kirisako, T., Ichimura, Y., Okada, H., Kabeya, Y., Mizushima, N., Yoshimori, T., Ohsumi, M., Takao, T., Noda, T., and Ohsumi, Y. (2000). The reversible modification regulates the membrane-binding state of Apg8/Aut7 essential for autophagy and the cytoplasm to vacuole targeting pathway. The Journal of Cell Biology *151*, 263–276.

Klionsky, D.J., Cuervo, A.M., Dunn, W.A., Levine, B., van der Klei, I., and Seglen, P.O. (2007). How shall I eat thee? Autophagy *3*, 413–416.

Kraft, C., Deplazes, A., Sohrmann, M., and Peter, M. (2008). Mature ribosomes are selectively degraded upon starvation by an autophagy pathway requiring the Ubp3p/Bre5p ubiquitin protease. Nat. Cell Biol. *10*, 602–610.

Kraft, C., Peter, M., and Hofmann, K. (2010). Selective autophagy: ubiquitin-mediated recognition and beyond. Nat. Cell Biol. *12*, 836–841.

Kreutzberg, G.W. (1996). Microglia: a sensor for pathological events in the CNS. Trends Neurosci. *19*, 312–318.

Krishnamoorthy, G., Lassmann, H., Wekerle, H., and Holz, A. (2006). Spontaneous opticospinal encephalomyelitis in a double-transgenic mouse model of autoimmune T cell/B cell cooperation. The Journal of Clinical Investigation *116*, 2385–2392.

Kuballa, P., Nolte, W.M., Castoreno, A.B., and Xavier, R.J. (2012). Autophagy and the immune system. Annu. Rev. Immunol. *30*, 611–646.

Kuchroo, V.K., Anderson, A.C., Waldner, H., Munder, M., Bettelli, E., and Nicholson, L.B. (2002). T cell response in experimental autoimmune encephalomyelitis (EAE): role of self and cross-reactive antigens in shaping, tuning, and regulating the autopathogenic T cell repertoire. Annu. Rev. Immunol. *20*, 101–123.

Lam, G.Y., Cemma, M., Muise, A.M., Higgins, D.E., and Brumell, J.H. (2013). Host and bacterial factors that regulate LC3 recruitment to Listeria monocytogenes during the early stages of macrophage infection. Autophagy *9*.

Lassmann, H., Brunner, C., Bradl, M., and Linington, C. (1988). Experimental allergic encephalomyelitis: the balance between encephalitogenic T lymphocytes and demyelinating antibodies determines size and structure of demyelinated lesions. Acta Neuropathol. *75*, 566–576.

Lee, H.K., Mattei, L.M., Steinberg, B.E., Alberts, P., Lee, Y.H., Chervonsky, A., Mizushima, N., Grinstein, S., and Iwasaki, A. (2010). In vivo requirement for Atg5 in antigen presentation by dendritic cells. Immunity *32*, 227–239.

Lee, J., Giordano, S., and Zhang, J. (2012). Autophagy, mitochondria and oxidative stress: cross-talk and redox signalling. Biochem. J. *441*, 523–540.

Lee, S.C., and Raine, C.S. (1989). Multiple sclerosis: Oligodendrocytes in active lesions do not express class II major histocompatibility complex molecules. J Neuroimmunol *25*, 261–266.

León, B., López-Bravo, M., and Ardavín, C. (2007). Monocyte-derived dendritic cells formed at the infection site control the induction of protective T helper 1 responses against Leishmania. Immunity *26*, 519–531.

Levine, B., and Deretic, V. (2007). Unveiling the roles of autophagy in innate and adaptive immunity. Nat Rev Immunol *7*, 767–777.

Levine, B., and Kroemer, G. (2008). Autophagy in the Pathogenesis of Disease. Cell *132*, 27–42.

Li, H., Gonnella, P., Safavi, F., Vessal, G., Nourbakhsh, B., Zhou, F., Zhang, G.-X., and Rostami, A. (2013). Low dose zymosan ameliorates both chronic and relapsing experimental autoimmune encephalomyelitis. J Neuroimmunol *254*, 28–38.

Li, M., Wang, I.X., Li, Y., Bruzel, A., Richards, A.L., Toung, J.M., and Cheung, V.G. (2011a). Widespread RNA and DNA sequence differences in the human transcriptome. Science *333*, 53–58.

Li, W.-W., Li, J., and Bao, J.-K. (2011b). Microautophagy: lesser-known self-eating. Cell. Mol. Life Sci. *69*, 1125–1136.

Ling, C., Sandor, M., and Fabry, Z. (2003). In situ processing and distribution of intracerebrally injected OVA in the CNS. J Neuroimmunol *141*, 90–98.

Linington, C., and Lassmann, H. (1987). Antibody responses in chronic relapsing experimental allergic encephalomyelitis: correlation of serum demyelinating activity with antibody titre to the myelin/oligodendrocyte glycoprotein (MOG). J Neuroimmunol *17*, 61–69.

Linington, C., Bradl, M., Lassmann, H., Brunner, C., and Vass, K. (1988). Augmentation of demyelination in rat acute allergic encephalomyelitis by circulating mouse monoclonal antibodies directed against a myelin/oligodendrocyte glycoprotein. The American Journal of Pathology *130*, 443–454.

Linthicum, D.S., Munoz, J.J., and Blaskett, A. (1982). Acute experimental autoimmune encephalomyelitis in mice. I. Adjuvant action of Bordetella pertussis is due to vasoactive amine sensitization and increased vascular permeability of the central nervous system. Cell. Immunol. *73*, 299–310.

Liu, Y.-J. (2005). IPC: professional type 1 interferon-producing cells and plasmacytoid dendritic cell precursors. Annu. Rev. Immunol. *23*, 275–306.

Lleo, A., Invernizzi, P., Selmi, C., Coppel, R.L., Alpini, G., Podda, M., Mackay, I.R., and Gershwin, M.E. (2007). Autophagy: highlighting a novel player in the autoimmunity scenario. J. Autoimmun. *29*, 61–68.

Lu, C., Pelech, S., Zhang, H., Bond, J., Spach, K., Noubade, R., Blankenhorn, E.P., and Teuscher, C. (2008). Pertussis toxin induces angiogenesis in brain microvascular endothelial cells. J. Neurosci. Res. *86*, 2624–2640.

Lublin, F.D., and Reingold, S.C. (1996). Defining the clinical course of multiple sclerosis. Neurology.

Lum, J.J., Bauer, D.E., Kong, M., Harris, M.H., Li, C., Lindsten, T., and Thompson, C.B. (2005). Growth factor regulation of autophagy and cell survival in the absence of apoptosis. Cell *120*, 237–248.

Macatonia, S.E., Taylor, P.M., Knight, S.C., and Askonas, B.A. (1989). Primary stimulation by dendritic cells induces antiviral proliferative and cytotoxic T cell responses in vitro. J. Exp. Med. *169*, 1255–1264.

Mann, M.K., Ray, A., Basu, S., Karp, C.L., and Dittel, B.N. (2012). Pathogenic and regulatory roles for B cells in experimental autoimmune encephalomyelitis. Autoimmunity *45*, 388–399.

Marta, M., Meier, U.C., and Lobell, A. (2009). Regulation of autoimmune encephalomyelitis by toll-like receptors. Autoimmun Rev *8*, 506–509.

Martiney, J.A., Rajan, A.J., Charles, P.C., Cerami, A., Ulrich, P.C., Macphail, S., Tracey, K.J., and Brosnan, C.F. (1998). Prevention and treatment of experimental autoimmune encephalomyelitis by CNI-1493, a macrophage-deactivating agent. J. Immunol. *160*, 5588–5595.

Martinez, J., Almendinger, J., Oberst, A., Ness, R., Dillon, C.P., Fitzgerald, P., Hengartner, M.O., and Green, D.R. (2011). Microtubule-associated protein 1 light chain 3 alpha (LC3)-associated phagocytosis is required for the efficient clearance of dead cells. Proc. Natl. Acad. Sci. U.S.a. *108*, 17396–17401.

Martinez, J., Verbist, K., Wang, R., and Green, D.R. (2013). The relationship between metabolism and the autophagy machinery during the innate immune response. Cell Metab. *17*, 895–900.

Matsushita, T., Yanaba, K., Bouaziz, J.-D., Fujimoto, M., and Tedder, T.F. (2008). Regulatory B cells inhibit EAE initiation in mice while other B cells promote disease progression. The Journal of Clinical Investigation *118*, 3420–3430.

Mazure, N.M., and Pouysségur, J. (2010). Hypoxia-induced autophagy: cell death or cell survival? Curr. Opin. Cell Biol.

McCarthy, D.P., Richards, M.H., and Miller, S.D. (2012). Mouse Models of Multiple Sclerosis: Experimental Autoimmune Encephalomyelitis and Theiler's Virus-Induced Demyelinating Disease. In Autoimmunity, (Totowa, NJ: Humana Press), pp. 381–401.

McCoy, L., Tsunoda, I., and Fujinami, R.S. (2006). Multiple sclerosis and virus induced immune responses: autoimmunity can be primed by molecular mimicry and augmented by bystander activation. Autoimmunity *39*, 9–19.

McLeod, J.G., Hammond, S.R., and Kurtzke, J.F. (2011). Migration and multiple sclerosis in immigrants to Australia from United Kingdom and Ireland: a reassessment. I. Risk of MS by age at immigration. J. Neurol. *258*, 1140–1149.

McMahon, E.J., Bailey, S.L., Castenada, C.V., Waldner, H., and Miller, S.D. (2005). Epitope spreading initiates in the CNS in two mouse models of multiple sclerosis. Nature Medicine *11*, 335–339.

Mendel, I., de Rosbo, N.K., and Ben-Nun, A. (1995). A myelin oligodendrocyte glycoprotein peptide induces typical chronic experimental autoimmune encephalomyelitis in H-2b mice: Fine specificity and T cell receptor Vβ expression of encephalitogenic T cells. Eur. J. Immunol. *25*, 1951–1959.

Menzies, F.M., Moreau, K., and Rubinsztein, D.C. (2011). Protein misfolding disorders and macroautophagy. Curr. Opin. Cell Biol. *23*, 190–197.

Mildner, A., Mack, M., Schmidt, H., Brück, W., Djukic, M., Zabel, M.D., Hille, A., Priller, J., and Prinz, M. (2009). CCR2+Ly-6Chi monocytes are crucial for the effector phase of autoimmunity in the central nervous system. Brain *132*, 2487–2500.

Miller, S.D., Karpus, W.J., and Davidson, T.S. (2010). Experimental autoimmune encephalomyelitis in the mouse. Curr Protoc Immunol *Chapter 15*, Unit15.1.

Mills, K.H.G. (2011). TLR-dependent T cell activation in autoimmunity. Nat Rev Immunol *11*, 807–822.

Milo, R., and Kahana, E. (2010). Multiple sclerosis: geoepidemiology, genetics and the environment. Autoimmun Rev *9*, A387–A394.

Miranda-Hernandez, S., Gerlach, N., Fletcher, J.M., Biros, E., Mack, M., Körner, H., and Baxter, A.G. (2011). Role for MyD88, TLR2 and TLR9 but not TLR1, TLR4 or TLR6 in experimental autoimmune encephalomyelitis. J. Immunol. *187*, 791–804.

Mizushima, N., Noda, T., Yoshimori, T., Tanaka, Y., Ishii, T., George, M.D., Klionsky, D.J., Ohsumi, M., and Ohsumi, Y. (1998). A protein conjugation system essential for autophagy. Nature *395*, 395–398.

Mizushima, N., and Komatsu, M. (2011). Autophagy: renovation of cells and tissues. Cell *147*, 728–741.

Mizushima, N., and Levine, B. (2010). Autophagy in mammalian development and differentiation. Nat. Cell Biol. *12*, 823–830.

Mizushima, N., Levine, B., Cuervo, A.M., and Klionsky, D.J. (2008). Autophagy fights disease through cellular self-digestion. Nature *451*, 1069–1075.

Moody, D.B., and Porcelli, S.A. (2003). Intracellular pathways of CD1 antigen presentation. Nat Rev Immunol *3*, 11–22.

Morlacchi, S., Soldani, C., Viola, A., and Sarukhan, A. (2011). Self-antigen presentation by mouse B cells results in regulatory T-cell induction rather than anergy or clonal deletion. Blood *118*, 984–991.

Morris-Downes, M.M., Smith, P.A., Rundle, J.L., Piddlesden, S.J., Baker, D., Pham-Dinh, D., Heijmans, N., and Amor, S. (2002). Pathological and regulatory effects of anti-myelin antibodies in experimental allergic encephalomyelitis in mice. J Neuroimmunol *125*, 114–124.

Mortensen, R. (2001). Overview of Gene Targeting by Homologous Recombination (Hoboken, NJ, USA: John Wiley & Sons, Inc.).

Münz, C. (2009). Enhancing immunity through autophagy. Annu. Rev. Immunol. *27*, 423–449.

Nakatogawa, H., Ichimura, Y., and Ohsumi, Y. (2007). Atg8, a ubiquitin-like protein required for autophagosome formation, mediates membrane tethering and hemifusion. Cell *130*, 165–178.

Nedjic, J., Aichinger, M., Emmerich, J., Mizushima, N., and Klein, L. (2008). Autophagy in thymic epithelium shapes the T-cell repertoire and is essential for tolerance. Nature *455*, 396–400.

Neefjes, J., Jongsma, M.L.M., Paul, P., and Bakke, O. (2011). Towards a systems understanding of MHC class I and MHC class II antigen presentation. Nat Rev Immunol *11*, 823–836.

Nimmerjahn, F., Milosevic, S., Behrends, U., Jaffee, E.M., Pardoll, D.M., Bornkamm, G.W., and Mautner, J. (2003). Major histocompatibility complex class II-restricted presentation of a cytosolic antigen by autophagy. Eur. J. Immunol. *33*, 1250–1259.

Noda, N.N., Ohsumi, Y., and Inagaki, F. (2010). Atg8-family interacting motif crucial for selective autophagy. FEBS Letters *584*, 1379–1385.

Olitsky, P.K., and Yager, R.H. (1949). Experimental disseminated encephalomyelitis in white mice. J. Exp. Med. *90*, 213–224.

Paludan, C., Schmid, D., Landthaler, M., Vockerodt, M., Kube, D., Tuschl, T., and Münz, C. (2005). Endogenous MHC class II processing of a viral nuclear antigen after autophagy. Science *307*, 593–596.

Paterson, P.Y. (1960). Transfer of allergic encephalomyelitis in rats by means of lymph node cells. J. Exp. Med. *111*, 119–136.

Pattingre, S., Tassa, A., Qu, X., Garuti, R., Liang, X.H., Mizushima, N., Packer, M., Schneider, M.D., and Levine, B. (2005). Bcl-2 antiapoptotic proteins inhibit Beclin 1-dependent autophagy. Cell *122*, 927–939.

Phan, U.T., Arunachalam, B., and Cresswell, P. (2000). Gamma-interferon-inducible lysosomal thiol reductase (GILT). Maturation, activity, and mechanism of action. J. Biol. Chem. *275*, 25907–25914.

Pickart, C.M. (2001). Mechanisms underlying ubiquitination. Annu. Rev. Biochem. *70*, 503–533.

Pierdominici, M., Vomero, M., Barbati, C., Colasanti, T., Maselli, A., Vacirca, D., Giovannetti, A., Malorni, W., and Ortona, E. (2012). Role of autophagy in immunity and autoimmunity, with a

special focus on systemic lupus erythematosus. Faseb J. *26*, 1400–1412.

Plantinga, T.S., Joosten, L.A.B., van der Meer, J.W.M., and Netea, M.G. (2012). Modulation of inflammation by autophagy: consequences for Crohn's disease. Curr Opin Pharmacol *12*, 497–502.

Platten, M., and Steinman, L. (2005). Multiple sclerosis: trapped in deadly glue. Nature Medicine *11*, 252–253.

Ponomarev, E.D., Shriver, L.P., Maresz, K., and Dittel, B.N. (2005). Microglial cell activation and proliferation precedes the onset of CNS autoimmunity. J. Neurosci. Res. *81*, 374–389.

Pöllinger, B., Krishnamoorthy, G., Berer, K., Lassmann, H., Bösl, M.R., Dunn, R., Domingues, H.S., Holz, A., Kurschus, F.C., and Wekerle, H. (2009). Spontaneous relapsing-remitting EAE in the SJL/J mouse: MOG-reactive transgenic T cells recruit endogenous MOG-specific B cells. Journal of Experimental Medicine *206*, 1303–1316.

Prescott, N.J., Fisher, S.A., Franke, A., Hampe, J., Onnie, C.M., Soars, D., Bagnall, R., Mirza, M.M., Sanderson, J., Forbes, A., et al. (2007). A nonsynonymous SNP in ATG16L1 predisposes to ileal Crohn's disease and is independent of CARD15 and IBD5. Gastroenterology *132*, 1665–1671.

Prinz, M., Garbe, F., Schmidt, H., Mildner, A., Gutcher, I., Wolter, K., Piesche, M., Schroers, R., Weiss, E., Kirschning, C.J., et al. (2006). Innate immunity mediated by TLR9 modulates pathogenicity in an animal model of multiple sclerosis. The Journal of Clinical Investigation *116*, 456–464.

Qiu, W., Pham, K., James, I., Nolan, D., Castley, A., Christiansen, F.T., Czarniak, P., Luo, Y., Wu, J., Garlepp, M., et al. (2013). The influence of non-HLA gene polymorphisms and interactions on disease risk in a Western Australian multiple sclerosis cohort. J Neuroimmunol.

Racke, M.K. (2001). Experimental Autoimmune Encephalomyelitis (EAE) - Current Protocols in Neuroscience - Racke - Wiley Online Library. Current Protocols in Neuroscience.

Raivich, G., and Banati, R. (2004). Brain microglia and blood-derived macrophages: molecular profiles and functional roles in multiple sclerosis and animal models of autoimmune demyelinating disease. Brain Res. Brain Res. Rev. *46*, 261–281.

Ramagopalan, S.V., Dyment, D.A., Cader, M.Z., Morrison, K.M., Disanto, G., Morahan, J.M., Berlanga-Taylor, A.J., Handel, A., De Luca, G.C., Sadovnick, A.D., et al. (2011). Rare variants in the CYP27B1 gene are associated with multiple sclerosis. Ann. Neurol. *70*, 881–886.

Randow, F., and Münz, C. (2012). Autophagy in the regulation of pathogen replication and adaptive immunity. Trends Immunol. *33*, 475–487.

Rao, P., and Segal, B.M. (2012). Experimental autoimmune encephalomyelitis. Methods Mol. Biol. *900*, 363–380.

Regnault, A., Lankar, D., Lacabanne, V., Rodriguez, A., Théry, C., Rescigno, M., Saito, T., Verbeek, S., Bonnerot, C., Ricciardi-Castagnoli, P., et al. (1999). Fcgamma receptor-mediated induction of dendritic cell maturation and major histocompatibility complex class I-restricted antigen presentation after immune complex internalization. J. Exp. Med. *189*, 371–380.

Richard, J.-F., Roy, M., Audoy-Rémus, J., Tremblay, P., and Vallières, L. (2011). Crawling phagocytes recruited in the brain vasculature after pertussis toxin exposure through IL6, ICAM1 and ITGαM. Brain Pathol. *21*, 661–671.

Riise, T., Nortvedt, M.W., and Ascherio, A. (2003). Smoking is a risk factor for multiple sclerosis. Neurology *61*, 1122–1124.

Rioux, J.D., Xavier, R.J., Taylor, K.D., Silverberg, M.S., Goyette, P., Huett, A., Green, T., Kuballa, P., Barmada, M.M., Datta, L.W., et al. (2007). Genome-wide association study identifies new susceptibility loci for Crohn disease and implicates autophagy in disease pathogenesis. Nat. Genet. *39*, 596–604.

Ryan, M., McCarthy, L., Rappuoli, R., Mahon, B.P., and Mills, K.H. (1998). Pertussis toxin potentiates Th1 and Th2 responses to co-injected antigen: adjuvant action is associated with enhanced regulatory cytokine production and expression of the co-stimulatory molecules B7-1, B7-2 and CD28. Int. Immunol. *10*, 651–662.

Sadler, R.H., Sommer, M.A., Forno, L.S., and Smith, M.E. (1991). Induction of anti-myelin antibodies in EAE and their possible role in demyelination. J. Neurosci. Res. *30*, 616–624.

Sadovnick, A.D. (2012). Genetic background of multiple sclerosis. Autoimmun Rev *11*, 163–166.

Sanjuan, M.A., and Green, D.R. (2008). Eating for good health: linking autophagy and phagocytosis in host defense. Autophagy *4*, 607–611.

Sanjuan, M.A., Dillon, C.P., Tait, S.W.G., Moshiach, S., Dorsey, F., Connell, S., Komatsu, M., Tanaka, K., Cleveland, J.L., Withoff, S., et al. (2007). Toll-like receptor signalling in macrophages links the autophagy pathway to phagocytosis. Nature *450*, 1253–1257.

Sanjuan, M.A., Milasta, S., and Green, D.R. (2009). Toll-like receptor signaling in the lysosomal pathways. Immunol. Rev. *227*, 203–220.

Satpathy, A.T., Wu, X., Albring, J.C., and Murphy, K.M. (2012). Re(de)fining the dendritic cell lineage. Nat Immunol *13*, 1145–1154.

Schluesener, H.J., Sobel, R.A., Linington, C., and Weiner, H.L. (1987). A monoclonal antibody against a myelin oligodendrocyte glycoprotein induces relapses and demyelination in central nervous system autoimmune disease. J. Immunol. *139*, 4016–4021.

Schmid, D., Pypaert, M., and Münz, C. (2007). Antigen-Loading Compartments for Major Histocompatibility Complex Class II Molecules Continuously Receive Input from Autophagosomes. Immunity.

Schmidt, H., Williamson, D., and Ashley-Koch, A. (2007). HLA-DR15 haplotype and multiple sclerosis: a HuGE review. Am. J. Epidemiol. *165*, 1097–1109.

Schulze, M.-S.E.D., and Wucherpfennig, K.W. (2012). The mechanism of HLA-DM induced peptide exchange in the MHC class II antigen presentation pathway. Curr. Opin. Immunol. *24*, 105–111.

Seamons, A., Perchellet, A., and Goverman, J. (2003). Immune tolerance to myelin proteins. Immunol. Res. *28*, 201–221.

Segura, E., and Amigorena, S. (2013). Inflammatory dendritic cells in mice and humans. Trends Immunol. *34*, 440–445.

Serafini, B., Rosicarelli, B., Magliozzi, R., Stigliano, E., Capello, E., Mancardi, G.L., and Aloisi, F. (2006). Dendritic cells in multiple sclerosis lesions: maturation stage, myelin uptake, and interaction with proliferating T cells. J. Neuropathol. Exp. Neurol. *65*, 124–141.

Shao, W.-H., and Cohen, P.L. (2011). Disturbances of apoptotic cell clearance in systemic lupus erythematosus. Arthritis Res. Ther. *13*, 202.

Shapira, Y., Agmon-Levin, N., and Shoenfeld, Y. (2010). Defining and analyzing geoepidemiology

and human autoimmunity. J. Autoimmun. *34*, J168–J177.

Shive, C.L., Hofstetter, H., Arredondo, L., Shaw, C., and Forsthuber, T.G. (2000). The enhanced antigen-specific production of cytokines induced by pertussis toxin is due to clonal expansion of T cells and not to altered effector functions of long-term memory cells. Eur. J. Immunol. *30*, 2422–2431.

Slavin, A.J., Soos, J.M., Stuve, O., Patarroyo, J.C., Weiner, H.L., Fontana, A., Bikoff, E.K., and Zamvil, S.S. (2001). Requirement for endocytic antigen processing and influence of invariant chain and H-2M deficiencies in CNS autoimmunity. The Journal of Clinical Investigation *108*, 1133–1139.

Sospedra, M., and Martin, R. (2005). Immunology of multiple sclerosis. Annu. Rev. Immunol. *23*, 683–747.

Spangrude, G.J., Braaten, B.A., and Daynes, R.A. (1984). Molecular mechanisms of lymphocyte extravasation. I. Studies of two selective inhibitors of lymphocyte recirculation. J. Immunol. *132*, 354–362.

Steinman, L. (2009). A molecular trio in relapse and remission in multiple sclerosis. Nat Rev Immunol *9*, 440–447.

Steinman, R.M., and Cohn, Z.A. (1973). Identification of a novel cell type in peripheral lymphoid organs of mice. J. Exp. Med. *137*, 1142–1162.

Stromnes, I.M., and Goverman, J.M. (2006a). Active induction of experimental allergic encephalomyelitis. Nat Protoc *1*, 1810–1819.

Stromnes, I.M., and Goverman, J.M. (2006b). Passive induction of experimental allergic encephalomyelitis. Nat Protoc *1*, 1952–1960.

Subramani, S., and Malhotra, V. (2013). Non-autophagic roles of autophagy-related proteins. EMBO Rep. *14*, 143–151.

Sundström, P., Nyström, L., and Hallmans, G. (2008). Smoke exposure increases the risk for multiple sclerosis. Eur. J. Neurol. *15*, 579–583.

Suzuki, G., Sawa, H., Kobayashi, Y., Nakata, Y., Nakagawa, K.I., Uzawa, A., Sakiyama, H., Kakinuma, S., Iwabuchi, K., and Nagashima, K. (1999). Pertussis toxin-sensitive signal controls the trafficking of thymocytes across the corticomedullary junction in the thymus. J. Immunol. *162*, 5981–5985.

Takeshita, F., Kobiyama, K., Miyawaki, A., Jounai, N., and Okuda, K. (2008). The non-canonical role of Atg family members as suppressors of innate antiviral immune signaling. Autophagy *4*, 67–69.

Tang, D., Kang, R., Coyne, C.B., Zeh, H.J., and Lotze, M.T. (2012). PAMPs and DAMPs: signal 0s that spur autophagy and immunity. Immunol. Rev. *249*, 158–175.

Teige, I., Treschow, A., Teige, A., Mattsson, R., Navikas, V., Leanderson, T., Holmdahl, R., and Issazadeh-Navikas, S. (2003). IFN-beta gene deletion leads to augmented and chronic demyelinating experimental autoimmune encephalomyelitis. J. Immunol. *170*, 4776–4784.

Teresa Bailey, P.B.F., Kristina Rowley, P.C., and Allison Bernknopf, P.B. (2011). A review of systemic lupus erythematosus and current treatment options. Formulary *46*, 178–194.

Tompkins, S.M., Padilla, J., Dal Canto, M.C., Ting, J.P.-Y., Van Kaer, L., and Miller, S.D. (2002).

De novo central nervous system processing of myelin antigen is required for the initiation of experimental autoimmune encephalomyelitis. J. Immunol. *168*, 4173–4183.

Tooze, S.A., and Yoshimori, T. (2010). The origin of the autophagosomal membrane. Nat. Cell Biol. *12*, 831–835.

Tran, E.H., Hoekstra, K., van Rooijen, N., Dijkstra, C.D., and Owens, T. (1998). Immune invasion of the central nervous system parenchyma and experimental allergic encephalomyelitis, but not leukocyte extravasation from blood, are prevented in macrophage-depleted mice. J. Immunol. *161*, 3767–3775.

Travassos, L.H., Carneiro, L.A.M., Ramjeet, M., Hussey, S., Kim, Y.-G., Magalhães, J.G., Yuan, L., Soares, F., Chea, E., Le Bourhis, L., et al. (2010). Nod1 and Nod2 direct autophagy by recruiting ATG16L1 to the plasma membrane at the site of bacterial entry. Nat Immunol *11*, 55–62.

Trotter, J.L., Clark, H.B., Collins, K.G., Wegeschiede, C.L., and Scarpellini, J.D. (1987). Myelin proteolipid protein induces demyelinating disease in mice. J. Neurol. Sci. *79*, 173–188.

Trotter, J., DeJong, L.J., and Smith, M.E. (1986). Opsonization with antimyelin antibody increases the uptake and intracellular metabolism of myelin in inflammatory macrophages. J. Neurochem. *47*, 779–789.

Valitutti, S., Müller, S., Cella, M., Padovan, E., and Lanzavecchia, A. (1995). Serial triggering of many T-cell receptors by a few peptide-MHC complexes. Nature *375*, 148–151.

van der Mei, I.A., Ponsonby, A.L., Blizzard, L., and Dwyer, T. (2001). Regional variation in multiple sclerosis prevalence in Australia and its association with ambient ultraviolet radiation. Neuroepidemiology *20*, 168–174.

Virgin, H.W., and Levine, B. (2009). Autophagy genes in immunity. Nat Immunol *10*, 461–470.

Voskuhl, R.R., and Gold, S.M. (2012). Sex-related factors in multiple sclerosis susceptibility and progression. Nat Rev Neurol *8*, 255–263.

Waldner, H., Collins, M., and Kuchroo, V.K. (2004). Activation of antigen-presenting cells by microbial products breaks self tolerance and induces autoimmune disease. The Journal of Clinical Investigation *113*, 990–997.

Walker, L.S.K., and Abbas, A.K. (2002). The enemy within: keeping self-reactive T cells at bay in the periphery. Nat Rev Immunol *2*, 11–19.

Wallin, M.T., Page, W.F., and Kurtzke, J.F. (2004). Multiple sclerosis in US veterans of the Vietnam era and later military service: race, sex, and geography. Ann. Neurol. *55*, 65–71.

Watts, C. (2001). Antigen processing in the endocytic compartment. Curr. Opin. Immunol. *13*, 26–31.

Wearsch, P.A., and Cresswell, P. (2008). The quality control of MHC class I peptide loading. Curr. Opin. Cell Biol. *20*, 624–631.

Weber, M.S., Hemmer, B., and Cepok, S. (2011). The role of antibodies in multiple sclerosis. Biochim. Biophys. Acta *1812*, 239–245.

Wekerle, H., Linington, C., and Lassmann, H. (1986). Cellular immune reactivity within the CNS. Trends Neurosci. *9*, 271–277.

Wekerle, H., and Sun, D.-M. (2010). Fragile privileges: autoimmunity in brain and eye. Acta

Pharmacol. Sin. *31*, 1141–1148.

White, E., Karp, C., Strohecker, A.M., Guo, Y., and Mathew, R. (2010). Role of autophagy in suppression of inflammation and cancer. Curr. Opin. Cell Biol. *22*, 212–217.

Wolf, S.D., Dittel, B.N., Hardardottir, F., and Janeway, C.A. (1996). Experimental autoimmune encephalomyelitis induction in genetically B cell-deficient mice. J. Exp. Med. *184*, 2271–2278.

Wong, E., and Cuervo, A.M. (2010). Autophagy gone awry in neurodegenerative diseases. Nat. Neurosci. *13*, 805–811.

Wong, G.H.W., Bartlett, P.F., Clark-Lewis, I., Battye, F., and Schrader, J.W. (1984). Inducible expression of H–2 and Ia antigens on brain cells. Nature *310*, 688–691.

Wu, G.F., Shindler, K.S., Allenspach, E.J., Stephen, T.L., Thomas, H.L., Mikesell, R.J., Cross, A.H., and Laufer, T.M. (2011). Limited sufficiency of antigen presentation by dendritic cells in models of central nervous system autoimmunity. J. Autoimmun. *36*, 56–64.

Xie, Z., and Klionsky, D.J. (2007). Autophagosome formation: core machinery and adaptations. Nat. Cell Biol. *9*, 1102–1109.

Xie, Z., Nair, U., and Klionsky, D.J. (2008). Atg8 controls phagophore expansion during autophagosome formation. Mol. Biol. Cell *19*, 3290–3298.

Xu, H., Wu, Z.-Y., Fang, F., Guo, L., Chen, D., Chen, J.X., Stern, D., Taylor, G.A., Jiang, H., and Yan, S.S. (2010). Genetic deficiency of Irgm1 (LRG-47) suppresses induction of experimental autoimmune encephalomyelitis by promoting apoptosis of activated CD4+ T cells. Faseb J. *24*, 1583–1592.

Xu, Y., Jagannath, C., Liu, X.-D., Sharafkhaneh, A., Kolodziejska, K.E., and Eissa, N.T. (2007a). Toll-like receptor 4 is a sensor for autophagy associated with innate immunity. Immunity *27*, 135–144.

Xu, Y., Zhan, Y., Lew, A.M., Naik, S.H., and Kershaw, M.H. (2007b). Differential development of murine dendritic cells by GM-CSF versus Flt3 ligand has implications for inflammation and trafficking. J. Immunol. *179*, 7577–7584.

Yogev, N., Frommer, F., Lukas, D., Kautz-Neu, K., Karram, K., Ielo, D., Stebut, von, E., Probst, H.-C., van den Broek, M., Riethmacher, D., et al. (2012). Dendritic cells ameliorate autoimmunity in the CNS by controlling the homeostasis of PD-1 receptor(+) regulatory T cells. Immunity *37*, 264–275.

Yousefi, S., Perozzo, R., Schmid, I., Ziemiecki, A., Schaffner, T., Scapozza, L., Brunner, T., and Simon, H.-U. (2006). Calpain-mediated cleavage of Atg5 switches autophagy to apoptosis. Nat. Cell Biol. *8*, 1124–1132.

Zamvil, S., Nelson, P., Trotter, J., Mitchell, D., Knobler, R., Fritz, R., and Steinman, L. (1985). T-cell clones specific for myelin basic protein induce chronic relapsing paralysis and demyelination. Nature *317*, 355–358.

Ziemssen, T., and Ziemssen, F. (2005). The role of the humoral immune system in multiple sclerosis (MS) and its animal model experimental autoimmune encephalomyelitis (EAE). Autoimmun Rev *4*, 460–467.

Acknowledgements

First of all, I would like to thank Prof. Dr. Jan Lünemann for giving me the chance to carry out my PhD studies in his laboratory and for a lot of help in every kind of issue.

Special thanks go to Prof. Dr. Christian Münz as beeing one of my PhD committee members, but also for sharing the infrastructure of his laboratory and giving me the opportunity to take part in the "Münz lab meeting" and for lots of theoretical input.

Additional thanks go to Prof. Dr. Burkhard Becher, who was the third, but definitely, not least, member of my PhD committee. I would like to thank him for intellectual input on any EAE-related questions and for sharing his mouse antibody toolbox with me.

I also would like to thank all members of the "Lünemann lab", namely Christian, Deeqa, Flavio, Isaak, Kristina, Miguel, and Patrick, for the friendly and constructive working atmosphere and their never ending encouragements. A special thank goes to Patrick for all his precise and reliable hands-on work.

Furthermore, I am thankful to all members of the Institute of Experimental Immunology for providing a great working environment and helpful advices. I would like to thank in particular all "autophagy people" and "EAE people" for a lot of input in theoretical and practical issues and sharing their knowledge with me.

Additionally, I would like to thank all the people that kept the place running: Anne, Dani, Jenny, Sabrina, Jan and Valérie, as well as Debi, Nicole, Ondrej, Monika and the Füllinsdorf team for taking care of all my mice.

All my thanks go to my family and friends for supporting and encouraging me durimg the years of my studies, especially during the times when I was far away from home.

And to Magnus: Thank you for everything!

Curriculum vitae

Personal

Name Christina Sina

Date of birth 17.08.1981

Place of birth Warstein, Germany

Nationality German

Family status Unmarried

Home address Burstwiesenstrasse 59
8055 Zurich
Switzerland

Education

08.1992 – 06.2001 **Gymnasium der Stadt Warstein, Germany**
Allgemeine Hochschulreife

10.2001 – 03.2008 **Christian-Albrechts-Universität zu Kiel, Germany**
Diplom-Biologin
Title of Diploma Thesis: "Functional Analysis of the Role of the CD34-Related Sialomucin, Podocalyxin, in Adhesion and Embryogenesis"

Work Experience

06.2008 – 12.2009 **Cytos Biotechnology AG, Schlieren, Switzerland**
Biologist in the Department of Research and Development

Doctoral Studies

Since 01.2010 **University of Zurich, Switzerland**
Institute of Experimental Immunology